UNIVERSITY OF CALIFORNIA, MERCED

Implications of the Renin Angiotensin System in Hepatic Lipid Metabolism During Metabolic Syndrome

A dissertation submitted in partial satisfaction of the requirements for the degree

Doctor of Philosophy

in

Quantitative and Systems Biology

by Jose Godoy Lugo

Committee in charge:

Frederick W. Wolf, chair

Jose P. Vazquez-Medina

Maria E. Zoghbi

Rudy M. Ortiz, advisor

2021

The Dissertation of Jose Godoy Lugo is approved, and it is acceptable in quality and form for publication on microfilm and electronically

Frederick W. Wolf, Chair

Jose P. Vazquez-Medina

Maria E. Zoghbi

Rudy M. Ortiz

University of California, Merced

2021

Table of Contents

List of Tables

List of Figures

Chapter I

Figure 5. Abundance of TAG and VLDL synthesis proteins. Western blot results, mean ± SD values for relative protein abundance of GPAM (A), DGAT1 (B), and ApoB (C), including Pearson's correlation test of ApoB vs time, during the glucose challenge in Long Evans Tokushima Otsuka (LETO; n=6), Otsuka Long Evans Tokushima Fatty (OLETF; n=6), OLETF + ARB (ARB; ARB x 8 weeks; n=6), and OLETF ± ARB (MINUS, ARB x 4 weeks, then removed x 4 weeks; n=6) rats. *Number at bottom of the bar number indicates n per group. * Significant difference from LETO (P < 0.05). ^ Significant difference from OLETF (P < 0.05). + Significant difference from ARB (P < 0.05).*

Figure 6. Summary of findings. In the liver of rats with AT1 blockade, basal TAG, NEFA, CD36 and ApoB were reduced. During the glucose challenge, TAG decreased and ApoB increased overtime. These results demonstrate that the chronic blockade of AT1 protects the liver from the inappropriate accumulation of TAG. This is associated with decreased CD36 abundance and an overtime increase of ApoB.

Chapter II

Figure 1. Plasma Ang 1-7 and RAS peptide receptors expression and abundance. Mean ± SD values for plasma Ang 1-7 (A), relative mRNA expression of MAS1 (B), AT1 (C), membrane abundance of MAS1 (D), and correlation test between MAS1 expression and membrane abundance during the glucose challenge in Long Evans Tokushima Otsuka (LETO; n=5), Otsuka Long Evans Tokushima Fatty (OLETF; n=8), OLETF + ARB (ARB; n=8) rats. * *Significant difference from LETO (P < 0.05).* ^ *Significant difference from OLETF (P < 0.05).*

Figure 2. Liver NEFA and gene expression of fatty acid transport, synthesis, and oxidation proteins. Mean ± SD values for liver NEFA (A), liver NEFA AUC (B), and mRNA expression of CD36 (C), FATP5 (D), ACC (E), FASN (F), CPT1A (G), and Acox1 (H) during the glucose challenge in Long Evans Tokushima Otsuka (LETO; n=5), Otsuka Long Evans Tokushima Fatty (OLETF; n=8), OLETF + ARB (ARB; n=8) rats. * *Significant difference from LETO (P < 0.05).* ^ *Significant difference from OLETF (P < 0.05).*

Figure 3. Liver TAG and gene expression of TAG synthesis enzymes. Mean ± SD values for liver TAG (A), liver TAG AUC (B), and mRNA expression of GPAT4 (C) and DGAT1 (D) during the glucose challenge in Long Evans Tokushima Otsuka (LETO; n=5), Otsuka Long Evans Tokushima Fatty (OLETF; n=8), OLETF + ARB (ARB; n=8) rats. * *Significant difference from LETO (P < 0.05).* ^ *Significant difference from OLETF (P < 0.05).*

Figure 4. Liver glucose and gene expression of gluconeogenic and glycolysis enzymes. Mean ± SD values for liver glucose (A), liver glucose AUC (B), and mRNA expression of PEPCK1 (A), G6PC1 (B), and GCK (C), and correlation test between liver glucose and GCK expression (F) during the glucose challenge in Long Evans Tokushima Otsuka (LETO; n=5), Otsuka Long Evans Tokushima Fatty (OLETF; n=8), OLETF + ARB (ARB; n=8) rats. * *Significant difference from LETO (P < 0.05).* ^ *Significant difference from OLETF (P < 0.05).*

Figure 5. Summary of findings. AT1 blockade increased Ang 1-7, and this increase was associated with decreased fatty acids and TAG levels, as well as decreased expression of genes of lipogenesis and gluconeogenesis in the liver, while decreasing glucose levels and increasing GCK expression. These results demonstrate that the progression of hepatic steatosis may be delayed, due to the reductions on lipogenesis. As well, the suggested improvement on glucose sensitivity, due to the increase in GCK and correlation with liver glucose levels, may contribute to the decrease in nutrient accumulation in the liver and systemic hyperglycemia.

Chapter III

Figure 1. Gene expression of GSH synthesis, usage, and cycling enzymes. Mean ± SD values for mRNA expression of GCLC (A), GCLM (B), GR (C), and GPx (D) during the glucose challenge in Long Evans Tokushima Otsuka (LETO; n=5), Otsuka Long Evans Tokushima Fatty (OLETF; n=8), OLETF + ARB (ARB; n=8) rats. * *Significant difference from LETO (P < 0.05).* ^ *Significant difference from OLETF (P < 0.05).*

Figure 2. Liver marker of fibrosis, hepatic mitochondrial catalase activity and gene expression of peroxide production enzyme. Mean ± SD values for plasma COL-4 levels (A), before the glucose challenge and catalase activity in mitochondria (B) and mRNA expression of NOX4 (C) during the glucose challenge in Long Evans Tokushima Otsuka (LETO; n=5), Otsuka Long Evans Tokushima Fatty (OLETF; n=8), OLETF + ARB (ARB; n=8) rats. * *Significant difference from LETO (P < 0.05).* ^ *Significant difference from OLETF (P < 0.05).*

Figure 3. Summary of findings. The expression of GCLC, gene of glutathione synthesis, was decreased after AT1 blockade. GR cycles GSH to its reduced form to be used in the reduction of oxidants, as in the reaction with GPx. The expression of these genes, GR and GPx, were decreased after AT1 blockade. Finally, AT1 blockade decreased catalase activity. Altogether, these results suggest that oxidant levels may be decreased with AT1 blockade, requiring less GSH production and cycling. The decrease in catalase activity and GPx expression support this argument, as both clear the H_2O_2, an oxidant in the cell.

List of Abbreviations

4-HNE, 4-hydroxy-2-nonenal
ACE, angiotensin-converting enzyme
ACE2, angiotensin-converting enzyme 2
Acox1, acyl-CoA oxidase 1
Ang 1-7, angiotensin 1-7
Ang I, angiotensin I
Ang II, angiotensin II
ANOVA, analysis of variance
ApoB, apolipoprotein B
ARB, angiotensin receptor blockers
AT1, angiotensin receptor type 1
AT2, angiotensin receptor type 2
ATP, adenosine triphosphate
AUC, area under the curve
B2M, beta-2-microglobulin
CD36, cluster of differentiation 36
CMC, carboxymethyl cellulose
COL-4, collagen type IV
CPT1A, carnitine palmitoyltransferase 1A
DGAT, diacylglycerol O-Acyltransferase
DNL, de novo lipogenesis
EDTA, Ethylenediaminetetraacetic acid
FAS, fatty acid synthase
FATP2, fatty acid transporter protein 2
FATP5, fatty acid transporter protein 5
FFA, free fatty acids
G6PC1, glucose 6-phosphatase catalytic subunit 1
GCLC, glutamate cysteine ligase catalytic subunit
GCLM, glutamate cysteine ligase modifier subunit
GGT, γ-glutamyl transpeptidase
GLUT2, glucose transporter 2
GNG, gluconeogenesis
GPAT, glycerol-3-phosphate acyltransferase
GPx, glutathione peroxidase
GR, glutathione reductase
GSH, glutathione
GSSG, glutathione disulfide
H_2O_2, hydrogen peroxide
IR, insulin resistance
KO, knockout

LETO, Long-Evans Tokushima Otsuka
MAS1, proto-oncogene MAS1
MDA, malondialdehyde
MetS, metabolic syndrome
NAFLD, nonalcoholic fatty liver disease
NASH, nonalcoholic steatohepatitis
NEFA, non-esterified fatty acids
Nox4, NADPH oxidase 4
OLETF, Otsuka Long Evans Tokushima Fatty
PEPCK1, phosphoenolpyruvate carboxykinase 1
PIC, protease inhibitor cocktail
RAS, renin-angiotensin system
SOD, superoxide dismutase
T0, baseline
T2D, type 2 diabetes mellitus
TAG, triacylglycerides
TC, total cholesterol
VLDL, very-low-density lipoprotein

Acknowledgements

I would like to thank my advisor, Dr. Rudy M. Ortiz, and my committee, composed by Dr. Frederick W. Wolf, Dr. Jose P. Vazquez-Medina, and Dr. Maria E. Zoghbi.

I would like to thank the University of California, the University of California Institute for Mexico and the United States (UC MEXUS), and the organism for science in Mexico, *Consejo Nacional de Ciencia y Tecnologia* (CONACYT). As well, I would like to thank the members of the Ortiz Lab and the Nishiyama Lab.

I would also like to thank my family, who took care of me, and specially thank my mom, Gloria G. Lugo Ramos, for all the sacrifices and difficulties that she endured throughout her life so I could be who and where I am.

Curriculum Vitae

Education

2016 B.S. Quimico Biologo Clinico. Unversidad de Sonora, Mexico.

2017-present Ph.D. Quantitative Systems Biology. University of California Merced, Merced, CA.

Advisor: Rudy M. Ortiz

Publications

1. **Godoy-Lugo JA**, Thorwald MA, Nakano D, Nishiyama A, Soñanez-Organis JG, Ortiz RM. Chronic angiotensin receptor activation promotes hepatic triacylglycerol accumulation during an acute glucose challenge in obese-insulin-resistant OLETF rats. *Endocrine*., 2021.
2. Rodriguez R, Escobedo B, Lee AY, Thorwald MA, **Godoy-Lugo JA**, Nakano D, Nishiyama A, Parkes DG, Ortiz RM. Simultaneous angiotensin receptor blockade and glucagon-like peptide-1 receptor activation ameliorate albuminuria in obese insulin-resistant rats. *Clin Exp Pharmacol Physiol*., 2020.
3. **Godoy-Lugo JA**, Miranda-Cruz MM, Rosas-Rodriguez JA, Icedo-Garcia R, Adan-Bante NP, Soñanez-Organis JG. Hypoxia inducible factor −1 regulates WSSV-induced glycolytic genes in the white shrimp Litopenaeus vannamei. *Fish Shellfish Immunol*., 2019.
4. Thorwald MA, **Godoy-Lugo JA**, Rodriguez GJ, Rodriguez MA, Jamal M, Kinoshita H, Nakano D, Nishiyama A, Forman HJ, Ortiz RM. Nrf2-related gene expression is impaired during a glucose challenge in type II diabetic rat hearts. *Free Radic. Biol. Med*., 2019.
5. Miranda-Cruz MM, Poom-Llamas JJ, **Godoy-Lugo JA**, Ortiz RM, Gomez-Jimenez S, Rosas-Rodriguez JA, Moran-Palacio EF, Soñanez-Organis JG. Silencing of HIF-1 in WSSV-infected white shrimp: effect on viral load and antioxidant enzymes. *Comp Biochem Physiol C Toxicol Pharmacol*., 2018.
6. Rodriguez R, Moreno M, Lee AY, **Godoy-Lugo JA**, Nakano D, Nishiyama A, Parkes D, Awayda MS, Ortiz RM. Simultaneous GLP-1 receptor activation and angiotensin receptor blockade increase natriuresis independent of altered arterial pressure in obese OLETF rats. *Hypertens Res*., 2018.
7. Hernandez-Palomares MLE, **Godoy-Lugo JA**, Gomez-Jimenez S, Gamez-Alejo LA, Ortiz RM, Muñoz-Valle JF, Peregrino-Uriarte AB, Yepiz-Plascencia G, Rosas-Rodriguez JA, Soñanez-Organis JG. Regulation of lactate dehydrogenase in response to WSSV infection in the shrimp Litopenaeus vannamei. *Fish Shellfish Immunol*., 2018.

8. Rosas-Rodriguez JA, Soñanez-Organis JG, **Godoy-Lugo JA**, Espinoza-Salazar JA, López-Jacobo CJ, Stephens-Camacho NA, González-Ochoa G. Betaine Aldehyde Dehydrogenase expression during physiological cardiac hypertrophy induced by pregnancy. *Biochem Biophys Res Commun*., 2017.
9. Martinez B, Soñanez-Organis JG, **Godoy-Lugo JA**, Horin LJ, Crocker DE, Ortiz RM. Thyroid hormone-stimulated increases in PGC-1α and UCP2 promote life history-specific endocrine changes and maintain a lipid-based metabolism. *Am J Physiol Regul Integr Comp Physiol*., 2017.
10. Soñanez-Organis JG, **Godoy-Lugo JA**, Hernández-Palomares MLE, Rodriguez-Martinez D, Rosas-Rodriguez JA, Gonzalez-Ochoa G, Virgen-Ortiz A, Ortiz RM. HIF-1α and PPARγ during physiological cardiac hypertrophy induced by pregnancy: Transcriptional activities and effects on target genes. *Gene*., 2016.

Pending publication

1. **Godoy-Lugo JA**, Rodriguez R, Nakano D, Nishiyama A, Ortiz RM. Improved hepatic lipogenesis is associated with increased plasma angiotensin 1-7 during AT1 receptor blockade in insulin-resistant OLETF rats. *Am. J. Physiol. - Endocrinol. Metab.*
2. Rodriguez R, Lee A, **Godoy-Lugo JA**, Martinez B, Ohsaki H, Nakano D, Nishiyama A, Parkes D, Vazquez-Medina JP, Ortiz RM. Chronic AT1 blockade improves hyperglycemia by decreasing adipocyte inflammation and decreasing hepatic PCK1 and G6PC1 expression in obese rats. *Am. J. Physiol. - Endocrinol. Metab.*
3. Thorwald MA, **Godoy-Lugo JA**, Rodriguez R, Stanhope KL, Graham JL, Havel PJ, Forman HJ, Ortiz RM. Cardiac NF- k B Acetylation Increases While Nrf2-related Gene Expression and Mitochondrial Activity are Impaired During the Progression of Diabetes in UCD-T2DM Rats. *Nutr. Metab.*

Abstract

Non-alcoholic fatty liver disease (NAFLD) afflicts 25% of the world's population and is projected to increase due to the increasing prevalence of diabetes and obesity. The metabolic syndrome (MetS) is a cluster of conditions that raise the risk of cardiovascular disease. A strong association exists between MetS and NAFLD, and these two conditions share many characteristics (e.g., increased waist circumference, triacylglycerol, glucose, and blood pressure), along with insulin resistance, that promote their pathogenesis. The classical signaling pathway of the renin-angiotensin system (RAS) has been related to the development and progression of metabolic disease. The objectives of these projects were to elucidate the mechanisms associated with RAS that promote hepatic steatosis in a metabolic syndrome model and to investigate the effects of a nutrient overload via a glucose challenge. The first chapter describes the potential mechanisms by which chronic blockade of the classical RAS pathway decreased hepatic lipid accumulation and increased insulin sensitivity. The second chapter describes that blockade of the classical RAS pathway increased angiotensin 1-7 (Ang 1-7), which acts on the non-classical pathway of RAS. Ang 1-7 signaling is suggested to counteract RAS pathogenic signaling. The increased Ang 1-7 was associated with decreased hepatic lipid levels, triacylglycerol synthesis, fatty acid oxidation, gluconeogenesis, and improved glucose tolerance. Finally, the third chapter examined part of the redox status, which is a component of the "hit" hypotheses describing the pathogenesis of NAFLD, through the expression of hepatic glutathione enzymes. Chronic blockade of the classical RAS pathway decreased the expression of enzymes regulating glutathione metabolism (synthesis, usage, and reduction). Collectively, these data demonstrated that the classical RAS pathway contributes to the dysregulation of metabolism in the liver, which promotes the pathogenesis of NAFLD and MetS. Additionally, overactivation of RAS via AT1-mediated signaling may worsen the hepatic redox status, affecting liver glutathione regulation, which has systemic impact in controlling increased oxidant production. Because the mechanisms behind the development of NAFLD are not fully elucidated, understanding the molecules that dysregulate the metabolic and oxidative homeostasis may provide specific targets for the treatment and prevention of metabolic diseases.

Introduction

Renin Angiotensin System and Hepatic Lipid Metabolism During Metabolic Syndrome

NAFLD is used as an umbrella term that encompasses from the simple fatty liver to the more progressive steatosis associated with hepatitis (inflammation of the liver), fibrosis, cirrhosis, and hepatocellular carcinoma [1]. NAFLD is diagnosed when there are no secondary causes of liver disease [2] where non-alcoholic fatty liver (NAFL) and non-alcoholic steatohepatitis (NASH) are forms of NAFLD. NAFL is characterized by hepatic steatosis with lesser or no inflammation and no evidence of injury. On the other hand, NASH is identified when necroinflammation and severe damage to the hepatocytes are present in a fatty liver [3]. Though many advancements have been made to understand the cause and development of NAFLD, its epidemiology remains incompletely characterized [2]. However, the "two-hit" and, a later proposed, "multiple-hit" hypotheses have been used to describe the pathogenesis of NAFLD [4, 5]. In the "two-hit" hypothesis, the "first hit" is lipid accumulation in the liver, while the "second hit" is multi-factorial, based on the promotion of hepatic injury, inflammation, increased oxidant production, and fibrosis [4, 6]. Insulin resistance (IR) is suggested as the main contributor to the "first hit", causing liver steatosis [7]. The later proposed "multiple-hit" hypothesis describes that multi-factorial events (i.e., obesity, IR, gut microbiome, increased adipokine secretion, hepatic oxidative stress, mitochondrial dysfunction, and genetic factors) help explain pathogenesis and progression of NAFLD to a greater extent [5].

Currently, reliable predictors of the progression of NAFLD are lacking [8], though metabolic disease progression (e.g., obesity, diabetes, metabolic syndrome) has frequently paralleled the histological development of this disease [3, 9]. In the case of metabolic syndrome (MetS), a strong association with NAFLD exists [10] and both of these conditions share many metabolic characteristics (e.g., increased waist circumference, IR, circulating TAG and glucose, and blood pressure, etc.) [10, 11]. MetS is a cluster of conditions (i.e., increased waist circumference, triacylglycerol, glucose, and arterial pressure, and reduced HDL cholesterol) that raise the risk of heart disease, stroke, and diabetes [12]. MetS is diagnosed when three or more of these characteristics are present simultaneously [12]. As with NAFLD, the pathogenic mechanisms of MetS are not completely elucidated [13]. A critical component of MetS pathogenesis, as well as in NAFLD and the "hits" hypotheses, is IR [14], which can increase circulating non-esterified fatty acids (NEFA). Insulin mediates the increase in glucose uptake in the liver, while it inhibits lipolysis and gluconeogenesis, while IR increases adipose lipolysis, increasing circulating NEFA. The increased NEFA stimulate the liver to increase gluconeogenesis and lipogenesis, leading to dysregulated glucose and lipid metabolism and promoting the disease progression [13].

Insulin signaling can be inhibited by elevated angiotensin II (Ang II) signaling, this is a peptide generated as part of the renin-angiotensin system (RAS) [15] and the most biologically active RAS peptide [16]. Inappropriately elevated Ang II and over-activation of its target receptor (AT1) contribute to the development of insulin resistance [17]. There are two pathways involved in RAS signaling, the classical pathway, mediated by the Ang II/AT1 axis, and the non-classical pathways, mediated by Ang II-Ang III/AT2 and the angiotensin 1-7 (Ang 1-7)/proto-oncogene Mas (MAS1) axes. For the classical pathway, the juxtaglomerular cells of the kidney secrete renin, which enzymatically cleaves angiotensinogen, which is secreted by the liver, to produce angiotensin I. Angiotensin I is then cleaved into Ang II by the angiotensin-converting enzyme (ACE) in circulation. For the non-classical pathway, Ang II is instead cleaved by ACE2 to produce Ang 1-7, but Ang I may also be enzymatically cleaved to produce Ang 1-7 [18]. It is reported that the non-classical pathways generally oppose the actions of the classical pathway [19], offering a mechanism to reverse the detriments of the Ang II-mediated effects.

Inappropriately elevated Ang II and over-activation of AT1 also contribute to the development of fatty liver [20]. Ang II-mediated activation of AT1 inhibits insulin signaling and may overload the liver partly by promoting *de novo* lipogenesis [21] and gluconeogenesis [22]. While chronic infusion of Ang II increased circulating insulin, it also increased TAG, NEFA, and liver TAG synthesis in rats [23, 24]. These characteristics derived from Ang II signaling are known to promote the development and progression of NAFLD [25] and MetS [10]. Angiotensin receptor blockers (ARBs) are used primarily to treat hypertension by blocking Ang II signaling [26, 27]. While ARBs are used to ameliorate hypertension, multiple studies have demonstrated improvements in substrate metabolism after chronic treatment, suggesting that over-activation of AT1 may impair substrate metabolism. Chronic blockade of AT1 can improvement insulin resistance [28], circulating components of the lipid profile [29], and hepatic steatosis [30] as well as increasing plasma Ang 1-7 [31]. Increased circulating Ang 1-7 decreased plasma TAG, total cholesterol, glucose, and insulin [32], as well as liver gluconeogenesis [33]. Ang 1-7 also increased glucose uptake in hepatocytes [34] and decreased adipose lipogenesis in rats with increased circulating Ang 1-7 [35]. Collectively, these findings highlight the connection between AT1 blockade and the activation of the non-classical pathways of RAS.

A key problem of NAFLD in humans is overnutrition [36]. In healthy livers, a carbohydrate rich diet contributes to approximately 5% of NEFA production, while in NAFLD patients this can increase to around 30% [37]. Low carbohydrate diets are beneficial, reducing body mass and intrahepatic TAG [38], and may ameliorate NAFLD [39, 40], while a high carbohydrate diet can induce NASH [41]. To better understand the impact of nutrient overload, studies have used acute oral delivery of nutrients (e.g.,

cholesterol, fructose, glucose, saturated fatty acids, etc.) [42, 43]. However, these efforts have addressed primarily superficial effects on metabolism, as many of these studies focus mainly on the measure of substrates. Furthermore, studies using these nutrient loads to analyze the impact on different cellular mechanisms [44, 45] are scarce in the investigation of NAFLD and MetS. Therefore, exposing the system acutely to high concentrations of nutrients (e.g., via a glucose challenge) may provide insight into the mechanisms derived from glucose (glucotoxicity) and lipids (lipotoxicity) that promote hepatic injury [46].

Although amelioration of the lipid profile and liver steatosis is reported with AT1 blockade [29, 30, 47, 48], the mechanisms promoting hepatic steatosis, and the effect that AT1 blockade may exert on them are not yet completely elucidated. This dissertation provides novel data on the effects of AT1 blockade in ameliorating lipid and glucose metabolism in the liver of insulin-resistant rats. It provides insight into hepatic TAG regulation in the liver of advanced stage-NAFLD and its amelioration through AT1 blockade, while also tackling into the prevention of NAFLD by describing changes in glucose and lipid metabolism, as well as redox biology, in an early stage of NAFLD. These data provide better understanding of the mechanisms that promote the development and progression of NAFLD during insulin-resistant conditions.

Chapter I
AT1 Blockade Reduces Hepatic Steatosis

Introduction

Non-alcoholic fatty liver disease (NAFLD) afflicts 25% of the world's population and is projected to increase due to the increasing prevalence of diabetes and obesity [49, 50]. While the renin-angiotensin system (RAS) is known for regulating cardiovascular function and renal hemodynamics, there is a relationship between obesity, and insulin resistance, and the activation of the RAS [51, 52]. Angiotensin II (Ang II) is the main mediator of the physiological actions of the RAS [16], and it is regarded as a risk factor for NAFLD [53]. Tangentially, the metabolic syndrome (MetS) is a cluster of disorders [12] (i.e., abdominal obesity, elevated circulating triacylglycerol (TAG), reduced HDL cholesterol levels, hypertension, and increased fasting glucose) that raise the risk of NAFLD [11].

Elevated Ang II and over-activation of its target receptor (AT1) contribute to impaired hepatic lipid metabolism [21], hepatic steatosis [20], and insulin resistance [17, 54]. Chronic infusion of Ang II increased circulating insulin, TAG, NEFA, and liver TAG synthesis in rats [23, 29], factors that ultimately contribute to the development of NAFLD [25]. Accordingly, obesity and insulin resistance contribute to the development of MetS [11], and while NAFLD is strongly associated with metabolic syndrome (MetS) [10, 11], because of the shared characteristics that promote their development, it is not yet clear which one precedes the other. AT1 receptor blockers were developed to decrease hypertension. AT1 blockers prevent Ang II from binding its receptor, inhibiting its signaling [26]. While these AT1 blockers have been used to decrease hypertension with great success, studies demonstrate improvements in substrate metabolism. Studies using AT1 blockade report improved insulin resistance [28], circulating components of the lipid profile [29], and hepatic steatosis [30], yet the mechanisms leading to this changes have not been fully described.

The sequestration of hepatic NEFA is mainly dependent on membrane fatty acid transporters, which include the fatty acid transport protein (FATP) family [55], cluster of differentiation 36 (CD36) [56], and caveolins [57]. In the liver, FATP5 and FATP2 are the most abundantly expressed of the 6 members of the FATP family, while hepatic expression of CD36 is typically low but increases with fatty liver [58, 59]. Knockdown [60] and knockout (KO) [61] of FATPs ameliorate hepatic steatosis. These studies also demonstrated a positive correlation between FATP levels and NEFA uptake in the liver [60, 61]. Accordingly, CD36 KO reduced NEFA uptake and utilization [62], while CD36 expression was increased by Ang II infusion [63]. Investigating these transporters may be

beneficial to elucidating the mechanisms behind the reduction of hepatis steatosis obtained after AT1 blockade [64, 65].

Increased TAG synthesis may lead to increased hepatic steatosis [66], which promotes the progression of NAFLD [67]. Glycerol-3-phosphate acyltransferase (GPAT) is one rate-limiting enzyme catalyzing the first step of TAG synthesis [68], while diacylglycerol O-acyltransferase (DGAT) catalyzes the last step of TAG formation [69]. These enzymes are key to produce TAG, GPAT expression is increased in the livers of NAFLD patients [70] and DGAT deficiency decreased TAG synthesis [71]. This suggest that changes in GPAT and DGAT may dictate the rate of TAG synthesis, while partially contributing to TAG accumulation by the increased production [66]. Tangentially, TAG can be shuttled out of the liver as VLDL [72]. Each VLDL particle contains one molecule of ApoB [73], suggesting that ApoB abundance may reflect the VLDL being produced in the liver, as TAG availability primarily determines the rate of VLDL synthesis [74]. This suggests that ApoB may serve as an alternate route to partially decrease intrahepatic TAG.

Though AT1 blockade is widely used to treat MetS-related hypertension and numerous beneficial effects in ameliorating lipid metabolism are reported [29, 30, 47, 48], the mechanisms promoting hepatic steatosis during MetS, and the effect that AT1 blockade may exert on them, are not completely understood. In this study, the static and dynamic (i.e., during a glucose challenge) responses to a glucose challenge are investigated, focusing on hepatic lipid accumulation and proteins mediating NEFA uptake, TAG and VLDL cholesterol synthesis, and fatty acid oxidation in rats with MetS, as well, the potential legacy-effect left after AT1 blockade removal is investigated.

Methods

All experimental procedures were reviewed and approved by the institutional animal care and use committees of the Kagawa Medical University (Japan) and the University of California, Merced (USA). Phenotypical data (i.e., body mass, oral glucose tolerance test curves, insulin levels, and blood pressure) has been previously published [44] with that study focused on redox signaling in the heart in response to a glucose challenge. The current study is unique, and it complements the previous one by extending the examination of the dynamic changes in hepatic lipid metabolism in response to a glucose challenge, which represents a nutrient overload that may appear in Western diets [75, 76]. We have included previously published body mass and plasma angiotensin II levels (78) (**Table 1**) to better illustrate our model and the efficacy of the AT1 blockade. As well, we have included data already published in this chapter [77]. Finally, we address treatment non-compliance and potential long-lasting effect after the initial treatment has stopped (legacy effect) [78]. Low compliance has proven to be a challenge when treating patients

Table 1. Mean (± SD) end of study body mass and plasma angiotensin II.

	LETO	OLETF	ARB	MINUS
Body Mass (g)	465 ± 29	610 ± 31*	598 ± 36*	602 ± 28*
Plasma AngII (fmol/ml)	58.9 ± 3.1	68.6 ± 11.6	211.3 ± 27.9*,^	65.2 ± 10.2+

*Significant difference from LETO ($P < 0.05$). ^ Significant difference from OLETF ($P < 0.05$). + Significant difference from ARB ($P < 0.05$).

with hypertension, dyslipidemia and diabetes [79, 80] and assessing treatment-legacy effect may provide a better understanding of the aftereffects of pharmacological AT1 blockade [81, 82].

In this study, we approach the obtained results from two perspectives: **(1)** the static outcomes following the chronic AT1 blockade and its removal (potential legacy effect) and **(2)** the dynamic response to a glucose challenge in our rat MetS model (OLETF), when it is treated to block AT1 (ARB), and during non-compliance (ARB/AT1 blockade-removal group, MINUS) with the angiotensin receptor blocker. In all cases, comparisons are made using the lean, strain-control (LETO) as a baseline.

Animals

OLETF rats are reported to develop insulin resistance and hyperglycemia by 17 weeks of age [83, 84]. For that reason, male, age matched, 17-week-old, lean strain-control Long Evans Tokushima Otsuka (LETO; 428 ± 8 g) and obese Otsuka Long Evans Tokushima Fatty (OLETF; 536 ± 6 g) rats (Japan SLC Inc., Hamamatsu, Japan) were used. Rats were assigned to the following groups (n=5–7 animals/group/time point): **(1)** untreated LETO, **(2)** untreated OLETF, **(3)** OLETF + angiotensin receptor blocker (ARB; 10 mg olmesartan/kg/d × 8 weeks) [85], and **(4)** OLETF ± ARB (MINUS; 10 mg olmesartan/kg/d × 4 weeks, then removed until dissection). ARB (Daiichi-Sankyo, Tokyo, Japan) was administered by oral gavage suspended in carboxymethyl cellulose (CMC) to conscious rats and untreated rats were gavaged with CMC only. Animals were maintained in groups of two to three animals per cage, given access to water and standard laboratory chow (MF; Oriental Yeast Corp., Tokyo, Japan), and maintained under controlled temperatures (23 - 24 °C) and humidity (~55%) with a light-dark cycle of 12-12 h.

For dissections, all animals were fasted for 12 h ± 15 min. To investigate the dynamic response to a glucose challenge, animals were dissected at baseline (T0, fasting) and after 3 (T3) and 6 h (T6) after a glucose load by gavage (2 g glucose/kg mass). Initiation of the overnight fasts and the glucose gavages were staggered to meet the exact dissections timepoints. Animals were decapitated and trunk blood collected in vials containing EDTA (Sigma-Aldrich, EDS) and proteinase inhibitor cocktail (Sigma-Aldrich, P2714). Livers were snap frozen in liquid nitrogen and kept at −80 °C until analyzed.

Biochemical Analyses & marker of hepatic NAFLD

Insulin, glucose, plasma total cholesterol (TC), TAG, and NEFA concentrations, as well as Collagen Type IV (COL-4), were measured using the commercially available reagents Insulin Rat ELISA Kit (Thermo Fisher Scientific, ERINS), Autokit glucose (Fujifilm

Wako Diagnostics, 997-03001), Total Cholesterol E (Fujifilm Wako Diagnostics, 999-02601), L-Type Triglyceride M (Fujifilm Wako Diagnostics, 994-02891 and 990-02991), HR Series NEFA-HR (2) (Fujifilm Wako Diagnostics, 999-34691, 995-34791, 991-34891, and 993-35191), and CIV ELISA (MyBioSource, MBS732756), respectively, following manufacturer's instructions. All samples were analyzed in duplicate and only accepting values that fell within percent coefficients of variability of less than 10% for all measurements.

Western blot analyses

A 25 mg piece of frozen liver was homogenized in phosphate buffer for a two-step extraction of cytoplasm and plasma membrane proteins. Briefly, phosphate buffer (50 mM Potassium Phosphates) (Fisher Scientific, P290 and P285) was used to homogenize the liver, then centrifuged at 15,000 x g to recover the supernatant containing the cytoplasmic fraction. Then, 50 mM potassium phosphate buffer + 1% Triton X-100 (Millipore-Sigma, T8787) was used to homogenize the pellet, which contained the plasma membrane fraction. The pellet homogenate was centrifuged at 15,000 x g, and the plasma membrane contents recovered from the supernatant. The buffers contained 3% protease inhibitor cocktail (Sigma-Aldrich, P2714) to help prevent protein degradation. The protein content of the fractions was quantified using the Bradford assay (Bio-Rad Laboratories, 5000203). Total protein (5-10 μg) was resolved in 10% Tris-HCL SDS gels. Proteins were electroblotted onto 0.45-μm polyvinyl difluoride (PVDF) (Millipore-Sigma, IPVH00010) membranes by semi-wet transfer using the Mini Gel Tank and Blot Module Set (Invitrogen, NW2000). Intercept blocking buffer (Li-Cor, 927-60001, 927-70001) was used to block the membranes then incubated 16 h with the corresponding primary antibody (diluted 1:1,000-1:2,000) against glycerol-3-phosphate acyltransferase 1 (GPAM) (abcam, ab69990), FATP5 (Invitrogen, PA5-42028), diacylglycerol O-acyltransferase 1 (DGAT1) (Thermo Fisher, PA5-79150), ApoB (Thermo Fisher, PA5-86950), CD36 (Thermo Fisher, PA1-16813), FATP2 (Thermo Fisher, PA5-30420), CPT1 (Proteintech, 15184-1-AP), Acox1 (Thermo Fisher, PA5-76341), and beta actin (Cell Signaling Technology, 3700S) (diluted 1:5,000). Membranes were washed, incubated with IRDye 800CW anti-rabbit (Li-Cor, 926-32213) and/or 680RD donkey anti-mouse IgG secondary antibodies (Li-Cor, 926-68072) (diluted 1:20,000), and rewashed. Blots were visualized using the Odyssey system (Li-Cor) and quantified using the Image Studio Lite ver. 5.2 (Li-Cor) using beta actin as a loading control. Plasma membrane and cytosolic fractions were tested for purity against Na^+/K^+ ATPase antibody (Abcam, ab76020) (diluted 1:40,000) and alpha tubulin (Abcam, ab52866) (diluted 1:40,000), respectively.

Statistics

Data was tested for normality using the Shapiro-Wilk test [86]. Means (±SD) were compared by ANOVAs. Means were considered significantly different at $p < 0.05$ using the Tukey test. Two-way-ANOVAs were used when analyzing datasets with all timepoints (T0, T1, T2) and groups, and one-way-ANOVA testing for multiple comparisons using the Tukey test, when analyzing datasets without timepoints (T0 only or group AUC). Correlations were calculated using the Pearson r coefficient [87, 88] to better assess changes over time. Area under the curve (AUC) analyses were calculated using the area under the concentration curve in batch designs [89] .Outliers were calculated and removed using the ROUT test [90] and one outlier was replaced with the mean of the corresponding group [91]. All statistical analyses were performed with GraphPad Prism 8.4.3 software (GraphPad Prism, La Joya, CA).

Results

To better recognize the difference between static (i.e., chronic AT1 blockade, reflected by differences at T0) and dynamic (i.e., during the acute glucose load) responses, the results were separated into two sections contained within each subheading, designated respectively to the response.

AT1 blockade improved the glucose:insulin ratio during the glucose challenge

Previous studies have shown that ARBs decrease plasma glucose [92, 93] and report improvements in insulin resistance [94], yet other studies report no changes [95, 96]. Therefore, to better address the existing discrepancies in the literature, we measured plasma glucose and insulin statically over time and dynamically in response to the glucose load.

Static Changes: Basal circulating glucose levels were 34%, 30%, and 46% greater in OLETF, ARB, and MINUS, respectively, than LETO (**Fig. 1A**). While levels in MINUS were 22% and 29% greater than OLETF and ARB, respectively (**Fig. 1A**). Basal plasma insulin was 80% and 73% greater in OLETF and MINUS, respectively, compared to LETO (**Fig. 1C**). The basal glucose-to-insulin ratios were not different among the groups (**Fig. 1E**).

Dynamic Changes: During the acute glucose challenge, circulating glucose levels were 40% and 30% greater in OLETF, 36% and 37% greater in ARB, and 31% and 55% greater in MINUS, when compared to LETO at T3 and T6, respectively (**Fig. 1A**). Levels in MINUS at T6 were 18% and 12% greater than OLETF and ARB, respectively (**Fig. 1A**). Mean glucose AUC was 38%, 38%, and 48% greater in OLETF, ARB and MINUS,

respectively, when compared to LETO, whereas mean AUC in MINUS was 8% greater than OLETF and ARB (**Fig. 1B**).

At T3, plasma insulin levels were 183% greater in OLETF compared to LETO, and 89% and 74% lesser in ARB and MINUS, respectively, compared to OLETF (**Fig. 1C**). At T6, levels were 75% and 145% greater in OLETF and MINUS, respectively, when compared to LETO (**Fig. 1C**). Plasma insulin levels were 30% and 50% lesser in ARB compared to OLETF and MINUS, respectively (**Fig. 1C**). Mean insulin AUC was 140%, 52%, and 99% greater in OLETF, ARB, and MINUS, respectively, when compared to LETO (**Fig. 1D**). Mean AUCs were 37% and 17% lesser in ARB and MINUS, respectively, compared to OLETF, whereas MINUS AUC was 31% greater compared to ARB (**Fig. 1D**).

At T3, the glucose-to-insulin ratio was 50% lesser in OLETF compared to LETO, while ratios in ARB and MINUS were 45% and 37% greater than OLETF (**Fig. 1E**). At T6, ratios in OLETF and MINUS were 43% and 53% lesser than LETO, while the ARB ratio was 39% greater than OLETF. The ratio on MINUS remained 49% lesser than ARB (**Fig. 1E**). Mean glucose-to-insulin ratio AUC was 38%, 9%, and 15% lesser in OLETF, ARB, and LETO, respectively, compared to LETO (**Fig. 1F**). Mean ratios in ARB and MINUS were 32% and 15% greater, respectively, compared to OLETF, while ratio on MINUS remained 25% lesser compared to ARB (**Fig. 1F**).

Contrasting with other studies [92, 93], ARB did not change the glucose levels, yet it lowered insulin levels during the glucose challenge and ameliorated the glucose-to-insulin ratio as seen previously [94, 95].

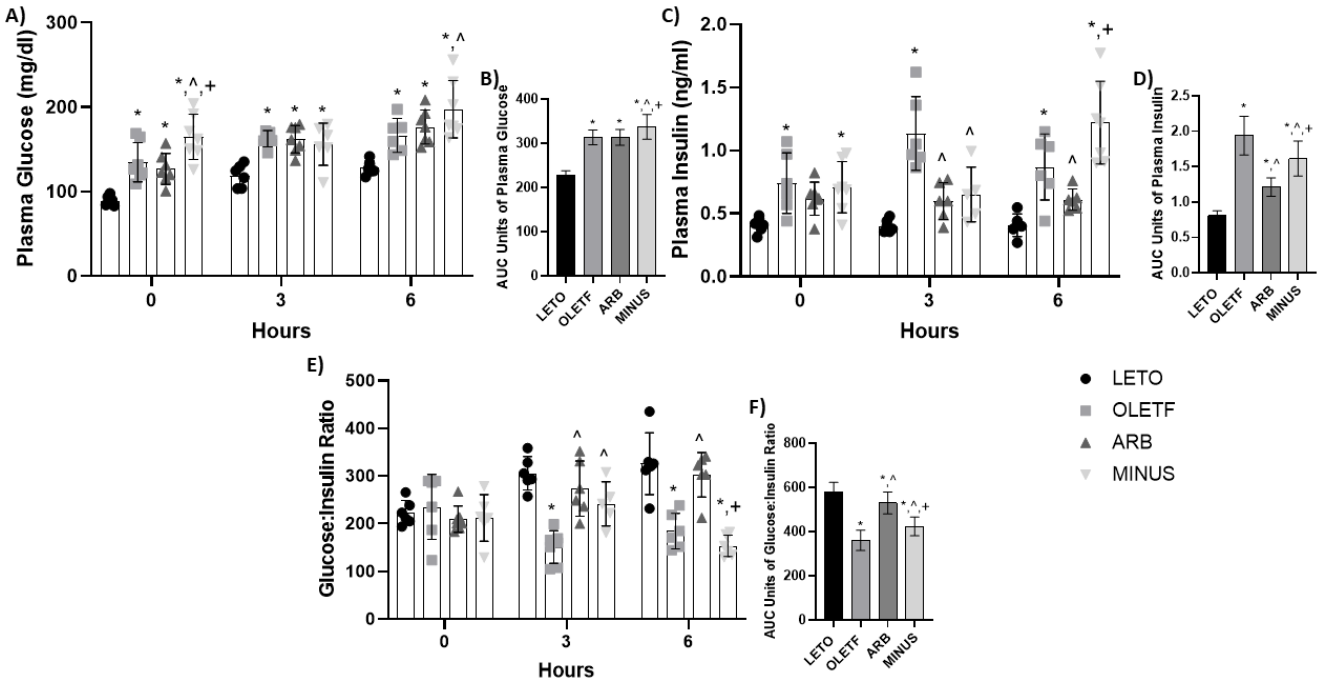

Figure 1. Plasma glucose and insulin levels. Mean ± SD values of plasma glucose (A), AUC of plasma glucose (B), plasma insulin (C), AUC of plasma insulin (D), glucose:insulin ratio (E), and AUC of glucose:insulin ratio (F), during the glucose challenge in Long Evans Tokushima Otsuka (LETO; n=6), Otsuka Long Evans Tokushima Fatty (OLETF; n=7), OLETF + ARB (ARB; ARB x 8 weeks; n=7), and OLETF ± ARB (MINUS, ARB x 4 weeks, then removed x 4 weeks; n=7) rats. * *Significant difference from LETO (P < 0.05).* ^ *Significant difference from OLETF (P < 0.05).* + *Significant difference from ARB (P < 0.05).*

AT1 blockade had no effect on circulating TAG or TC levels

COL-4 has been shown to accurately detect NAFLD with levels representing the degree of severity [97, 98].

Static Changes: COL-4 levels were 178% and 157% greater in OLETF and MINUS, respectively, compared to LETO (**Fig. 2A**). Levels were 155% lesser in ARB compared to OLETF (**Fig. 2A**). Levels in MINUS were intermediate between ARB and OLETF with levels 135% greater than ARB (**Fig. 2A**). These results suggest that liver fibrosis is decreased with ARB, while the removal of the treatment led to an intermediary phenotype associated with loss of most of the ARB benefits.

While it is known that ARB treatment improves circulating NEFA, TAG, and TC [29, 47, 48], these variables were measured here to better interpret the changes as they relate to the changes in the proteins associated with their metabolism and to ascertain the effects of the glucose challenge on lipid metabolism. *Static Changes*: Basal plasma NEFA was 38% and 50% greater in ARB and MINUS, respectively, compared to LETO (**Fig. 2B**). Plasma TAG was 174%, 110%, and 194% greater in OLETF, ARB and

MINUS, respectively, compared to LETO, while MINUS remained 40% greater than ARB (**Fig. 2D**). Plasma TC was 47%, 47%, and 73% greater in OLETF, ARB, and MINUS, respectively, compared to LETO (**Fig. 2F**).

Dynamic Changes: During the glucose challenge, plasma NEFA in MINUS was 43% and 30% greater than LETO and OLETF at T3, respectively (**Fig. 2B**). At T6, levels in OLETF, ARB and MINUS were 76%, 79%, and 93% greater, respectively, compared to LETO (**Fig. 2B**). Mean plasma NEFA AUC was 17%, 42%, and 64% greater in OLETF, ARB and MINUS, respectively, compared to LETO (**Fig. 2C**). Mean AUC in ARB and MINUS was 17% and 29%, respectively, greater than OLETF, while MINUS remained 14% greater than ARB (**Fig. 2C**).

At T3, plasma TAG levels in OLETF, ARB, and MINUS remained 275%, 227%, and 320% greater, respectively, than LETO (**Fig. 2D**). At T6, levels in OLETF, ARB, and MINUS were 162%, 211%, and 302% greater, respectively, than LETO. While MINUS remained 53% and 29% greater compared to the OLETF and ARB groups, respectively (**Fig. 2D**). Mean plasma TAG AUC was 222%, 195%, and 285% greater in OLETF, ARB, and MINUS, respectively, compared to LETO, while MINUS remained 20% and 30% greater than ARB and OLETF, respectively (**Fig. 2E**).

At T3, plasma TC levels were 23% and 98% greater in MINUS than LETO and OLETF, respectively (**Fig. 2F**). At T6, levels were 30%, 22%, and 38% greater in OLETF, ARB, and MINUS, respectively, compared to LETO, while MINUS remained 13% greater than ARB (**Fig. 2F**). Mean plasma TC AUC was 21%, 22%, and 39% greater in OLETF, ARB, and MINUS, respectively, compared to LETO, and MINUS remained 15% and 14% greater than OLETF and ARB, respectively (**Fig. 2G**).

ARB plasma NEFA AUC was greater than OLETF, while plasma TAG AUC remained unchanged. On the other hand, MINUS AUCs were all greater than ARB, which demonstrates the detrimental effect of treatment removal. AT1 activation triggers mechanisms that induce insulin resistance and hypertension [81], the progression insulin resistance in these animals is exponential during the its youth [83]. In our study, we treated our rats during its early stages of MetS (17 weeks of age) and the more developed stage (21 weeks of age), when the rat presents pronounced hepatic steatosis [83, 99]. During the initial phase of AT1 blockade (4 weeks of treatment), the measured parameters may be ameliorated. Though when the treatment is removed, the impact of Ang II signaling may worsen, acting stronger, which may be explained as a drug-derived re-bound effect [100].

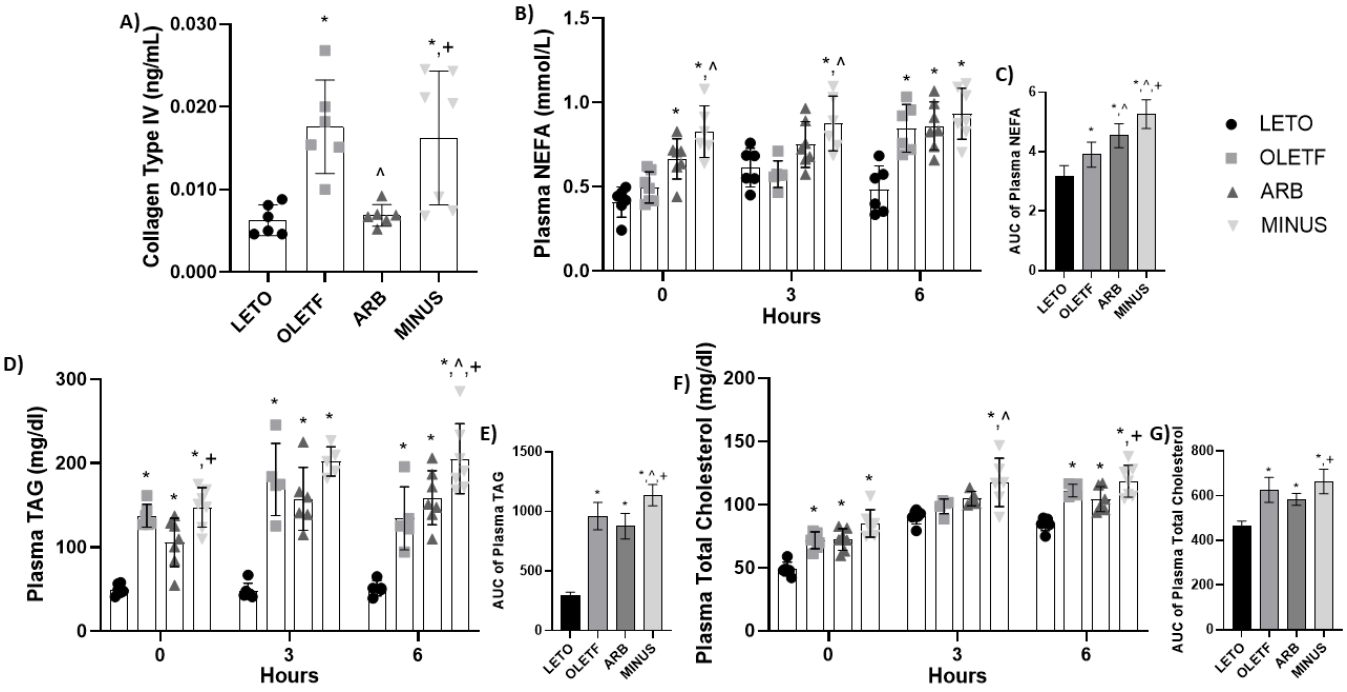

Figure 2. Plasma lipid profile levels. Mean ± SD values of COL-4 (A) plasma NEFA (B), AUC of plasma NEFA (C), plasma TAG (D), AUC of plasma TAG (E), plasma total (F) and AUC (G) of total cholesterol, during the glucose challenge in Long Evans Tokushima Otsuka (LETO; n=6), Otsuka Long Evans Tokushima Fatty (OLETF; n=7), OLETF + ARB (ARB; ARB x 8 weeks; n=7), and OLETF ± ARB (MINUS, ARB x 4 weeks, then removed x 4 weeks; n=7) rats. *Number at bottom of the bar number indicates n per group. * Significant difference from LETO (P < 0.05). ^ Significant difference from OLETF (P < 0.05). + Significant difference from ARB (P < 0.05).*

AT1 blockade protected against the glucose-induced accumulation of hepatic TAG

We measured part of the hepatic lipid profile to confirm this effect and further investigate it during a glucose challenge.

Static Changes: Basal liver NEFA was 47% greater in OLETF than LETO, while ARB was 39% lesser than OLETF (**Fig. 3A**). Liver TAG was 1880%, 787%, and 670% greater in OLETF, ARB, and MINUS, respectively, compared to LETO, while levels in ARB and MINUS remained 55% and 61% lesser than OLETF (**Fig. 3C**). Liver TC was 58% and 64% greater in OLETF and ARB, respectively, compared to LETO (**Fig. 3E**).

Dynamic Changes: During the glucose challenge, liver NEFA levels in ARB and MINUS were 53% and 81% greater than LETO at T3, respectively, while MINUS remained 33% greater than OLETF (**Fig. 3A**). Mean liver NEFA AUC was 40%, 38%, and 62% greater in OLETF, ARB, and MINUS, respectively, compared to LETO, while MINUS remained 15% and 17% greater than OLETF and ARB, respectively (**Fig. 3B**).

At T3, liver TAG levels were 4790% and 2760% greater in OLETF and MINUS, respectively, compared to LETO, and remained 41% lesser in MINUS compared to OLETF, and 138% greater than ARB (**Fig. 3C**). At T6, levels were 2600% and 1040% greater in OLETF and MINUS, respectively, compared to LETO, while ARB levels were 72% lesser than OLETF, and MINUS levels were 70% greater than ARB (**Fig. 3C**). Mean liver TAG AUC was 3260%, 900%, and 1935% greater in OLETF, ARB, and MINUS, respectively, compared to LETO. ARB and MINUS mean liver TAG remained 40% and 70% lesser, respectively, than OLETF, while MINUS remained 50% greater than ARB (**Fig. 3D**).

At T3, liver TC levels were 195%, 74%, and 90% greater in OLETF, ARB and MINUS, respectively, compared to LETO, while ARB and MINUS remained 41% and 36% lesser than OLETF, respectively (**Fig. 3E**). At T6, levels were 159%, 76%, and 143% greater in OLETF, ARB, and MINUS, respectively, compared to LETO. ARB remained 32% lesser than OLETF and MINUS remained 28% greater than ARB (**Fig. 3E**). Mean liver TC AUC was 145%, 71%, and 89% greater in OLETF, ARB, and MINUS, respectively, compared to LETO, while ARB and MINUS remained 30% and 23% lesser than OLETF, respectively (**Fig. 3F**).

ARB improved hepatic NEFA and TAG levels and protected it from TC accumulation during the glucose challenge. Notably, the MINUS group showed ameliorated basal hepatic TAG accumulation; however, during the glucose challenge, TAG and NEFA increased, along with their respective AUC. We attributed this to the re-bound effect [100], as thoroughly discussed above, here MINUS demonstrates more detrimental effects following non-compliance.

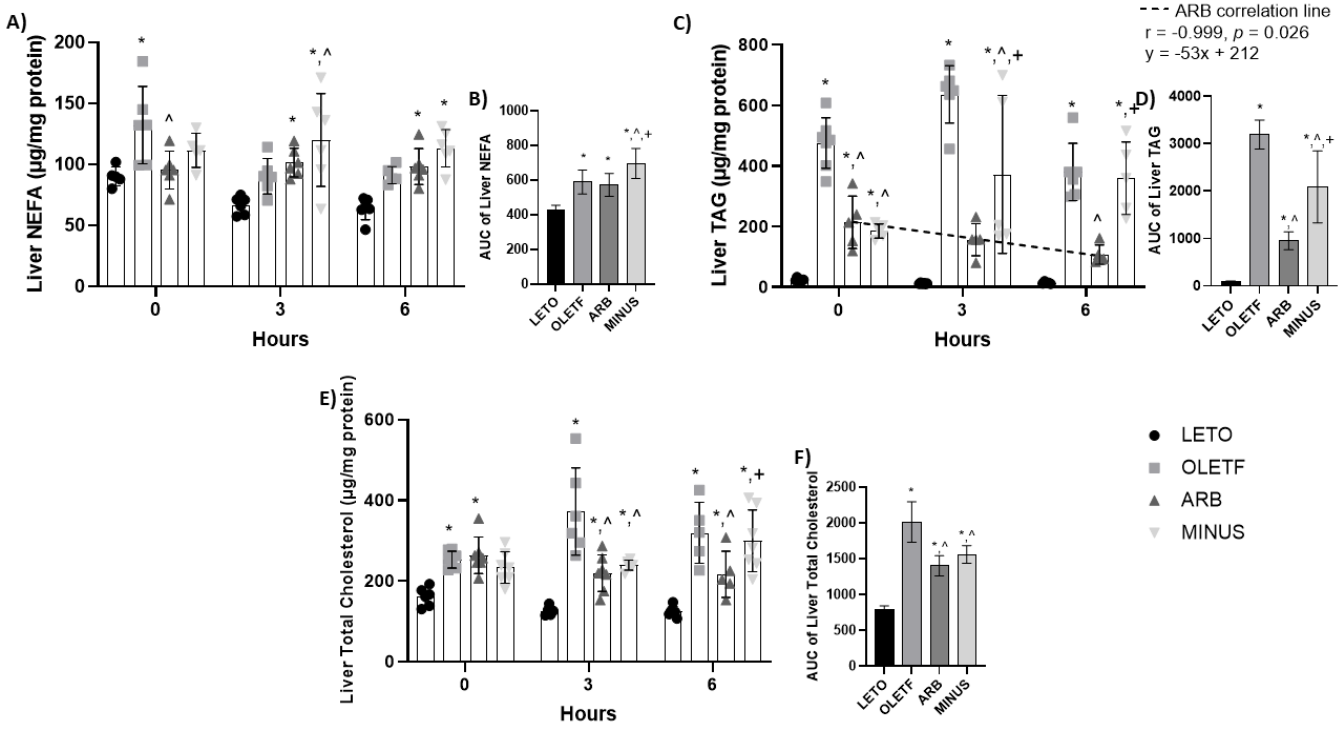

Figure 3. Liver lipid profile levels. Mean ± SD values of liver NEFA (A), AUC of NEFA (B), TAG (C), AUC of TAG (D), total cholesterol (E), and AUC of total cholesterol (F), during the glucose challenge in Long Evans Tokushima Otsuka (LETO; n=6), Otsuka Long Evans Tokushima Fatty (OLETF; n=6), OLETF + ARB (ARB; ARB x 8 weeks; n=6), and OLETF ± ARB (MINUS, ARB x 4 weeks, then removed x 4 weeks; n=6) rats. *Number at bottom of the bar number indicates n per group. * Significant difference from LETO (P < 0.05). ^ Significant difference from OLETF (P < 0.05). + Significant difference from ARB (P < 0.05).*

AT1 blockade decreased basal the abundance of CD36, and β-oxidation proteins in the liver following the glucose challenge

Because the liver-specific deletion of AT1 reduces hepatic steatosis [101], we wanted to assess the potential for decreased sequestration of NEFA as a contributing factor. Therefore, we measured the protein abundance of CD36, FATP5, and FATP2, which are the main liver NEFA transporters [55, 102, 103].

Static Changes: Basal CD36 protein abundance was 79%, 53%, and 74% greater in OLETF, ARB and MINUS, respectively, compared to LETO and remained 28% and 20% lower in ARB and MINUS, respectively, compared to OLETF (**Fig. 4A**). CD36 abundance and basal levels of fasting plasma insulin were significantly and positively correlated (r = 0.9836, p = 0.008) (**Fig. 4D**). FATP5 protein abundance was 52%, 62%, and 50% greater in MINUS than LETO, OLETF, and ARB, respectively (**Fig. 4B**). FATP2 protein abundance was 46% and 35% greater in MINUS compared to OLETF and ARB, respectively (**Fig. 4C**).

Dynamic Changes: During the glucose challenge, CD36 protein abundance was 70%, 75%, and 73% greater in OLETF, ARB, and MINUS, respectively, compared to LETO at T3 (**Fig. 4A**). At T6, protein abundance was 80%, 75%, and 73% greater in OLETF, ARB, and MINUS, respectively, compared to LETO (**Fig. 4A**). While ARB was 25% greater than OLETF and 28% lesser than MINUS (**Fig. 4A**).

At T3, FATP5 protein abundance was 34% and 44% greater in MINUS than LETO and ARB, respectively (**Fig. 4B**). At T6, protein abundance was 47%, 57%, and 79% greater in OLETF, ARB and MINUS than LETO, and remained 60% and 51% greater in MINUS than OLETF and ARB, respectively (**Fig. 4B**).

At T3, FATP2 protein abundance was 51%, 50%, and 43% lesser in OLETF, ARB, and MINUS, respectively, compared to LETO (**Fig. 4C**). At T6, protein abundance was 29% and 28% lesser in ARB than OLETF and LETO, respectively (**Fig. 4C**).

Collectively, the ARB-induced decrease in basal CD36 may partially explain the amelioration in hepatic lipid accumulation [104] while the greater abundance in FATP2 and FATP5 in the MINUS group may be responsible of the increased TAG accumulation [105].

On the other hand, Ang II signaling can increase hepatic lipids by decreasing fatty acid oxidation [21] and both Acox1 and CPT1 are essential mediators of lipid β-oxidation [57, 106]. We hypothesized that chronic blockade of AT1 increases β-oxidation.

Static Changes: No basal changes in Acox1 (**Fig. 4E**) or CPT1A (**Fig. 4F)** were detected among the groups suggesting that AT1 activation at this stage of MetS is not sufficient to profoundly impair oxidation.

Dynamic Changes: During the glucose challenge, Acox1 protein abundance was 46% and 44% greater in MINUS compared to LETO and OLETF, respectively (**Fig. 4D**). At T6, protein abundance was 39% and 38% greater in OLETF and ARB than LETO, respectively, and remained 34% and 33% lesser in MINUS than OLETF and ARB, respectively (**Fig. 4D**).

At T3, CPT1A protein abundance was 75%, 68%, and 81% greater in OLETF, ARB, and MINUS than LETO, respectively (**Fig. 4F**). At T6, protein abundance was 50%, 52%, and 81% lesser in OLETF, ARB, and MINUS than LETO, respectively, and remained 62% and 59% lesser in MINUS than ARB and MINUS, respectively (**Fig. 4F**). CPT1A abundance in MINUS tended to decrease ($r = 0.9944$, $p = 0.07$) in response to glucose over time.

The protein abundance for Acox1 and CPT1A in MINUS remained lower than OLETF and ARB at 6 h following the glucose challenge suggesting that the TAG accumulation in this group was partially attributed to a reduction in lipid oxidation. This

distinct behavior further demonstrates the detriment of non-compliance that is masked by analyzing static changes alone.

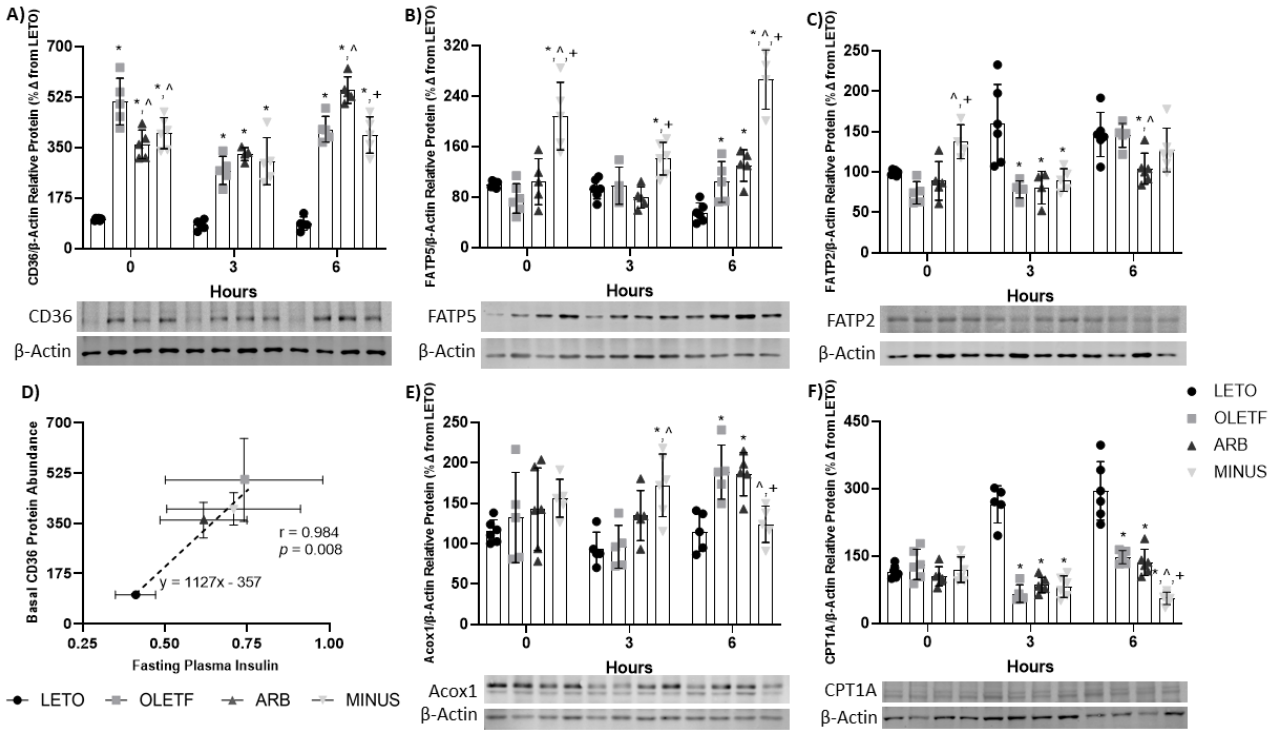

Figure 4. Abundance of membrane transporters and fatty acid oxidation proteins. Western blot results, mean ± SD values for relative liver membrane protein abundance of CD36 (A), FATP5 (B), FATP2 (C), Acox1 (D) and CPT1A (E), during the glucose challenge in Long Evans Tokushima Otsuka (LETO; n=6), Otsuka Long Evans Tokushima Fatty (OLETF; n=6), OLETF + ARB (ARB; ARB x 8 weeks; n=6), and OLETF ± ARB (MINUS, ARB x 4 weeks, then removed x 4 weeks; n=6) rats. *Number at bottom of the bar number indicates n per group. * Significant difference from LETO (P < 0.05). ^ Significant difference from OLETF (P < 0.05). + Significant difference from ARB (P < 0.05).*

AT1 blockade decreased basal ApoB abundance but not abundance of TAG synthesis proteins

Insulin can activate the liver-X-receptor, which promotes the transcription of genes of hepatic lipogenesis [107]. Previously, we demonstrated that ARB treatment decreased plasma insulin [108]. Therefore, we hypothesized that ARB treatment decreases TAG accumulation through suppression of TAG synthesis. The first committed step in TAG synthesis is catalyzed by glycerol-3-phosphate acyltransferase [68] while diglyceride acyltransferase (DGAT) mediates the last step of TAG synthesis [69].

Static Changes: In our study, basal GPAM protein abundance remained unchanged (**Fig. 5A**), and DGAT1 abundance was 15%, 10%, and 11% lesser in OLETF, ARB, and MINUS, respectively, compared to LETO (**Fig. 5B**).

Dynamic Changes: During the glucose challenge, no profound changes in GPAM were detected among groups or over time, except for a 40% decrease in MINUS at T6 when compared to ARB (**Fig. 5A**). In OLETF, GPAM abundance tended ($r = 0.9940$, $p = 0.07$) to increase in response to glucose over time. At T3, DGAT1 protein abundance was 14%, 11%, and 12% lesser in MINUS compared to LETO, OLETF and ARB, respectively, and at T6, was 11% lesser in ARB than LETO (**Fig. 5B**).

TAGs can be used to form VLDL with ApoB, which is secreted from the liver [72] and hepatic secretion of VLDL increases with insulin resistance [73]. Therefore, we measured ApoB to gain insight into hepatic VLDL formation and the effects of ARB on its production. *Static Changes*: Basal ApoB was 29% greater in OLETF compared to LETO, and 29% lesser in ARB than OLETF (**Fig. 5C**).

Dynamic Changes: During the glucose challenge, ApoB protein abundance was 39% and 43% greater in OLETF and ARB, respectively, than LETO, at T3 (**Fig. 5C**). At T6, ApoB protein abundance remained 46% and 45% greater in OLETF and ARB than LETO, respectively, and was 34% and 33% lesser in MINUS compared to OLETF and ARB, respectively (**Fig. 5C**). ApoB levels increased linearly ($r = 0.9985$, $p = 0.04$) over 6 h in ARB (**Fig. 5C**).

Hepatic sequestration of NEFA and chylomicron remnants is routed for oxidation or TAG esterification. TAG is also produced from excess glucose through *de novo* lipogenesis [21]. In our study, the abundance of TAG synthesis proteins remained unchanged with ARB treatment, while its removal caused their abundance to decrease during the glucose challenge. Elevated Ang II can alter VLDL secretion [21] and here we demonstrated that ARB treatment decreased ApoB protein abundance, a key protein for VLDL assembly [72] suggesting that less VLDL is present or being made in the liver. Furthermore, the linear increase in ApoB during the glucose challenge suggests that TAG is incorporated into VLDL to be secreted from the liver, preventing TAG accumulation.

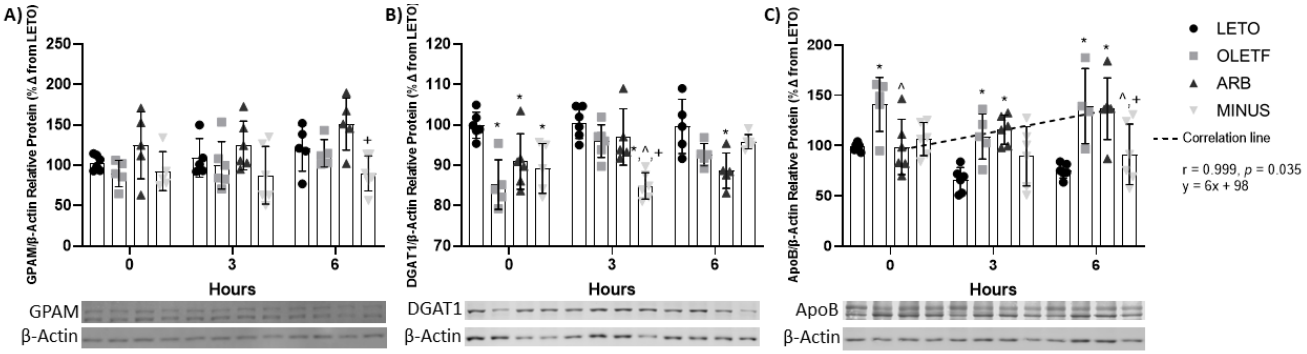

Figure 5. Abundance of TAG and VLDL synthesis proteins. Western blot results, mean ± SD values for relative protein abundance of GPAM (A), DGAT1 (B), and ApoB (C), including Pearson's correlation test of ApoB vs time, during the glucose challenge in Long Evans Tokushima Otsuka (LETO; n=6), Otsuka Long Evans Tokushima Fatty (OLETF; n=6), OLETF + ARB (ARB; ARB x 8 weeks; n=6), and OLETF ± ARB (MINUS, ARB x 4 weeks, then removed x 4 weeks; n=6) rats. *Number at bottom of the bar number indicates n per group. * Significant difference from LETO (P < 0.05). ^ Significant difference from OLETF (P < 0.05). + Significant difference from ARB (P < 0.05).*

Discussion

Hepatic TAG accumulation is the hallmark of NAFLD [11, 109], which affects 25% of the world's population [49]. NAFLD is strongly associated with metabolic syndrome (MetS) [10, 11], though it is not known if NAFLD is a cause or a consequence to MetS [110]. Increased Ang II signaling can cause obesity, insulin resistance, dyslipidemia, and hypertension [21], characteristics associated with NAFLD and MetS [10, 110]. Though the mechanisms promoting hepatic steatosis during MetS [58, 111], and in relation to Ang II signaling [16, 21], are not completely understood. In this study, the Ang II receptor (AT1) was blocked, as static and dynamic responses (i.e., to a glucose challenge) were investigated on liver steatosis and protein mediating NEFA uptake, TAG and VLDL cholesterol synthesis, and NEFA oxidation. With AT1 blockade, liver NEFA and TAG, as well as CD36 and ApoB abundance were decreased; while during the glucose challenge, liver TC and TAG were decreased (**Fig. 6**). Together, these results indicate that chronic AT1 blockade may improve liver steatosis by lowering liver TAG levels, while the decreased NEFA may be due to the decrease on CD36. Further, the increase on ApoB during the glucose challenge seen with AT1 blockade may partially contribute to the decrease on TAG, by promoting their export through VLDL.

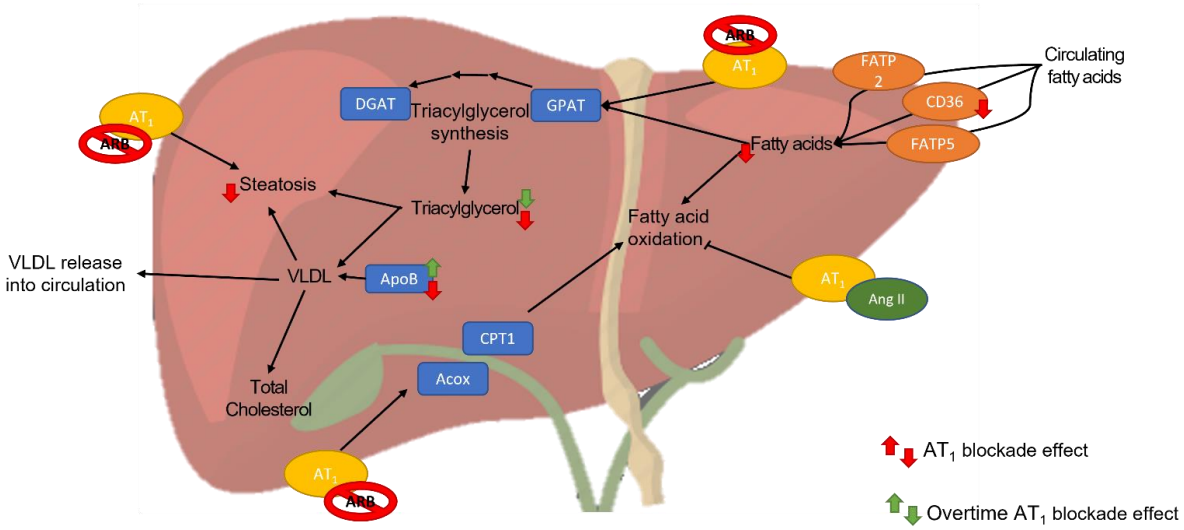

Figure 6. Summary of findings. In the liver of rats with AT1 blockade, basal TAG, NEFA, CD36 and ApoB were reduced. During the glucose challenge, TAG decreased and ApoB increased overtime. These results demonstrate that the chronic blockade of AT1 protects the liver from the inappropriate accumulation of TAG. This is associated with decreased CD36 abundance and an overtime increase of ApoB.

NAFLD patients often present hyperglycemia [112] and dyslipidemia [113]. Studies show that AT1 blockade ameliorates hyperglycemia by decreasing circulating glucose [92, 93] and improving insulin sensitivity [94], while other report no changes on either [95, 96]. Accordingly, the glucose:insulin ratio can be used to estimate insulin resistance [114], where lower values represent higher insulin resistance. In this study, AT1 blockade did not change plasma glucose levels, though it improved plasma insulin and the glucose:insulin ratio during the glucose challenge. Moreover, AT1 blockade also improves the lipid profile (i.e., circulating NEFA, TAG, and TC) [29, 47], yet the results are also contradictory [115, 116]. In this study, plasma TAG nor TC changed with AT1 blockade. Altogether, these data suggest that AT1 blockade with may ameliorate insulin resistance, as reflected by the improved glucose:insulin ratio, without improving circulating components of the lipid profile during this study conditions. On the other hand, the AT1 blockade removal decreased insulin sensitivity, as shown by the decreased glucose:insulin ratio, as well as having increased plasma NEFA and TAG, demonstrating the detrimental effects of treatment non-compliance. Finally, COL-4 is a non-invasive biomarker associated with the presence, and degree of severity, of NAFLD [97, 98]. AT1 blockade decreased the levels of COL-4, while after AT1 removal, the mean reversed to untreated OLETF levels. The results suggest that liver fibrosis may be decreased with AT1 blockade, while the removal of the blockade led to a split on the mean, that may be described by treatment ‘memory’ or complete loss of the benefit.

Prolonged hepatic steatosis accelerates the progression of NAFLD into its more severe stages [117]. Deletion of the AT1 receptor in mice [101] and AT1 blockade in Zucker fatty rats [29] decrease liver steatosis, which may delay the evolution of NAFLD. In this study, AT1 blockade decreased basal hepatic NEFA and TAG, as well as decreasing TAG and TC during the glucose challenge. This may be due to decreased basal CD36 abundance [118, 119], which may decrease the uptake of NEFA and potential TAG synthesis, more so than the FAPTs, as their abundance did not change with AT1 blockade. The suggestion that reduction of CD36 abundance decreases NEFA uptake may be substantiated by the correlation between reduced basal insulin and CD36 abundance, reflecting the improved responsiveness of the liver to insulin [104], as it decreased membrane CD36 presence and therefore the capacity to uptake NEFA. Reduced NEFA uptake may contribute to reduced hepatic NEFA levels more than increased NEFA oxidation, as AT1 blockade did not change the abundance of Acox1 or CPT1A. Furthermore, although no changes in GPAM or DGAT abundance were detected, TAG synthesis may have still been downregulated by decreasing the activity of these enzymes, more so than their abundance or stability, as insulin can regulate GPAM activity [68], while increased hepatic TAG levels can stimulate DGAT activity [120] in the liver. With AT1 blockade, both circulating insulin and liver TAG levels are decreased, which supports the suggestion that GPAM and DGAT activity may be downregulated, as insulin and increased liver TAG can regulate their activity. Moreover, AT1 blockade may improve hepatic steatosis by increasing VLDL export [72]. Each VLDL particle contains one molecule of ApoB [73], suggesting that ApoB abundance may reflect the VLDL being produced in the liver. Therefore, the linear increase in ApoB abundance throughout the glucose challenge suggest that with AT1 blockade, the available TAG may be mainly shuttled out of the liver as VLDL, preventing hepatic steatosis.

On the other hand, while basal liver TAG was decreased after AT1 removal, it increased during the glucose challenge, along with liver NEFA and TC. The increase on NEFA after AT1 blockade removal may be due to increased NEFA uptake from circulation, through the FAPT transporters [121], more so than CD36, as its abundance was reduced. The reduction on CD36 after AT1 blockade removal may be explained the decreased levels of circulating insulin, as they correlated among the different groups, where CD36 abundance and insulin levels were greater than with chronic AT1 blockade, yet lesser than untreated OLETF. Nonetheless, the liver NEFA AUC, FAPT5 and FATP2 abundance were increased after removal of the AT1 blockade, suggesting that increased NEFA uptake may be mediated mainly by FATP5 in these dysregulated conditions, following non-compliance. Interestingly, the increase on liver TAG following the glucose challenge may be due to increased TAG synthesis and reduced secretion of TAG via VLDL. This is suggested by the possible dysregulation due to a re-bound effect [100], caused by the removal of AT1 blockade, where the impact of Ang II signaling may

worsen, increasing NEFA uptake and TAG production, which may be through further stimulation of FATP membrane translocation, and DGAT activity [120], respectively, as it may be the case in OLETF, whose NEFA and TAG are increased. Accordingly, plasma NEFA, TAG and TC may be increased after removal of AT1 blockade due to the same argument around the re-bound effect [100], which suggests that treatment non-compliance may be more detrimental than the lack of treatment. Therefore, while most hepatic benefits of AT1 blockade were kept chronically, they were lost after AT1 blockade removal during a nutrient overload, stimulated by the glucose challenge, highlighting the detriments of treatment non-compliance [79, 122, 123]. This may be explained by lack of treatment 'memory' [78], and further substrate dysregulation [100], as reflected by increased parameters of the lipid profile, both circulating and in the liver.

Table 2. Results for ARB and MINUS groups compared to OLETF.

	AT_1 Blockade (ARB)			ARB removal (MINUS)		
Measurements	**0 h**	**3 h**	**6 h**	**0 h**	**3 h**	**6 h**
Substrates of hepatic lipid profile						
NEFA	v	-	-	-	^	-
TAG	v	v	v	v	v	-
Cholesterol	-	v	v	-	v	-
Proteins of fatty acid transport						
FATP5	-	-	-	^	^	^
FATP2	-	-	v	^	-	-
CD36	v	-	^	v	-	-
Proteins of fatty acid oxidation						
Acox1	-	-	-	-	^	v
CPT1A	-	-	-	-	-	v
Proteins of TAG synthesis						
GPAT1	-	-	-	-	-	-
DGAT1	-	-	-	-	v	-
Protein of TAG secretion						
ApoB	v	-	-	-	-	v

^ *increase; v decrease; - no difference*

In summary, these results demonstrate that AT1 blockade may protect the liver from TAG accumulation by modulating NEFA uptake and increasing TAG export via ApoB

(**Fig. 6**). While treatment non-compliance reverted many of the potential benefits observed with AT1 blockade, with the added detriment of altering the sensitivity of the cellular responses to a glucose load. This may leave the liver be more susceptible to further lipid accumulation over time, due to the dysregulation in lipid substrates.

Chapter II
Improved Hepatic Gluconeogenesis and Lipogenesis are Associated with Increased Plasma Angiotensin 1-7

Introduction

The renin-angiotensin system (RAS) is well known for its critical role in regulating cardiovascular function and renal hemodynamics. Angiotensin II (Ang II) is the peptide responsible for most physiological actions of RAS [16]. Inappropriately elevated Ang II and over-activation of its target receptor (AT1) contribute to the development of insulin resistance [17] and fatty liver [20]. Ang II-mediated activation of AT1 may overload the liver partly by promoting *de novo* lipogenesis [21] and gluconeogenesis (GNG) [22]. Chronic infusion of Ang II increased circulating insulin, triacylglycerol (TAG), NEFA, and liver TAG synthesis in rats [23, 24]. Increased circulating lipids and lipogenesis promote the development of non-alcoholic fatty liver disease (NAFLD), which is an umbrella term that encompasses the spectrum of liver lesions, ranging from simple TAG accumulation to cirrhosis [11]. NAFLD is strongly associated with metabolic syndrome (MetS) and its characteristics [10, 11]. MetS is a cluster of conditions (e.g., increased circulating TAG and glucose, waist circumference, and blood pressure) that increases the risk of severe cardiovascular and metabolic disease [12]. NAFLD afflicts 25% of the world's population [49], nonetheless, the hepatic mechanisms promoting NAFLD and MetS [58], and in connection to Ang II signaling [21], are not completely understood.

Angiotensin receptor blockers (ARB) displace Ang II from the angiotensin receptor [26], inhibiting Ang II signaling. While ARBs are widely used to ameliorate MetS-related hypertension [124], they also improve components of the lipid profile and hepatic lipid accumulation in animal studies [125, 126] and clinical trials [47, 116]; however, the mechanisms that promote these improvements are not fully understood. Angiotensin 1-7 (Ang 1-7) is another RAS peptide, which may counteract the adverse effects derived from Ang II signaling [127]. AT1 blockade in rats has shown increased plasma Ang 1-7 [31]. Increased circulating Ang 1-7 decreased plasma TAG, total cholesterol (TC), glucose, and insulin [32], as well as liver GNG and glycogenolysis [33]. Ang 1-7 also increased glucose uptake in hepatocytes [34] and decreased adipose lipogenesis in rats with increased circulating Ang 1-7 [35]; however, GNG was increased in hyperglycemic hepatocytes treated with ARB [128]. These contrasting data demonstrate that it is not clear if the increase in Ang 1-7, produced by AT1 blockade [31], has the same effects as direct (i.e. cell incubation with Ang 1-7) or transgenic (i.e. through a fusion protein) increase in Ang 1-7.

Hepatic NEFA uptake is increased with NAFLD [58], and cluster of differentiation 36 (CD36) and fatty acid transporter 5 (FATP5) are the main liver fatty

acid transporters [129]. Their deletion reduced hepatic NEFA, among other lipid species [61, 118]. Liver-specific deletion of the Ang II receptor (AT1) reduced hepatic steatosis [101]. CD36 expression was increased with Ang II infusion in mice [63], while mice lacking an Ang II precursor, angiotensinogen, showed decreased hepatic steatosis but no difference in FATP5 or CD36 expression [130]. NAFLD patients present increased *de novo* lipogenesis (DNL) [131], which increases liver NEFA. Acetyl-CoA carboxylase (ACC) and fatty acid synthetase (FASN) catalyze rate-limiting steps of DNL [132]. While Ang II can act as a lipogenic activator in adipose tissue [133], contrasting results exist regarding DNL and Ang II signaling. AT1 blockade reduced DNL in obese rats [134], while Ang II infusion did not change genes of DNL in rats [135]. On the other hand, NAFLD can be attenuated by increasing NEFA oxidation [136]. In the liver, carnitine palmitoyl transferase 1 (CPT1) and acyl-CoA oxidase 1 (Acox1), participate in mitochondrial and peroxisomal NEFA oxidation, respectively [137]. Ang II downregulated NEFA oxidation in rat cardiomyocytes [138], while ARB treatment increased genes of NEFA oxidation in the liver of rats [21], but had no effects in enzymes of NEFA oxidation in skeletal muscle of humans [139].

NAFLD is closely linked to hepatic insulin resistance [140]. Hyperinsulinemia may drive NAFLD through increased TAG synthesis [66], as TAG accumulation is the hallmark of NAFLD [58]. The rate-limiting enzyme in TAG synthesis is glycerol-3-phosphate acyltransferase (GPAT) [68], while the last step of TAG formation is catalyzed by diacylglycerol O-acyltransferase (DGAT) [69]. In the livers of patients with NAFLD, GPAT expression is elevated [70]. Accordingly, DGAT deficiency protected primary hepatocytes from lipid deposition by decreasing TAG synthesis [71]. AT1 blockade decreased liver TAG accumulation in Zucker fatty rats [29], while others report no change in liver TAG [141]. On the other hand, hepatic GNG can be stimulated during NAFLD [140]. Normally, insulin suppresses hepatic GNG [142], but in insulin resistant subjects, the gluconeogenic flux is increased [143], contributing to the hyperglycemia and dyslipidemia. Phosphoenolpyruvate carboxykinase 1 (PEPCK1) and glucose-6-phosphatase catalytic subunit 1 (G6PC1) mediate hepatic GNG [144]. PEPCK1 silencing improve postprandial glycemia and plasma TAG in mice [145], while patients with G6PC1 deficiency showed fasting-induced postprandial hypoglycemia [146]. Ang II infusion increased plasma glucose in both fasted and fed rats [22]. As aforementioned, AT1 blockade increased GNG in hyperglycemic hepatocytes [128], yet increased circulating Ang 1-7 decreased GNG [33].

Although advances in Ang II and Ang 1-7 signaling in relation to metabolic improvement exist, studies examining specific proteins of lipid metabolism and GNG may be of interest to fully elucidate the benefits of modulating RAS signaling. Here, we investigate the impact of AT1 blockade on circulating Ang 1-7 levels, and their associations to changes in hepatic lipogenesis and glucose regulation.

Methods

All experimental procedures were reviewed and approved by the institutional animal care and use committees of the Kagawa Medical University (Japan) and the University of California, Merced (USA). The work presented here complements our previous studies in the same animals, where we assessed the contribution of AT1 activation in relation to cardiac redox biology [108], and to renal function through regulation of inflammation and blood pressure [147]. Therefore, previously presented phenotypical data (i.e., body mass, blood pressure, plasma glucose, insulin, glucagon, TAG, and NEFA) will be included in **Table 1** of this manuscript, to demonstrate the efficacy of the AT1 blockade.

Table 1. Mean (± SD) of end-of study basal measurements.

	LETO	OLETF	ARB
Body mass (g)	366 ± 15	503 ± 9*	481 ± 4
Blood pressure (mmHg)	114 ± 3	142 ± 2*	120 ± 2^
Glucose (mg/dl)	106 ± 7	139 ± 8*	120 ± 6*,^
Insulin (ng/ml)	0.23 ± 0.03	1.52 ± 0.73*	1.53 ± 0.67*
Glucagon (pmol/L)	1.9 ± 0.8	3.3 ± 1.3*	3.3 ± 1.6*
TAG (mg/dl)	59 ± 22	116 ± 8*	88 ± 33
NEFA (mEq/L)	0.53 ± 0.3	0.65 ± 0.1	0.71 ± 0.1

* Significant difference from LETO ($P < 0.05$). ^ Significant difference from OLETF ($P < 0.05$).

Animals

Male, age matched, 10-week-old, lean strain-control Long Evans Tokushima Otsuka (LETO; 279 ± 7 g) and obese Otsuka Long Evans Tokushima Fatty (OLETF; 359 ± 3 g) rats (Japan SLC Inc., Hamamatsu, Japan) were used. NAFLD is not yet strongly present at this age in these rats [99], providing the opportunity of examining the animals during the development of more severe hepatic disease. Rats were assigned to the following groups (n=5–8 animals/group/time point): **(1)** untreated LETO (n=5), **(2)** untreated OLETF (n=8), **(3)** OLETF + angiotensin receptor blocker (ARB; 10 mg olmesartan/kg/d × 6 weeks; n=8). ARB (Daiichi-Sankyo, Tokyo, Japan) was administered by oral gavage suspended in carboxymethyl cellulose (CMC) to conscious rats and untreated rats were gavaged with CMC only. Animals were maintained in groups of two to three animals per cage, given access to water and standard laboratory chow (MF; Oriental Yeast Corp., Tokyo, Japan), and maintained under controlled temperatures (23 - 24 °C) and humidity (~55%) with a light-dark cycle of 12-12 h.

For dissections, all animals were randomly assigned to a corresponding subgroup. Animals were fasted for 12 h ± 15 min. To investigate the dynamic response to a glucose challenge (nutrient overload), animals were dissected at baseline (T0, fasting) and after 1 (T1) and 2 h (T2) after a glucose load by gavage (2 g glucose/kg mass). Staggered times were used to ascertain correct dissection timing at 1 and 2 h after glucose. Trunk blood

was collected after decapitation in vials containing EDTA (Sigma-Aldrich, EDS) and proteinase inhibitor cocktail (Sigma-Aldrich, P2714). Livers were snap frozen in liquid nitrogen and kept at −80 °C until analyzed.

Biochemical Analyses

Plasma glucose, NEFA, TAG, and TC were measured using commercial kits: Autokit Glucose (Fujifilm Wako Diagnostics, 997-03001), HR Series NEFA-HR (2) (Fujifilm Wako Diagnostics, 999-34691, 995-34791, 991-34891and 993-35191), Triglyceride Colorimetric Assay Kit (Cayman Chemicals, 10010303), and Cholesterol Fluorometric Assay Kit (Cayman Chemicals, 10007640), respectively. All procedures were carried out following the manufacturer's instructions. All samples were analyzed in duplicate and only accepting values that fell within percent coefficients of variability of less than 10% for all measurements.

Measurements of Ang 1-7 and MAS1

Plasma Ang 1-7 was measured through ELISA (Cloud-Clone Corp, CES085Mi), using 50 μL of EDTA plasma. MAS1 receptor was measured in the plasma membrane of the liver. We obtained the membrane protein extract as follows: A 25 mg piece of frozen liver was homogenized in phosphate buffer for extraction of both cytoplasm and plasma membrane protein fractions. Briefly, phosphate buffer (50 mM potassium phosphates) (Fisher Scientific, P290 and P285) was used to homogenize the liver, then centrifuged at 15,000 x g to recover the supernatant containing the cytoplasmic fraction. Then, 50 mM potassium phosphate buffer + 1% Triton X-100 (Millipore-Sigma, T8787) was used to homogenize the pellet, which contained the plasma membrane fraction. The pellet homogenate was centrifuged at 15,000 x g, and the plasma membrane contents were recovered from the supernatant. The buffers contained 3% protease inhibitor cocktail (Sigma-Aldrich, P2714) to help prevent protein degradation. All centrifugations were carried out at 4°C. The protein content of the fractions was quantified using the Bradford assay (Bio-Rad Laboratories, 5000203). MAS1 receptor was measured in liver membrane samples using the Rat MAS1 / MAS (Sandwich ELISA) ELISA Kit (LSBio, LS-F66779) using 5 μL of the membrane protein extract, equivalent to 20 μg of total membrane protein. All procedures were carried out following the manufacturer's instructions. All samples were analyzed in duplicate and only accepting values that fell within percent coefficients of variability of less than 10% for all measurements.

qPCR mRNA quantification

Total RNA was obtained using TRIzol reagent (Invitrogen, 15596026) from a 25 mg piece of frozen liver, with 2 h for the RNA precipitation step. Genomic DNA was degraded using DNase I enzyme (Roche, 04716728001). Complementary DNA was reverse transcribed from gDNA-free RNA using the High-Capacity cDNA Reverse

Transcription Kit (Applied Biosystems, 4368814) using oligo dT. Quantitative PCR reactions were performed in duplicate, using an equivalent to 50 ng of RNA per reaction, using specific primers for MAS1, AT1, CD36, FATP5, ACC1, FASN, CPT1A, Acox1, GPAT4, DGAT1, G6PC1, PEPCK1, and GCK, and normalized using Beta-2-Microglobulin (B2M) mRNA levels. The primer sequences used for qPCR analyses are shown in **Table 2**.

Table 2. Primers used for qPCR.

Primer name	Sequence	NCBI Reference Sequence
B2M F	ATGGGAAGCCCAACTTCCTC	NM_012512.2
B2M R	ATACATCGGTCTCGGTGGGT	
MAS1 F	AACACATGGGCCTCCCATTC	XM_017588808.1
MAS1 R	AACAGGTAGAGGACCCGCAT	
AT1 F	TCTCAGCTCTGCCACATTCC	NM_030985.4
AT1 R	CGAAATCCACTTGACCTGGTG	
CD36 F	TCATGCCGGTTGGAGACCTA	NM_031561.2
CD36 R	CTTCCTCTGGGTTTTGCACG	
FATP5 F	GCCACACCTCATTTCATCCG	NM_024143.2
FATP5 R	GTTTCGGCCTTGTTGTCCAG	
ACC F	ATTGGGGCTTACCTTGTCCG	NM_022193.1
ACC R	TGCATTATCTGGATGCCCCC	
FASN F	CTGCTGCGGGCCAAGACAG	NM_017332.1
FASN R	GCTGTGGATGATGTTGATGATAG	
CPT1A F	ATTGGCAAGCGGGACCATAG	XM_017588838.1
CPT1A R	TGCAGGAACCAGTAAGGGGA	
Acox1 F	CTCACTCGAAGCCAGCGTTA	NM_017340.2
Acox1 R	TTGAGGCCAACAGGTTCCAC	
GPAT4 F	TACCGTGGTTGGATACCTGC	NM_001047849.1
GPAT4 R	ATCAATGGGCGACGTATGGT	
DGAT1 F	GCTATCCGGACAACCTGACC	NM_053437.1
DGAT1 R	CATCTCAAGAACCCGCCGTA	
PEPCK1 F	GGATGTGGCCAGGATCGAAA	NM_198780.3
PEPCK1 R	ATACATGGTGCGGCCTTTCA	
G6PC1 F	AACTCCAGCATGTACCGCAA	NM_013098.2
G6PC1 R	GGGCTAGGCAGTAGGGGATA	
GCK F	CGGGAGGCATCTACTCCACA	XM_006251179.4
GCKR	GAACCGGTGGCCTCTAGACA	

Statistics

Data was tested for normality using the Shapiro-Wilk test [86]. Means (±SD) were compared by ANOVAs. Means were considered significantly different at $p < 0.05$ using the Tukey test. Two-way-ANOVAs were used when analyzing datasets with all timepoints (T0, T1, T2) and groups, and one-way-ANOVA testing for multiple comparisons using the Tukey test, when analyzing datasets without timepoints (T0 only or group AUC). Correlations were calculated using the Pearson r coefficient [87] to better assess changes over time. Area under the curve (AUC) analyses were calculated using the area under the concentration curve in batch designs [88, 89]. Outliers were calculated and removed using the ROUT test [90] and one outlier was replaced with the mean of the

corresponding group [91]. All statistical analyses were performed with GraphPad Prism 8.4.3 software (GraphPad Prism, ver. 8.4.3).

Results

To better recognize the difference between static (i.e., chronic AT1 blockade, reflected by differences at T0) and dynamic (i.e., during the acute glucose load) responses, the results were separated into two sections contained within each subheading, designated respectively to the response.

AT1 blockade increased plasma Ang 1-7 levels while decreasing Mas1 membrane abundance

Ang 1-7 is a RAS peptide proposed to counteract the adverse effects of elevated Ang II signaling [127] and MAS1 is recognized as the Ang 1-7 receptor [148]. The activation of the Ang 1-7/MAS1 axis shows improved hepatic steatosis [149]. Therefore, measuring the levels of circulating Ang 1-7, and its receptor (MAS1) levels in hepatocyte membrane may provide insight to the mechanisms contributing to the benefits that AT1 blockade has in the liver.

Static changes: Basal Ang 1-7 levels in ARB were 58% and 80% greater than LETO and OLETF, respectively **(Fig. 1A)**. MAS1 expression was 29% and 35% lesser in OLETF and ARB, respectively, than LETO **(Fig. 1B)**. MAS1 membrane abundance was 21% and 34% lesser in OLETF and ARB, respectively, than LETO, and ARB was 16% lesser than OLETF **(Fig. 1C)**. AT1 expression was 31% lesser in ARB than OLETF **(Fig. 1D)**.

Dynamic changes: During the glucose challenge, Ang 1-7 levels in ARB remained 80% and 90% greater than LETO and OLETF at T1, and 13% and 54% greater than LETO and OLETF, respectively **(Fig. 1A)**. At T1, MAS1 expression was 62% and 45% lesser in ARB than LETO and OLETF, respectively, while at T2, MAS1 expression in OLETF and ARB were 38% and 59% lesser, respectively, than LETO **(Fig. 1B)**. At T1, MAS1 membrane abundance was 24% and 48% lesser in OLETF and ARB, respectively, than LETO, and membrane MAS1 in ARB was 32% lesser than OLETF, while at T2, membrane MAS1 in OLETF and ARB were 35% and 49% lesser than LETO, and 20% lesser in ARB than OLETF **(Fig. 1C)**. At T1, AT1 expression was 54% and 50% lesser in ARB than LETO and OLETF, respectively, while at T2, AT1 in OLETF and ARB were 64% and 50% lesser, respectively, than LETO **(Fig. 1D)**.

Ang 1-7 levels in ARB were negatively correlated ($r = -0.995$, $p = 0.043$) overtime, before and during the glucose challenge **(Fig. 1A)**. In all groups, MAS1

membrane abundance correlated with its gene expression (LETO r = 0.995, $p = 0.047$; OLETF r = 0.997 and $p = 0.037$; ARB r = 0.998 and $p = 0.030$) **(Fig. 1E)**.

Collectively, the data suggest that AT1 blockade increased the levels of Ang 1-7, while decreasing both AT1 and MAS1 receptors. The increase of Ang 1-7 alone may suffice to mediate its beneficial signaling [32, 150], which may contribute to the improvements to counteract NAFLD [33].

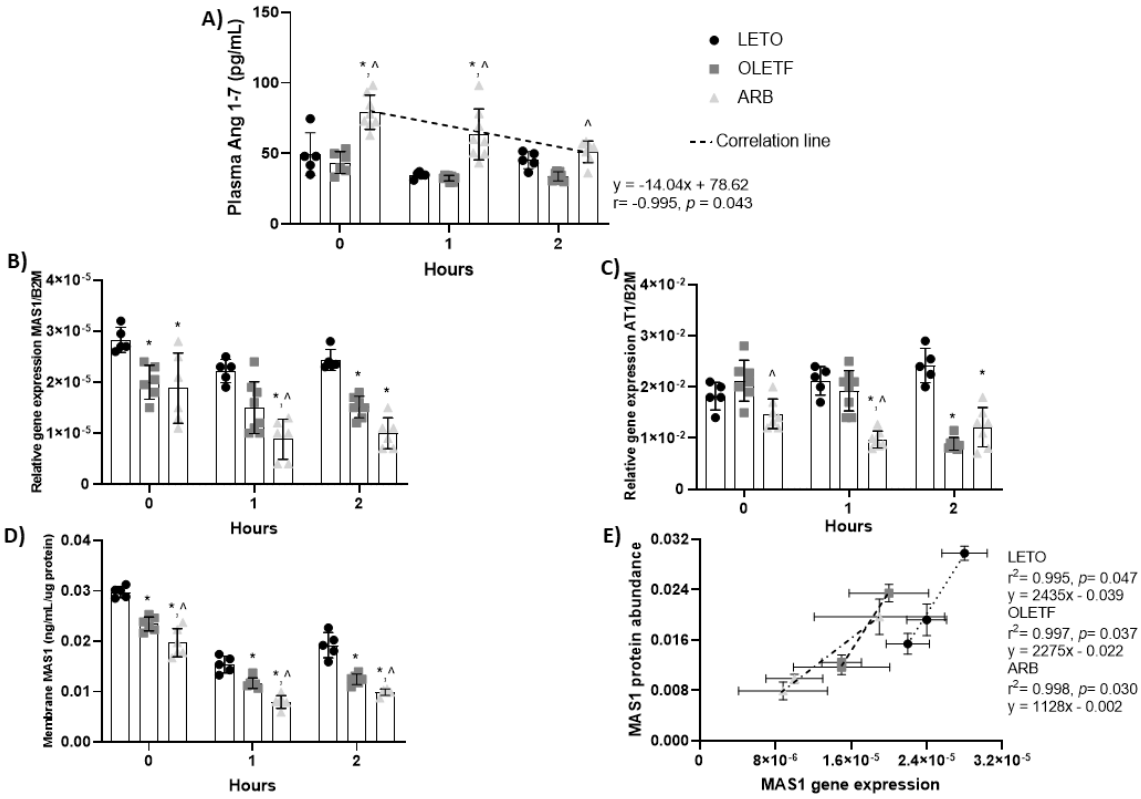

Figure 1. Plasma Ang 1-7 and RAS peptide receptors expression and abundance. Mean ± SD values for plasma Ang 1-7 (A), relative mRNA expression of MAS1 (B), AT1 (C), membrane abundance of MAS1 (D), and correlation test between MAS1 expression and membrane abundance during the glucose challenge in Long Evans Tokushima Otsuka (LETO; n=5), Otsuka Long Evans Tokushima Fatty (OLETF; n=8), OLETF + ARB (ARB; n=8) rats. * *Significant difference from LETO (P < 0.05).* ^ *Significant difference from OLETF (P < 0.05).*

AT1 blockade decreased liver NEFA, as well as FATP5 and FASN expression

Hepatic NEFA uptake, which is mainly mediated by CD36 and FATP5 [129], and synthesis (through DNL) [131] is increased with NAFLD [58]. Ang II infusion increased hepatic steatosis [24], while AT1 blockade [29] and increased Ang 1-7/MAS1 axis signaling [149] decreased it. Moreover, NAFLD can be attenuated by increasing NEFA oxidation [136]. Therefore, measuring the expression of genes related to these pathways

during AT1 blockade, and during a glucose challenge, may provide insight about the mechanisms promoting hepatic steatosis during MetS.

Static changes: Basal liver NEFA in OLETF and ARB were 160% and 112% greater, respectively, than LETO, while levels in ARB were 18% lesser than OLETF **(Fig. 2A)**. FATP5 expression in OLETF and ARB was 28% and 51% lesser, respectively, than LETO, and 33% lesser in ARB than OLETF **(Fig. 2D)**. ACC expression was 33% lesser in OLETF than LETO **(Fig. 2E)**. FASN expression in OLETF and ARB was 30% and 67% lesser, respectively, than LETO, and 53% lesser in ARB than OLETF **(Fig. 2F)**. CPT1A expression in OLETF and ARB was 27% and 35% lesser, respectively, than LETO **(Fig. 2G)**. Acox1 expression was 82% greater in OLETF than LETO, while levels were 65% lesser in ARB than OLETF **(Fig. 2H)**.

Dynamic changes: During the glucose challenge, liver NEFA in OLETF and ARB were 78% and 33% greater, respectively, than LETO, while levels in ARB were 25% lesser than OLETF at T1, and at T2, levels in OLETF and ARB were 81% and 51% greater, respectively, than LETO, and 17% lesser in ARB than OLETF **(Fig. 2A)**. NEFA AUC in OLETF and ARB was 88% and 49% greater, respectively, than LETO, 21% lesser in ARB than OLETF **(Fig. 2B)**. At T2, CD36 expression in OLETF was 132% greater than LETO, and 65% lesser in ARB than OLETF **(Fig. 2C)**. At T1, FATP5 expression in ARB was 63% and 54% lesser in ARB than LETO and OLETF, respectively, while at T2, levels in OLETF and ARB were 22% and 64%, respectively, lesser than LETO, and 53% lesser in ARB than OLETF **(Fig. 2D)**. At T1, ACC expression in OLETF was 74% greater than LETO, and 42% and 67% lesser in ARB than LETO and OLETF, respectively. At T2, levels in OLETF were 51% greater than LETO, 29% and 53% lesser in ARB than LETO and OLETF, respectively **(Fig. 2E)**. At T1, FASN expression in OLETF was 88% greater than LETO, and 53% lesser in ARB than OLETF. At T2, levels in OLETF were 15% greater than LETO, and 74% and 77% lesser in ARB than LETO and OLETF, respectively **(Fig. 2F)**. At T1, CPT1 expression in OLETF and ARB was 58% and 78% lesser, respectively, than LETO, and 47% lesser in ARB than OLETF. At T2, levels in ARB were 45% and 49% lesser than LETO and OLETF, respectively **(Fig. 2G)**. At T1, Acox1 expression in OLETF was 26% greater than LETO, and 70% and 76% lesser in ARB than LETO and OLETF, respectively. At T2, levels in OLETF and ARB were 80% and 88% lesser, respectively, than LETO **(Fig. 2H)**.

FASN expression in OLETF correlated positively over time ($r = 0.997$, $p = 0.036$), before and during the glucose challenge **(Fig. 2F)**.

These data suggest AT1 blockade may decrease liver NEFA by decreasing their uptake and synthesis, through decreased FATP5, and FASN expression, without increasing their oxidation, as supported by the decreased expression of CPT1A and

Acox1. As well, this may help downregulate DNL during nutrient overload, as suggested by the decrease in FASN and ACC expression.

Figure 2. Liver NEFA and gene expression of fatty acid transport, synthesis, and oxidation proteins. Mean ± SD values for liver NEFA (A), liver NEFA AUC (B), and mRNA expression of

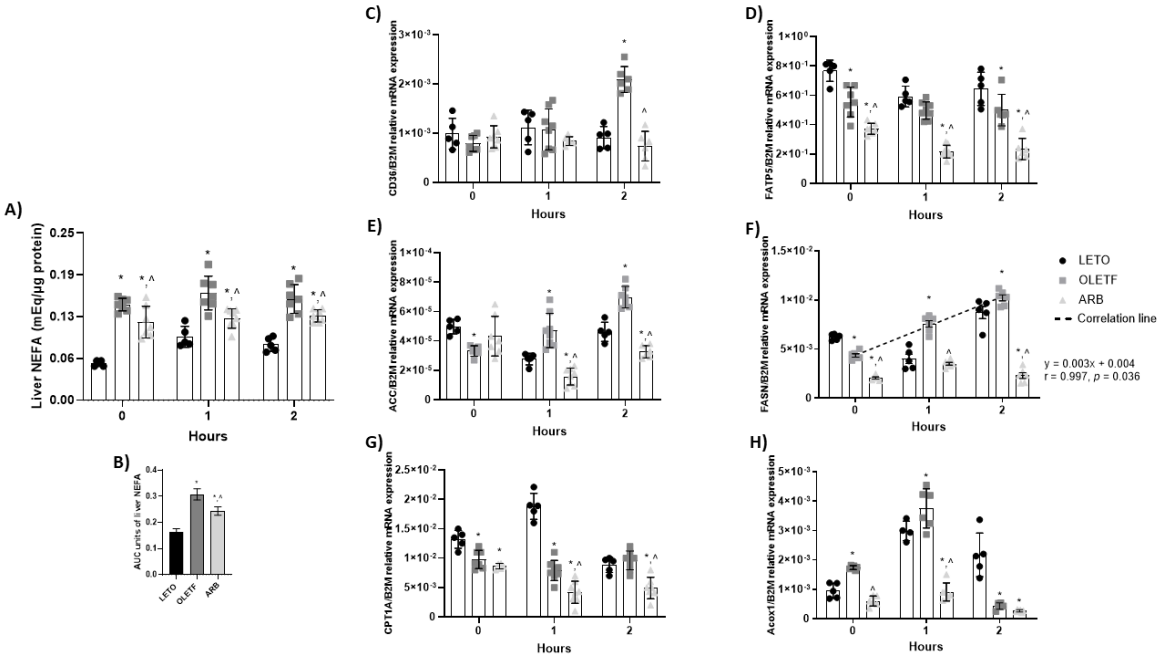

CD36 (C), FATP5 (D), ACC (E), FASN (F), CPT1A (G), and Acox1 (H) during the glucose challenge in Long Evans Tokushima Otsuka (LETO; n=5), Otsuka Long Evans Tokushima Fatty (OLETF; n=8), OLETF + ARB (ARB; n=8) rats. * *Significant difference from LETO (P < 0.05).* ^ *Significant difference from OLETF (P < 0.05).*

AT1 blockade decreased basal hepatic TAG and decreased genes of TAG synthesis during the glucose challenge

TAG accumulation is the hallmark of NAFLD [58]. TAG synthesis in the liver is initiated by GPAT, while DGAT catalyzes the last step to create new TAG [68, 69]. AT1 blockade [29] and increased Ang 1-7 signaling [149] have demonstrated benefits in decreasing hepatic TAG. Thus, measuring liver TAG levels, and the expression of genes for enzymes responsible for TAG synthesis during AT1 blockade, and after a glucose load, may provide further insight into the mechanisms involved in the improvements on hepatic TAG accumulation, and the detriments of nutrient overload derived from the glucose challenge.

Static changes: Basal liver TAG in OLETF and ARB were 125% and 79% greater, respectively, than LETO, and 20% lesser in ARB than OLETF **(Fig. 3A)**. GPAT4 **(Fig. 3C)** and DGAT1 **(Fig. 3D)** expression in ARB was 32% and 36% greater, respectively, than LETO.

Dynamic changes: During the glucose challenge, liver TAG levels in OLETF and ARB were 40% and 32% greater, respectively, than LETO at T2 **(Fig. 3A)**. TAG AUC in OLETF and ARB was 37% and 25% greater than LETO, and 8% lesser in ARB than OLETF **(Fig. 3B)**. At T1, GPAT4 expression in OLETF and ARB was 37% and 43% lesser, respectively, than LETO, while at T2, levels in OLETF were 43% greater than LETO and 43% lesser in ARB than OLETF **(Fig. 3C)**. At T1, DGAT1 expression in OLETF was 65% greater than LETO, and 32% lesser in ARB than OLETF, while at T2, levels were 64% and 59% lesser in ARB than LETO and OLETF, respectively **(Fig. 3D)**.

DGAT1 expression in ARB correlated negatively over time (r = -0.996, p = 0.039), before and during the glucose challenge **(Fig. 3D)**.

Thus, the data indicate that chronic AT1 blockade decreased liver TAG levels. This reduction may be partially mediated by decreased TAG synthesis during nutrient overload, more so than during the fasted state, as suggested by the decrease in GPAT4 at T2 and the linear decrease of DGAT1.

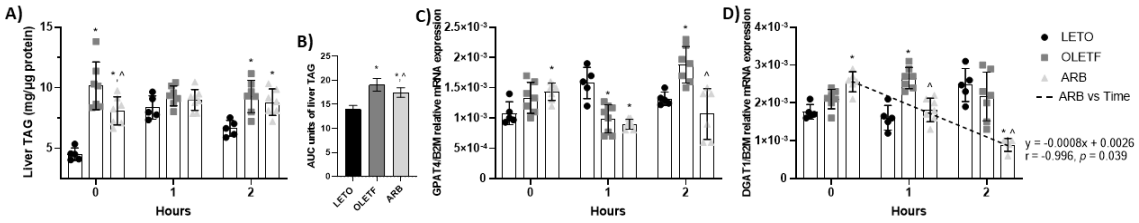

Figure 3. Liver TAG and gene expression of TAG synthesis enzymes. Mean ± SD values for liver TAG (A), liver TAG AUC (B), and mRNA expression of GPAT4 (C) and DGAT1 (D) during the glucose challenge in Long Evans Tokushima Otsuka (LETO), Otsuka Long Evans Tokushima Fatty (OLETF), OLETF + ARB (ARB) rats. ** Significant difference from LETO ($P < 0.05$). ^ Significant difference from OLETF ($P < 0.05$).*

AT1 blockade decreased genes of gluconeogenesis, while increasing GCK expression and reducing hepatic glucose levels

NAFLD [140] and insulin resistance [143] can increase GNG and its flux. During healthy conditions, insulin signaling suppresses hepatic GNG [142]. AT1 blockade suppressed renal GNG [151] while Ang 1-7 signaling improved insulin signaling [34]. Therefore, examining GNG and the genes that regulate its flux during AT1 blockade, and during glucose overload, may provide insight on the regulation of hepatic GNG during MetS, and its potential contribution to promoting the severity of NAFLD. Furthermore, glucokinase (GCK) regulates hepatic glucose disposal and its metabolism [152], thus, changes in GCK may help to better understand hepatic glucose sensitivity.

Static changes: Basal liver glucose in OLETF and ARB was 137% and 58% greater, respectively, than LETO, and 33% lesser in ARB than OLETF **(Fig. 4A)**.

PEPCK1 expression in OLETF was 151% greater than LETO, and 76% and 91% lesser in ARB than OLETF and LETO, respectively **(Fig. 4C)**. G6PC1 expression in OLETF was 186% greater than LETO, and 69% lesser in ARB than OLETF **(Fig. D)**. GCK expression in ARB was 3850% and 240% greater than LETO and OLETF, respectively **(Fig. 4E)**.

Dynamic changes: During the glucose challenge, liver glucose in OLETF was 59% greater than LETO and 21% lesser in ARB than OLETF at T1. At T2, levels in OLETF and ARB were 92% and 15% greater, respectively, than LETO, and 40% lesser in ARB than OLETF **(Fig. 4A)**. Glucose AUC in OLETF and ARB was 80% and 41% greater, respectively, than LETO, and 21% lesser in ARB than OLETF **(Fig. 4B)**. At T1, PEPCK1 expression in OLETF was 85% greater than LETO, and 61% lesser in ARB than OLETF, while at T2, levels in OLETF were 62% lesser than LETO and 206% greater in ARB than OLETF **(Fig. 4C)**. At T1, G6PC1 expression in OLETF was 840% greater than LETO and 62% lesser in ARB than OLETF **(Fig. 4D)**. At T1, GCK expression in OLETF and ARB was 88% and 57% lesser, respectively, than LETO, and 261% greater in ARB than OLETF. At T2, levels in OLETF and ARB were 43% and 29% lesser, respectively, than LETO, and 23% greater in ARB than OLETF **(Fig. 4E)**.

GCK expression in ARB correlated positively over time ($r = 0.995$, $p = 0.047$), before and during the glucose challenge **(Fig. 4E)**. Additionally, basal expression levels correlated with liver glucose in LETO ($r = 0.996$, $p = 0.039$) and ARB ($r = 0.998$, $p = 0.028$) **(Fig. 4F)** but not OLETF.

Altogether, these data suggest that chronic AT1 blockade may reduce hepatic GNG, as reflected by the decreased expression of PEPCK1 and G6PC1, while also improving the response of GCK expression to increased hepatic glucose levels. This is further supported by decreased hepatic glucose levels, the linear increase of GCK over time and the correlation found in LETO and ARB between GCK expression and liver glucose content before and during the glucose challenge.

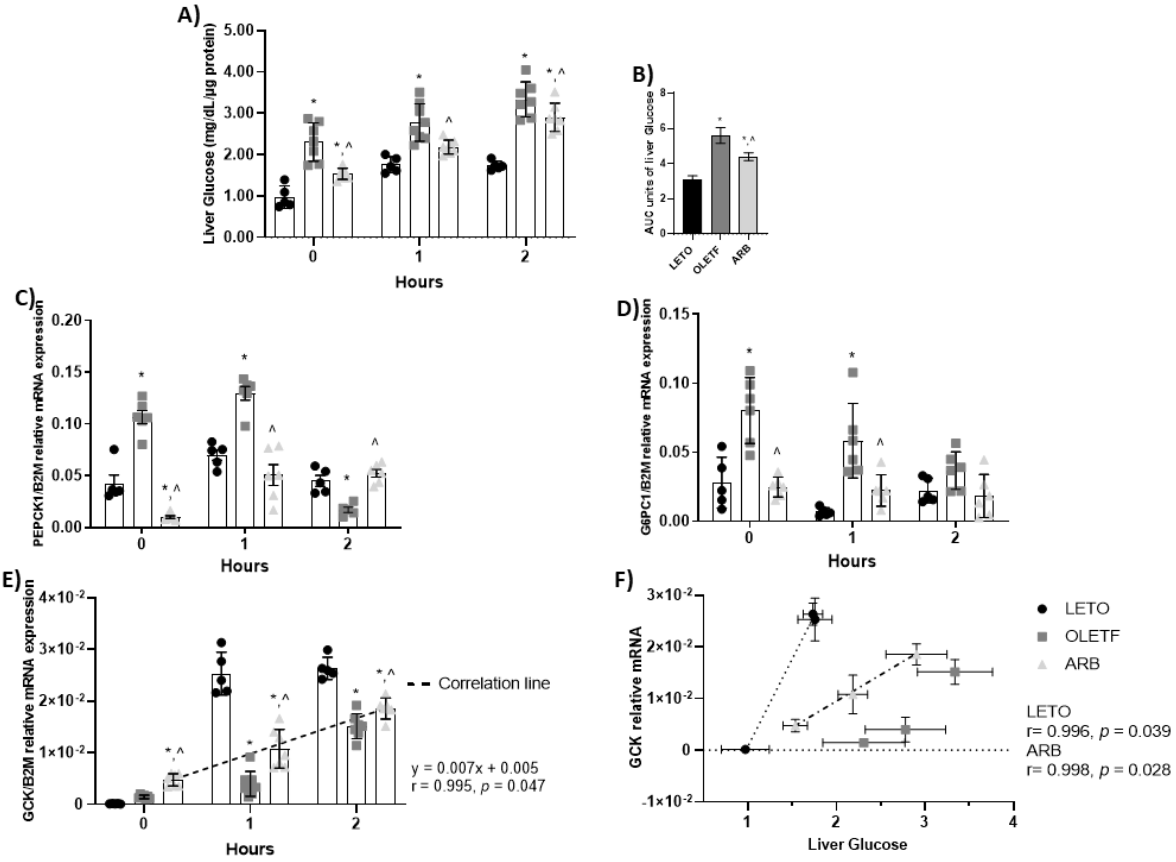

Figure 4. Liver glucose and gene expression of gluconeogenic and glycolysis enzymes. Mean ± SD values for liver glucose (A), liver glucose AUC (B), and mRNA expression of PEPCK1 (A), G6PC1 (B), and GCK (C), and correlation test between liver glucose and GCK expression (F) during the glucose challenge in Long Evans Tokushima Otsuka (LETO; n=5), Otsuka Long Evans Tokushima Fatty (OLETF; n=8), OLETF + ARB (ARB; n=8) rats. * *Significant difference from LETO (P < 0.05).* ^ *Significant difference from OLETF (P < 0.05).*

Discussion

Inappropriately elevated RAS, characterized by increased plasma Ang II, [53] and over-activation of the Ang II receptor (AT1) [20] contribute to the development of NAFLD. Ang 1-7 is a RAS peptide proposed to counteract the adverse effects of elevated Ang II signaling [127]. In this study, Ang 1-7 was increased with AT1 blockade associated with improved hepatic metabolism (**Fig. 5**). Liver TAG accumulation is the hallmark of NAFLD [58] and the changes in synthesis, oxidation, secretion, and storage of TAG is crucial and can reflect the changes in lipid metabolism that lead to NAFLD development. With AT1 blockade, genes promoting hepatic lipogenesis were decreased both basally and during the glucose challenge, as demonstrated by the changes in the expression of FATP5, ACC, FASN, and DGAT1, which may consequentially lower TAG production.

Finally, chronic AT1 blockade may have sensitized the response of the liver to glucose given the changes in the expression of GCK.

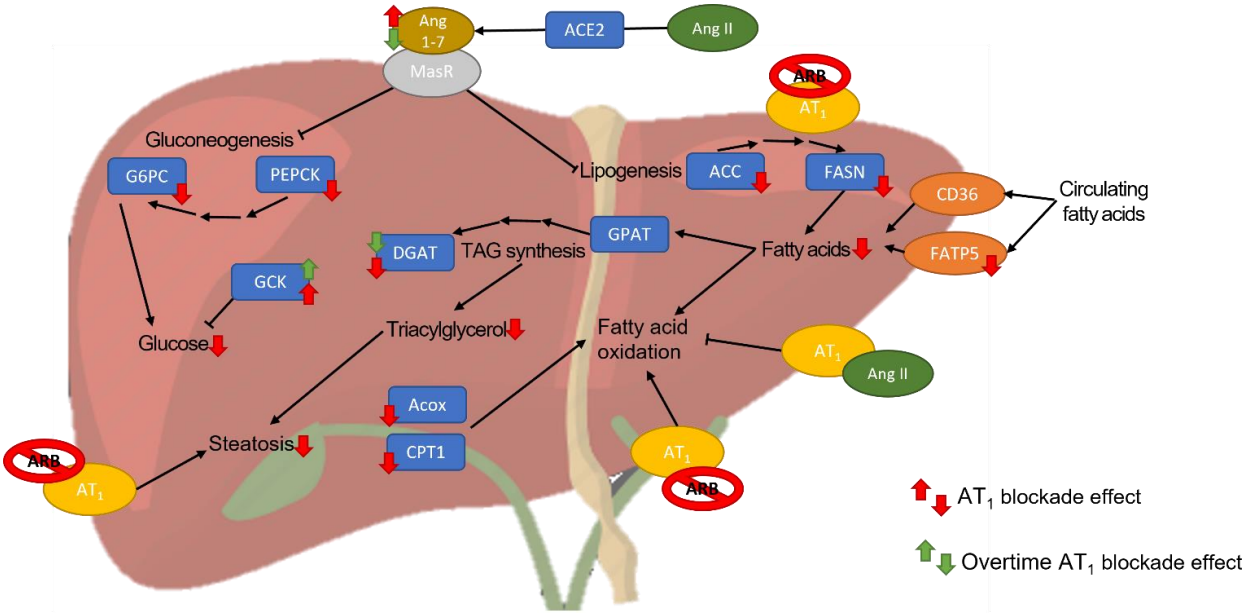

Figure 5. Summary of findings. AT1 blockade increased Ang 1-7, and this increase was associated with decreased fatty acids and TAG levels, as well as decreased expression of genes of lipogenesis and gluconeogenesis in the liver, while decreasing glucose levels and increasing GCK expression. These results demonstrate that the progression of hepatic steatosis may be delayed, due to the reductions on lipogenesis. As well, the suggested improvement on glucose sensitivity, due to the increase in GCK and correlation with liver glucose levels, may contribute to the decrease in nutrient accumulation in the liver and systemic hyperglycemia.

The increased plasma levels on Ang 1-7 may be due to increased angiotensin converting enzyme activity during the AT1 blockade [153]. Though Ang 1-7 was elevated with AT1 blockade and during the glucose challenge, its membrane receptor proto-oncogene Mas (MAS1) abundance was decreased. This may be due to AT1 blockade maintaining MAS1 expression during the early stages of the ARB treatment [154], suggesting that hepatocyte Ang 1-7 signaling may have acclimated to these lower levels of receptor expression [155] to promote homeostasis due to the increased levels of Ang 1-7 [156]. Alternatively, maintained MAS1 receptor expression is often reported with increased Ang 1-7 through infusion [157], which may not mimic the Ang 1-7 increase mediated by AT1 blockade. Finally, Ang 1-7 signaling may be suppressed during pathological conditions, which may explain the lack of changes Ang 1-7 levels in OLETF [158]. MAS1 gene expression and protein abundance were correlated in all groups, even during the glucose challenge. This suggests that MAS1 may not have post-transcriptional or post-translational regulation in the liver of these rats during metabolic

syndrome. Similarly, AT1 expression was decreased with AT1 blockade [159], and this decrease remained during the early stage of the glucose challenge. Thus, the increased circulating Ang 1-7, with no increase on its receptor (MAS1), may be sufficient to contribute to the beneficial effects produced by AT1 blockade.

Hepatic NEFA uptake is increased during NAFLD [58], and our study provides evidence for elevated Ang II/AT1 axis signaling contributing to hepatic lipid accumulation, which may be mediated by increased hepatic CD36 and FATP5 expression during metabolic syndrome. The decrease on liver NEFAs associated with AT1 blockade may be derived from decreased FATP5 expression, as FAPT5 is a main hepatic NEFA transporter [129]. Additionally, the decrease in CD36 at the end of the glucose challenge may demonstrate how the liver may be protected from excessive NEFA accumulation after a nutrient overload (e.g., glucose challenge) [119]. Accordingly, the liver can produce NEFA through DNL [131]. The increase in liver NEFA AUC in OLETF may have resulted from the increases in FASN and ACC [160]. AT1 blockade decreased FASN expression, while ACC expression was only decreased during the glucose challenge. These data suggest that AT1 activation may contribute to hepatic steatosis during the progression of MetS by upregulating DNL. Conversely, increased NEFA oxidation may not contribute significantly to the decrease in liver NEFA. With chronic AT1 blockade, basal Acox1 was decreased, and both Acox1 and CPT1A expression were decreased during the glucose challenge, suggesting that NEFA oxidation may be decreased with AT1 blockade. Alternatively, this decrease could reflect a shift from NEFA to glucose oxidation to meet cellular energetic needs [161], which may contribute to ameliorating MetS-associated hyperglycemia. Collectively, these results suggest that AT1 blockade may decrease hepatic steatosis by decreasing NEFA uptake and DNL, ultimately preventing the increase and accumulation of TAG in the liver by reducing available NEFA.

NAFLD can develop during hyperinsulinemia, increasing TAG synthesis and accumulation [66], with GPAT [68] and DGAT [69] driving TAG production. AT1 blockade decreased GPAT4 and DGAT1 expression, which may decrease basal hepatic TAG, suggesting that AT1 activation may promote hepatic TAG accumulation by up-regulating the expression of the rate-limiting enzymes of TAG synthesis. After the nutrient load, DGAT1 expression decreased linearly overtime with AT1 blockade, while GPAT4 decreased only 2 h after the glucose load. This suggest that the decrease in TAG production during the glucose load may reflect changes in nutrient processing by the liver [161]. OLETF rats overfeed themselves with greater meal sizes, rather than increasing the number of meals [162] repeatedly generating nutrient overloads. However, the expression of these genes was not measured during the chow fed-state, only during fasting and the glucose challenge. Nonetheless, the results demonstrate that AT1 blockade may decrease hepatic TAG synthesis by suppressing transcription of the rate-limiting enzymes, thus

desensitizing the liver to nutrient loads, preventing hepatic TAG accumulation, which may be derived from *ad libitum* feeding.

Hepatic GNG can be stimulated during NAFLD [140]. During insulin resistance, the gluconeogenic flux is increased [143], stimulating glucose production, which contributes to hyperglycemia and, ultimately, dyslipidemia [163]. The primary mediators of hepatic GNG are PEPCK1 and G6PC1 [144]. In this study, chronic AT1 blockade decreased PEPCK1 and G6PC1 expression, which may be responsible for the reduced liver glucose content. This suggests that AT1 activation may increase liver GNG and therefore glucose levels, which promotes hyperglycemia [163]. Conversely, the results obtained with AT1 blockade demonstrate a behavior closer to the lean control, where GNG is not stimulated and GCK expression is increased during the nutrient overload, both contributing to reducing glucose levels. Additionally, because Ang 1-7 signaling improves insulin signaling and glucose uptake [32], the increased circulating Ang 1-7 in this study may benefit the liver by improving its response to glucose. Thus, the improvements in hepatic substrate metabolism conferred by chronic AT1 blockade may be mediated, at least in part, by increased Ang 1-7 signaling, through improvements on insulin sensitivity [32, 164], which are supported by our previous findings where AT1 blockade reduced insulin resistance index in these rats [165].

Increased circulating Ang 1-7 decreased plasma glucose and increased its uptake in rat adipocytes [32] and skeletal muscle *in vivo* [164]. Hyperglycemia can indirectly contribute to NAFLD development by increasing NEFA synthesis and reducing NEFA oxidation in the presence of abundant lipids [166]. GCK regulates hepatic glucose disposal through the phosphorylation of glucose [152]. A relationship between GCK expression and liver TAG in humans suggested that increased GCK is detrimental [152], while GCK activity was decreased in obese diabetic subjects [167]. In this study, GCK was not correlated with liver TAG. GCK expression increased with AT1 blockade, both basally and linearly during the glucose challenge. This suggests that the overactivation of AT1, associated with MetS, may decrease GCK activity, which alters the balance in lipid and glucose metabolism. Furthermore, GCK expression correlated with glucose levels during AT1 blockade and in the lean controls, highlighting the contributions of GCK to increasing hepatic glucose tolerance. This suggests that GCK is sensitive to the increasing levels of glucose, unlike the untreated OLETF, where hepatic glucose remained elevated before and throughout the glucose challenge, while GCK expression was suppressed. These results suggest that chronic AT1 blockade may improve hepatic glucose metabolism (i.e., reduced uptake and increase oxidation) during conditions of glucose intolerance, which may partly decrease systemic hyperglycemia and improve insulin resistance.

In summary, these results demonstrate that chronic AT1 blockade and the subsequential increase in Ang 1-7 ameliorate hepatic steatosis by reducing NEFA uptake

and TAG synthesis in the hepatocyte (**Fig. 5**). Overactivation of hepatic AT1 may be one of the most critical components contributing to the imbalance in substrate metabolism associated with NAFLD and MetS. Chronic AT1 blockade may also sensitize the liver to glucose, as shown by the correlation between liver glucose and GCK expression. This would help maintain homeostatic balance in substrate metabolism, especially during post-prandial elevations, stimulated by the glucose challenge used in this study. Finally, all these improvements were not dependent on a constant increase in MAS1 receptor expression or membrane abundance, suggesting that Ang 1-7 signaling may not require elevated MAS1 abundance to exert effective signaling [168] at this stage of the disease.

Table 3. Results for ARB group compared to OLETF.

Measurements	ARB group		
	0 h	1 h	2 h
Elements of Ang (1-7) signaling			
Plasma Ang (1-7)	^	^	^
MAS1 receptor expression	-	v	-
MAS1 receptor membrane abundance	v	v	v
Substrates of hepatic lipid profile			
NEFA	v	v	v
TAG	v	-	-
Genes of fatty acid transport			
FATP5	v	v	v
CD36	-	-	v
Genes of fatty acid oxidation			
Acox1	v	v	-
CPT1A	-	v	v
Genes of lipid synthesis			
ACC	-	v	v
FAS	v	v	v
DGAT1	-	v	v
Elements of hepatic glucose regulation			
Liver glucose	v	v	v
PEPCK1	v	v	v
G6PC1	v	v	-
GCK	^	^	^

^ *increase; v decrease; - no difference*

However, the contributions of the Ang 1-7/MAS1 signaling axis to the regulation of cellular metabolism in the prevention and amelioration of NAFLD or MetS warrant

further investigation, as the relation between metabolic regulation and the Ang 1-7/MAS1 axis are not fully elucidated. The regulatory effects of the Ang 1-7/MAS1 axis to counteract the detrimental effects of the Ang II/AT1axis are more widely accepted than before, yet the extent of this counter regulation is still not fully defined. Several studies show that increasing circulating Ang 1-7 and MAS1 receptor activation can improve liver fibrosis [169], muscle atrophy [170], fat mass [32, 150], increased insulin secretion [148], and insulin response in various tissues (i.e., adipose, cardiac, skeletal muscle, and liver) [171]. Thus, AT1 blockade alone should exert beneficial effects similar to those present when the Ang 1-7/MAS1 axis is stimulated. Conversely, other studies report a lack of the AT1 blockade-mediated benefits associated with increased Ang 1-7/MAS1 axis signaling. AT1 blockade in hypertensive diabetic rats did not improve glucose metabolism [172] or have significant effects on the expression of insulin-signaling components in the muscle [54]. These findings highlight the importance of elucidating the mechanisms by which Ang 1-7/MAS1 signaling counters the Ang II/AT1 axis effects during metabolic disorders. In this study, we demonstrated that chronic AT1 blockade increased circulating Ang 1-7 and liver GCK gene expression, while decreasing hepatic and plasma glucose levels, liver NEFA and TAG, and genes of gluconeogenesis, and NEFA uptake and synthesis. Knowing which genes are simultaneously sensitive to the AT1 blockade and increase with Ang 1-7 or MAS1 activation, warrants better understanding of the contributions of these RAS signaling components to the development of impaired substrate metabolism that is associated with MetS.

Chapter III
AT1 blockade improves the redox state during hepatic steatosis

Introduction

The “two-hit” hypothesis is often the working model that describes non-alcoholic fatty liver disease (NAFLD) pathogenesis. The “first hit” is lipid accumulation in the liver cells, while the “second hit” is multi-factorial, based on the promotion of hepatic injury, inflammation, increased oxidant production, and fibrosis [4, 6]. Insulin resistance is suggested as the main contributor to the “first hit”, causing liver steatosis by increasing lipogenesis and reducing non-esterified fatty acid (NEFA) oxidation [7]. Excessive NEFA may then be used to generate reactive oxygen species [173]. An updated hypothesis is the “multiple-hit”, which describes multi-factorial events (i.e., obesity, insulin resistance, gut microbiome, increased adipokine secretion, hepatic oxidative stress, mitochondrial dysfunction, and genetic factors) that better explain the pathogenesis and progression of NAFLD [5]. Among these factors, oxidative stress is considered one of the main contributors to the development [174] and progression [175] of NAFLD. Oxidative stress is generated when there is an imbalance between the production of oxidants and antioxidant defenses, which may result in damage to the biological system [176].

Glutathione (GSH) is a tripeptide that is present in all mammalian cells [177] where it serves many functions, including the reduction of harmful oxidant species and toxicants [178]. Low GSH levels are associated with metabolic disease pathology, including type 2 diabetes [177] and NAFLD [179]. While GSH supplementation decreased circulating markers of liver and oxidative damage [180], and its dietary consumption is suggested to reduce body mass in patients with metabolic syndrome [181]. GSH is primarily produced by glutamate cysteine ligase (GCL), which is composed by two subunits, catalytic (GCLC) and modifier (GCLM) [182]. GCLC has all the catalytic activity to produce GSH [183] while GCLM is not enzymatically active, but increases the affinity of GCLC to its substrate [184]. GSH can be used to reduce peroxides, through glutathione peroxidase (GPx) [185], which ameliorates the redox status. GSH is glutathione reductase (GR) catalyzes the reduction of glutathione disulfide (GSSG) back to GSH to replenish the GSH pool [182]. GSH is also found in plasma, where it can be broke down by other tissues, through γ-glutamyl transpeptidase (GGT), to uptake GSH components and increase its intracellular production [186]. Most of the circulating GSH is secreted by the liver [187], therefore hepatic dysregulation of GSH production may then have a greater systematical impact [182].

Hyperglycemia, hyperlipidemia [188], and NEFA overload [189] increase oxidant production. Elevated glucose levels can produce oxidants through glucose auto-oxidation

[190], and metabolism and formation of advanced glycosylation end products [191]. Increased NEFA oxidation and induction of endoplasmic reticulum stress by lipotoxic lipids can also generate oxidants (e.g., hydrogen peroxide, H_2O_2; malondialdehyde, MDA; 4-hydroxynonenal, HNE) [189, 192]. Angiotensin receptor blockers (ARBs) block the AT1 receptor, preventing Ang II signaling. Because of the anti-inflammatory and anti-fibrotic effects, ARBs are suggested as potential therapeutic drugs for NAFLD treatment [193]. Chronic ARB treatment can decrease hyperglycemia [93], dyslipidemia [194], hepatic steatosis [29], and oxidant production [195, 196].

Because of the increased redox state in NAFLD, and the systematic relevance of hepatic GSH levels, it is important to investigate the regulation of GSH during hepatic steatosis. Furthermore, the dynamic effects of a nutrient overload (through a glucose challenge) on a compromised liver, such as present during NAFLD are scarce and further study is needed to provide additional insight on GSH metabolism and regulation, which may partly counteract the redox state during the "multifactorial hits" to prevent NAFLD progression. This study may also enhance the understating of how a nutrient overload may alter the redox response and promote NAFLD. In this study, the gene expression of enzymes that regulate GSH metabolism (synthesis and cycling) were investigated, as well as the mitochondrial activity of the anti-oxidant, catalase, after chronic AT1 blockade and during nutrient overload.

Methods

All experimental procedures were reviewed and approved by the institutional animal care and use committees of the Kagawa Medical University (Japan) and the University of California, Merced (USA). The work presented here complements our previous studies in the same animals, where we assessed the contribution of AT1 activation in relation to cardiac redox biology [108], and to renal function through regulation of inflammation and blood pressure [147]. Therefore, previously presented data in this document will be used to contrast and complement what is presented here.

Animals

Male, age matched, 10-week-old, lean strain-control Long Evans Tokushima Otsuka (LETO; 279 ± 7 g) and obese Otsuka Long Evans Tokushima Fatty (OLETF; 359 ± 3 g) rats (Japan SLC Inc., Hamamatsu, Japan) were used. NAFLD is not yet strongly present at this age in these rats [99], providing the opportunity of examining the animals during the development of more severe hepatic disease. Rats were assigned to the following groups (n=5–8 animals/group/time point): **(1)** untreated LETO (n=5), **(2)** untreated OLETF (n=8), and **(3)** OLETF + angiotensin receptor blocker (ARB; 10 mg olmesartan/kg/d × 6 weeks; n=8). ARB (Daiichi-Sankyo, Tokyo, Japan) was administered by oral gavage suspended in carboxymethyl cellulose (CMC) to conscious rats and untreated rats were gavaged with CMC only. Animals were maintained in groups

of two to three animals per cage, given access to water and standard laboratory chow (MF; Oriental Yeast Corp., Tokyo, Japan), and maintained under controlled temperatures (23 - 24 °C) and humidity (~55%) with a light-dark cycle of 12-12 h.

For dissections, all animals were randomly assigned to a corresponding subgroup. Animals were fasted for 12 h ± 15 min. To investigate the dynamic response to a glucose challenge (nutrient overload), animals were dissected at baseline (T0, fasting) and after 1 (T1) and 2 h (T2) after a glucose load administered by gavage (2 g glucose/kg mass). Staggered times were used to ascertain correct dissection timing at 1 and 2 h post-glucose loading. Trunk blood was collected after decapitation in vials containing EDTA (Sigma-Aldrich, EDS) and proteinase inhibitor cocktail (Sigma-Aldrich, P2714). Livers were snap frozen in liquid nitrogen and kept at −80 °C until analyzed.

Plasma marker of hepatic fibrosis

Collagen Type IV (COL-4) was measured in plasma using the commercially available reagents from the kit CIV ELISA (MyBioSource, MBS732756) following manufacturer's instructions. All samples were analyzed in duplicate and only accepting values that fell within percent coefficients of variability of less than 10% for all measurements.

qPCR mRNA quantification

Total RNA was obtained using TRIzol reagent (Invitrogen, 15596026) from a 25 mg piece of frozen liver, allowing 2 h for the RNA precipitation step. Genomic DNA was degraded using DNase I enzyme (Roche, 04716728001). Complementary DNA was reverse transcribed from gDNA-free RNA using the High-Capacity cDNA Reverse Transcription Kit (Applied Biosystems, 4368814) using oligo dT. Quantitative PCR reactions were performed in duplicate, using an equivalent to 50 ng of RNA per reaction, using specific primers for GCLC, GCLM, GPx1, GR, NADPH oxidase 4 (NOX4), and normalized using Beta-2-Microglobulin (B2M) mRNA levels. The primer sequences used for qPCR analyses are shown in **Table 1**.

Table 1. Primers used for qPCR.

Primer name	Sequence	NCBI Reference Sequence
B2M F	ATGGGAAGCCCAACTTCCTC	NM_012512.2
B2M R	ATACATCGGTCTCGGTGGGT	
GCLC	AGTGGAGGTAAAAGCGACCC	NM_012815.2
GCLC	TCACTTGTGGGCAACTGGAA	
GCLM F	GAAAAAGTGTCCGTCCACGC	NM_017305.2
GCLM R	CCACTGCATGGGACATGGTA	
GR F	CGAGGAAGACGAAATGCGTG	NM_053906.2
GR R	CGAAGCCCTGAAGCATCTCA	
GPx1 F	GGTGTTCCAGTGCGCAGATA	NM_030826.4
GPx1 R	CTTAGGGGTTGCTAGGCTGC	
NOX4 F	AGATGTTGGGCCTAGGATTGTG	NM_053524.1
NOX4 R	TGTGATCCGCGAAGGTAAGC	

Statistics

Data was tested for normality using the Shapiro-Wilk test [86]. Means (±SD) were compared by ANOVAs. Means were considered significantly different at $p < 0.05$ using the Tukey test. Two-way-ANOVAs were used when analyzing datasets with all timepoints (T0, T1, T2) and groups, and one-way-ANOVA testing for multiple comparisons using the Tukey test, when analyzing datasets without timepoints (T0 only or group AUC). Correlations were calculated using the Pearson r coefficient [87] to better assess changes over time. Area under the curve (AUC) analyses were calculated using the area under the concentration curve in batch designs [88, 89]. Outliers were calculated and removed using the ROUT test [90] and one outlier was replaced with the mean of the corresponding group [91]. All statistical analyses were performed with GraphPad Prism 8.4.3 software (GraphPad Prism, ver. 8.4.3).

Results

To better recognize the differences between static (i.e., chronic AT1 blockade, reflected by differences at T0) and dynamic (i.e., during the acute glucose load) responses, the results were separated into two sections contained within each subheading, designated respectively to the response.

GCLC, GR, and GPx expression is decreased with AT1 blockade

The liver is a unique organ because it can produce cysteine, a GSH precursor [197]. Alterations in the hepatic ability to produce or export GSH impacts its systemic homeostasis [182]. Patients with NAFLD show increased hepatic GPx activity [179]. Thus, measuring the gene expression of enzymes that participate in GSH synthesis and cycling, as well as GPx, which uses GSH as a substrate, may provide insight into GSH homeostasis after chronic AT1 blockade.

Static changes: Basal GCLC expression in OLETF was 38% greater than LETO and was 23% lesser in ARB than OLETF **(Fig. 1A)**. GR expression in OLETF and ARB was 32% and 46% lesser, respectively, than LETO and OLETF, and 22% percent lesser in ARB than OLETF **(Fig. 1C)**. GPx expression in OLETF was 55% greater than LETO, while its expression in ARB was 22% lesser than OLETF **(Fig. 1D)**.

Dynamic changes: During the glucose challenge, GCLC expression in ARB was 22% lesser than OLETF at T1 **(Fig. 1A)**. GR expression in OLETF and ARB was 30% and 54% lesser, respectively, than LETO, and 34% percent lesser in ARB than OLETF at T1, while at T2, OLETF and ARB were 48% and 45%, respectively, lesser than LETO **(Fig. 1C)**. GPx expression in OLETF was 56% greater than LETO, while its expression in ARB was 27% lesser than OLETF at T1 **(Fig. 1D)**.

GR expression in ARB was positively correlated (r = 0.997, p = 0.047) overtime, before and during the glucose challenge **(Fig. 1AC)**.

Collectively, these data suggest that GSH synthesis may be reduced with chronic AT1 blockade, representing a suppression of oxidant generation in this group and an overall decrease in the demand for anti-oxidants, as well as during the first hour of the glucose challenge.

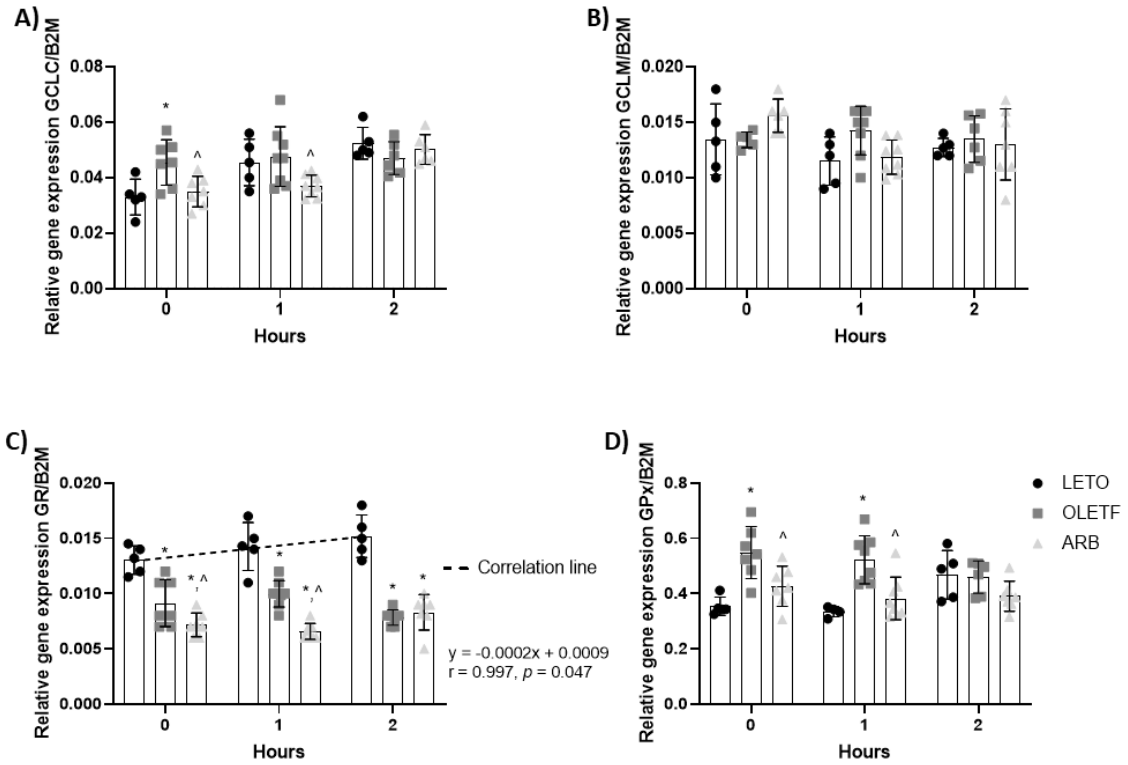

Figure 1. Gene expression of GSH synthesis, usage, and cycling enzymes. Mean ± SD values for mRNA expression of GCLC (A), GCLM (B), GR (C), and GPx (D) during the glucose challenge in Long Evans Tokushima Otsuka (LETO; n=5), Otsuka Long Evans Tokushima Fatty (OLETF; n=8), OLETF + ARB (ARB; n=8) rats. * *Significant difference from LETO (P < 0.05).* ^ *Significant difference from OLETF (P < 0.05).*

AT1 blockade decreased mitochondrial catalase activity and plasma marker of fibrosis COL-4

Chronic AT1 blockade decreased hepatic fibrosis in patients with NAFLD [193]. Recently, non-invasive markers have gained traction to evaluate the levels of hepatic fibrosis and inflammation, COL-4 levels have been shown to accurately represent the severity of hepatic fibrosis during NAFLD [97, 98]. Additionally, elevated levels of oxidants in hepatocytes increased catalase activity in its mitochondria [198]. NOX4 is a pro-oxidant enzyme that primarily produces H_2O_2 [199]. NOX4 was increased in the liver of patients with NAFLD [200]. However, NOX4 KO in mice increased insulin resistance

after feeding with a high fat diet [201], suggesting that NOX4 may have beneficial effects in certain tissues during specific conditions. Therefore, investigating the effect of AT1 blockade on COL-4, may support the traction that new non-invasive markers are gaining. Additionally, measuring NOX4 expression and mitochondrial catalase activity may provide a better understanding of the regulation of H_2O_2 levels in the liver when exposed to a nutrient overload, and their potential contribution to NAFLD.

Static changes: Basal COL-4 levels in OLETF and ARB were 107% and 49% greater, respectively, than LETO, and 28% lesser in ARB than OLETF **(Fig. 2)**. Mitochondrial catalase activity in OLETF was 36% greater than LETO, and 33% lesser in ARB than OLETF **(Fig. 2)**. Nox4 expression in OLETF and ARB was 61% and 41% lesser, respectively, than LETO, and 51% greater in ARB than OLETF **(Fig. 2)**.

Dynamic changes: During the glucose challenge, mitochondrial catalase activity in OLETF was 85% greater than LETO, and 26% lesser in ARB than OLETF at T1 **(Fig. 2)**. Nox4 expression in OLETF and ARB was 52% and 74% lesser, respectively, than LETO, and 45% lesser in ARB than OLETF **(Fig. 2)**. At T2, Nox4 expression in OLETF and ARB was 57% and 71% lesser, respectively, than LETO **(Fig. 2)**.

The decrease in COL-4 suggests that liver fibrosis may be reduced with chronic AT1 blockade, supported by previous studies that confirmed decreased fibrosis with ARB treatment [193]. The decrease in mitochondrial catalase activity with chronic AT1 blockade may represent a decreased oxidant state. Finally, increased NOX4 in ARB suggests that its expression may be beneficial to the liver, as reflected by the higher NOX4 expression in the healthy LETO.

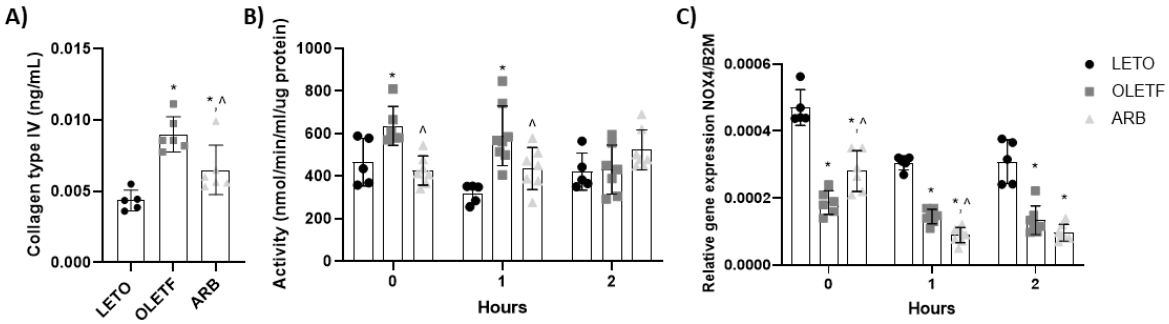

Figure 2. Liver marker of fibrosis, hepatic mitochondrial catalase activity and gene expression of peroxide production enzyme. Mean ± SD values for plasma COL-4 levels (A), before the glucose challenge and catalase activity in mitochondria (B) and mRNA expression of NOX4 (C) during the glucose challenge in Long Evans Tokushima Otsuka (LETO), Otsuka Long Evans Tokushima Fatty (OLETF), OLETF + ARB (ARB) rats. ** Significant difference from LETO ($P < 0.05$).* ^ *Significant difference from OLETF ($P < 0.05$).*

Discussion

Oxidative stress is considered as one of the main contributors to the development [174] and progression [175] of NAFLD. GSH participates in the reduction of harmful oxidant species and toxicants [178]. Low GSH levels are associated with NAFLD in humans [179]. The circulating pool of GSH is supplied mainly from GSH synthesized in the liver, which generates approximately 85% of circulating GSH [202]. Accordingly, GSH and redox homeostasis in the liver are also maintained by GR, which cycles GSH by reducing GSSG to GSH [177]. Thus, hepatic production and export of GSH is key to maintain systemic GSH homeostasis [182]. In this study, basal GCLC and GR expression were reduced with chronic ARB treatment (**Fig. 3**), suggesting that GSH production may be decreased over time due to the AT1-blockade mediated reduction in oxidant production [203]. This suggests that in the liver of insulin-resistant rats with hepatic steatosis, AT1 blockade may improve the redox state, reducing the need for GSH production.

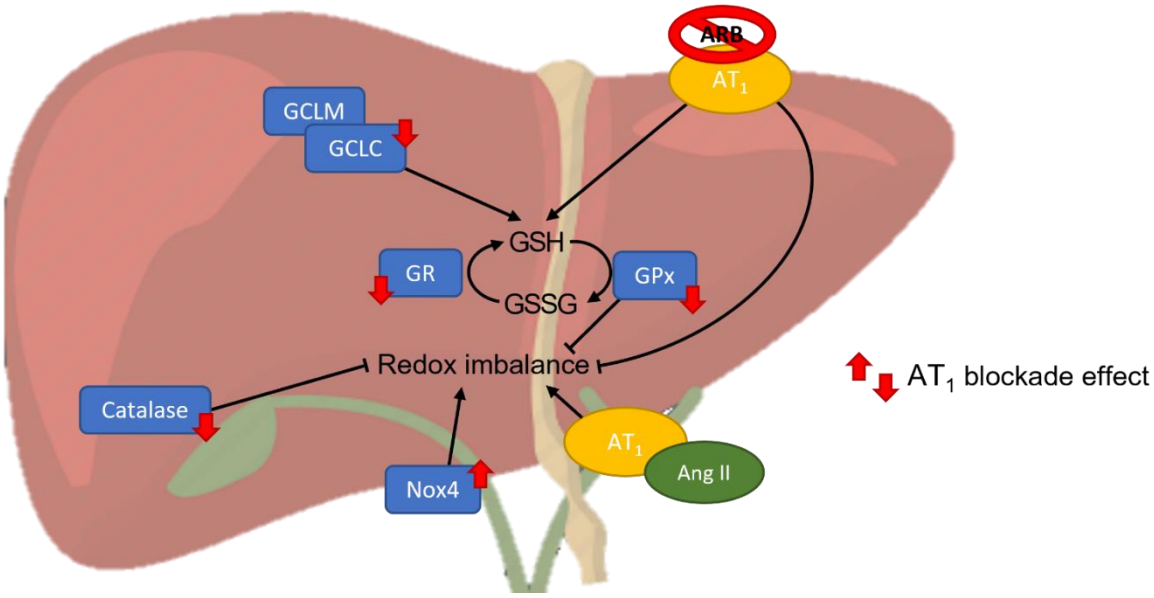

Figure 3. Summary of findings. The expression of GCLC, gene of glutathione synthesis, was decreased after AT1 blockade. GR cycles GSH to its reduced form to be used in the reduction of oxidants, as in the reaction with GPx. The expression of these genes, GR and GPx, were decreased after AT1 blockade. Finally, AT1 blockade decreased catalase activity. Altogether, these results suggest that oxidant levels may be decreased with AT1 blockade, requiring less GSH production and cycling. The decrease in catalase activity and GPx expression support this argument, as both clear the H_2O_2, an oxidant in the cell.

The decrease in GCLC, GR, and GPx in the ARB group 1 h after the glucose challenge may reflect the improved redox state of the hepatocyte. Contrarily, low GSH levels have been associated with NAFLD in humans [179], suggesting that chronically compromised livers have impaired GSH production. However, the NAFLD progression

may not be as severe in this stage [99]. Therefore, while in early stages of NAFLD, there may be an increase on GSH demand because of the increased oxidant production [179], the AT1 blockade improved the redox state and therefore decreased the need for GSH production and cycling. Moreover, during late-stage diabetes, the response from enzymes that counteract oxidants is reduced [204], supporting the argument that during advanced NAFLD, GSH levels may be decreased due to impaired mechanisms of oxidant reduction [179] and not due to the lack of a cellular demand. The increase in GCLC and GPx genes in OLETF suggests that more GSH production and oxidant clearance may be needed during the early stages of NAFLD [205], to counteract the increased production of oxidants in the liver [189], while chronic AT1 may have decreased oxidant production, supported by the decrease in GCLC and GPx expression. Separately, GCLM interacts with GCLC to increase its catalytic efficiency [206]. In this study, GCLM expression did not change. This suggests that in the liver of OLETF rats, GCLC may be the subunit more sensitive to AT1 blockade. This is relevant because GCLC regulates GCL formation and its consequential activity [207]. On the other hand, GR expression was reduced in OLETF and with AT1 blockade and remained so throughout the glucose challenge. This suggests that GR expression may be decreased at the very early stages of NAFLD in MetS, decreasing the cycling of GSSG back to GSH and promoting an increased oxidative state [189]. While with chronic AT1 blockade, this decrease may be partially due to the lesser need of GSH, derived from the improved oxidative state [208]. Additionally, the glucose challenge induced a linear increase in GR expression in LETO, while levels were lower in OLETF and ARB groups and remained so in response to the glucose load. This suggests that the livers in OLETF rats, despite the ARB-associated benefits, may still be sensitive to glucotoxicity [46], which impairs GR expression. This study reveals that the GR-mediated aspect of GSH cycling may be independent of AT1 signaling and sensitive to glucotoxicity, even during the early stages of MetS and NAFLD. Thus, chronic AT1 blockade may not be sufficient to ameliorate the glucose-induced suppression of GR expression, as shown by the difference between the LETO and ARB animals during the glucose challenge.

It is suggested that oxidative stress mediates the progression of liver fibrosis, by producing hepatic injury, initiating fibrogenesis [209]. AT1 blockade decreased fibrosis in the liver of patients with NAFLD [193]. COL-4 accurately represented the severity of hepatic fibrosis during NAFLD [97, 98]. In this study, COL-4 was decreased after chronic AT1 blockade, suggesting that the degree of liver fibrosis is ameliorated [98]. This also suggests that activation of AT1 early in MetS may be a contributing mechanism in the manifestation of fibrosis associated with NAFLD. The improvement in COL-4 may also represent amelioration of a pro-oxidative state produced by overactivation of AT1 [195, 196]. Accordingly, in the older OLETF rats [44] (chapter 1, fig. 2A), AT1 blockade also decreased COL-4, suggesting that even during more advanced stages of NAFLD

[99], chronic AT1 blockade may also improve the redox state in the liver, ameliorating liver fibrosis or its progression.

H_2O_2 is regarded as a major redox metabolite, which when properly regulated serves as an important intracellular signaling molecule [210]; however, when present in supraphysiological concentrations, it contributes to an oxidizing environment [211]. GPx uses GSH to catalyze the conversion of H_2O_2 to water [185]. Catalase also reduces H_2O_2 to water and oxygen. Elevated oxidants in hepatocytes may mainly increase mitochondrial catalase activity [198]. In this study, the decrease in mitochondrial catalase activity with AT1 blockade decreased in parallel with GPx expression. This suggests that with chronic AT1 blockade, cellular H_2O_2 levels may be reduced [212], reflected by the decreased GPx expression [213]. H_2O_2 production may also not be greatly stimulated by glucose at this stage of NAFLD progression, as neither GPx expression nor catalase activity showed a behavior that reached correlation overtime during the glucose challenge.

On the other hand, NOX4 is a pro-oxidant enzyme that primarily produces H_2O_2 [199]. Hepatic NOX4 was increased in patients with NAFLD [200], though NOX4 KO in mice led to increased insulin resistance after feeding with a high fat diet [201], demonstrating that NOX4 may presence is beneficial to achieve normal physiology. In this study, basal NOX4 expression was lower in OLETF and ARB groups, suggesting that NOX4 may exert beneficial effects for the liver. The increase in NOX4 expression in ARB, compared to OLETF, may be beneficial, as its levels would be closer to healthy LETO levels, which suggest that NOX4 expression may be needed in the liver of healthy LETO rats, as suggested by the increased obesity and IR in a mice study with NOX4 KO [201]. This expression pattern suggests that NOX4 may supply the liver with H_2O_2 to participate in insulin signaling [214] and as a second messenger, more so than to contribute to the oxidant imbalance [215]. This is supported by the findings of chapter II, where AT1 blockade may have ameliorated insulin sensitivity in the liver (Fig. 4). In the heart of OLETF rats, NOX4 was also increased after ARB treatment [216] where its increase may be beneficial for the heart [217, 218], though more research is needed to fully understand the role of NOX4 during metabolic alterations.

Table 2. Results for ARB group compared to OLETF.

Measurements	AT_1 Blockade (ARB) 0 h	1 h	2 h
Genes of GSH synthesis & cycling			
GCLM	v	-	-
GCLC	v	v	v
GR	-	v	v
H_2O_2 production			
NOX4	-	-	-
H_2O_2 reduction			
Catalase	v	-	^
GPx			

^ *increase; v decrease; - no difference*

In summary, these data suggest that AT1 blockade may benefit the redox state in the liver, as reflected by reduced expression of GCLC and GR (**Fig. 3**). The reduction of oxidants may be achieved by reducing H_2O_2 accumulation, supported by decreased mitochondrial catalase activity and GPx expression. Accordingly, NOX4 may participate to benefit the liver signaling, as suggested by its increased expression in the healthy LETO animals and increased expression on the AT1 blockade group, when compared to the diseased OLETF. These results support the argument that early intervention [219], in this case through AT1 blockade, helps prevent the rapid progression of NAFLD that may be derived from increased oxidant production [5, 175].

Conclusions and future directions

Non-alcoholic fatty liver disease (NAFLD) afflicts 25% of the world's population and is projected to increase due to the raising prevalence of diabetes and obesity [49, 50]. While the renin-angiotensin system (RAS) is well known for regulating cardiovascular function and renal hemodynamics, a relationship among obesity, insulin resistance, and RAS activation has been reported [51, 52]. Inappropriately elevated angiotensin II (Ang II) is the primary mediator of detrimental actions of the classical RAS pathway [16]. On the other hand, metabolic syndrome (MetS) was found to be associated with NAFLD. MetS is a cluster of conditions that raise the risk of cardiovascular disease [12] and shares many characteristics with NAFLD [10, 11]. However, the mechanisms of pathogenesis for NAFLD and MetS are not completely elucidated. Therefore, this dissertation aimed to evaluate parts of the mechanisms that participate in metabolic dysregulation, which may promote the development and progression of NAFLD and MetS. Additionally, this work investigated the impact of nutrient overload in a model of MetS, through a glucose challenge, to gain further insight into the regulation and tolerance of the system during MetS. The unique study designs allowed for the study of chronic, static changes over time versus the acute, dynamic changes in response to a glucose challenge over time in hours. Because of the study designs, this dissertation therefore took a unique approach to the study of the classical and non-classical RAS signaling pathways in relation to NAFLD and MetS.

In the first chapter, angiotensin receptor 1 (AT1) blockade is used to ameliorate MetS and NAFLD characteristics, with the pursuit of reversing these, improving the prognosis of these alterations. With the older rats used in the first chapter, it is documented that by the age of dissection (26 weeks old) they display advanced MetS and further progression of NAFLD [99, 220]. The results obtained demonstrate that chronic AT1 blockade may protect the liver from triacylglycerol (TAG) accumulation by modulating non-esterified fatty acids (NEFA) uptake, likely mediated by the decreased CD36 membrane abundance, and increasing TAG export, via apolipoprotein B. In the second chapter, rats were younger at the time of dissection (16 weeks old). Here, AT1 blockade was associated with increased circulating angiotensin 1-7 (Ang 1-7), part of the non-classical signaling of RAS, which is proposed to counteract the detrimental Ang II signaling. Chronic AT1 blockade decreased liver NEFA, TAG and glucose, in these younger animals. While these substrate levels were not reverted to healthy LETO levels, a physiological improvement was suggested by the correlation between decreasing expression of DGAT1 during the glucose challenge, which would downregulate the synthesis of TAG. On the same note, a correlation between the increasing expression of GCK during the glucose challenge, indicating an improved response to elevated glucose levels. Furthermore, GCK expression correlated with liver glucose levels in the healthy LETO and AT1-dblocked groups. This indicates that the liver was responsive to the

increasing glucose levels, supported by the decreased expression of gluconeogenic enzymes, which would prevent increased hyperglycemia. Therefore, the results presented demonstrate that blockade of AT1, and therefore the classical pathway of RAS, ameliorates characteristics of NAFLD and MetS. While the characteristics of MetS evaluated could not be reversed, they were profoundly improved.

Although the pathogenesis of NAFLD is not fully understood, the "two-hit" hypothesis has been used to describe it, the first hit is increased steatosis and the second one is based on the promotion of hepatic injury. An updated version is the "multiple-hit" hypothesis, where the events are multi-factorial (i.e., obesity, insulin resistance, gut microbiome, increased adipokine secretion, hepatic oxidative status, mitochondrial dysfunction, and genetic factors). Of these, increase oxidant status is proposed as one of the main contributors to NAFLD pathogenesis [174, 175]. Glutathione (GSH) is a ubiquitous tripeptide that reduces harmful oxidant species and toxicants [178]. Circulating GSH can be used to supply the intracellular pools during increased oxidant presence [177], with the liver secreting almost 85% of the GSH found in circulation [202]. In the third chapter, the expression of GSH enzymes was evaluated in the younger rats to gain insight into GSH homeostasis in the early stages of NAFLD [99]. The expression of GSH synthesis enzyme subunit glutamate-cysteine ligase catalytic (GCLC) was decreased with chronic AT1 blockade. Suggesting decreased GSH production and an overall decreased need for GSH, which may be due to decreased oxidant presence. This is supported by the reduced catalase activity and decreased expression of glutathione peroxidase, which reduces the oxidant hydrogen peroxide using GSH. Interestingly, chronic AT1 blockade did not improve glutathione reductase expression, which remained increased in the healthy LETO and throughout the glucose challenge. This suggests that, as aforementioned, the demand for reduced GSH is lesser or AT1 blockade could not reverse the impaired expression of GR, as the levels remained the same as the untreated OLETF rats.

Nonetheless, investigating the contribution of the non-classical arm of RAS, especially though the signaling of Ang 1-7, to the amelioration of metabolism dysregulation is promising given the available literature and the data here presented. While the Ang 1-7/proto-oncogene Mas (MAS1) axis is proposed to counter the actions of the RAS classical pathway [127], the extent of this counter regulation is still not fully defined. Moreover, the relation between metabolic regulation and the Ang 1-7/MAS1 axis are not fully elucidated. Nonetheless, multiple studies demonstrate the benefits of this axis. Increased Ang 1-7 in circulation or the activation of its MAS1 receptor improved liver fibrosis [169], muscle atrophy [170], fat mass [32, 150], increased insulin secretion [148], and insulin response. It is also important to elucidate the specific mechanisms by which Ang 1-7/MAS1 signaling may counter that of the Ang II/AT1 axis during metabolic disorders. Knowing the pathways that may be simultaneously sensitive

to the AT1 blockade and to the increase of Ang 1-7 or MAS1 activation, warrants better understanding of the contributions of these RAS signaling components to the development of impaired substrate metabolism that is associated with MetS.

Today, the study of the Ang 1-7/MAS1 axis during metabolic disorder is an emerging area of interest. Recent studies employ exclusively increasing circulating Ang 1-7 or MAS1 activation. Oral Ang 1-7 is delivered through hydroxypropyl-β-cyclodextrin vehicles (HPβCD/Ang 1-7) [221], or microorganism secretion of the fusion protein (*Lactobacillus paracasei*) [222]. The MAS1 receptor has been activated using pharmacological agonists AVE0991 [168] and 20-hydroxyecdysone [223]. Metabolic improvements were reported in some of these studies, which broaden the options for treatment of metabolic disease, based on the effects of the Ang 1-7/MAS1 axis.

Because of the counteraction proposed between the classical and non-classical RAS pathways, ascertaining the role of Ang 1-7 signaling during NAFLD may provide a more profound understanding of the complexities behind RAS signaling. While investigating the organism with Ang 1-7 stimulation or MAS1 activation has provided insight into its signaling mechanism, in-depth longitudinal studies using transcriptomic, proteomic and/or metabolomic methods could be an initial grand-scale approach to identifying the targets that mediate the beneficial effects of increased Ang 1-7 signaling. Accordingly, benefits obtained from chronic AT1 blockade on substrate metabolism may be enhanced by simultaneously inducing the activation of Ang 1-7 signaling, through novel modes of activation or stimulation that may not rely completely on pharmaceutical interventions [221, 222]. Therefore, results from those studies may improve current treatments for NAFLD, and to prevent and ameliorate diseases related to metabolic alterations.

References

1. Sayiner M, Koenig A, Henry L, Younossi ZM, (2016) Epidemiology of Nonalcoholic Fatty Liver Disease and Nonalcoholic Steatohepatitis in the United States and the Rest of the World. *Clin Liver Dis* 20: 205-214.
2. Nyberg LM, Cheetham TC, Patton HM, Yang SJ, Chiang KM*, et al.*, (2021) The Natural History of NAFLD, a Community-Based Study at a Large Health Care Delivery System in the United States. *Hepatol Commun* 5: 83-96.
3. Kanwar P, Kowdley KV, (2016) The Metabolic Syndrome and Its Influence on Nonalcoholic Steatohepatitis. *Clin Liver Dis* 20: 225-243.
4. Nagata K, Suzuki H, Sakaguchi S, (2007) Common pathogenic mechanism in development progression of liver injury caused by non-alcoholic or alcoholic steatohepatitis. *J Toxicol Sci* 32: 453-468.
5. Buzzetti E, Pinzani M, Tsochatzis EA, (2016) The multiple-hit pathogenesis of non-alcoholic fatty liver disease (NAFLD). *Metabolism* 65: 1038-1048.
6. Day CP, James OF, (1998) Steatohepatitis: a tale of two "hits"? *Gastroenterology* 114: 842-845.
7. Chen Z, Yu Y, Cai J, Li H, (2019) Emerging Molecular Targets for Treatment of Nonalcoholic Fatty Liver Disease. *Trends Endocrinol Metab* 30: 903-914.
8. Calzadilla Bertot L, Adams LA, (2016) The Natural Course of Non-Alcoholic Fatty Liver Disease. *Int J Mol Sci* 17.
9. Pais R, Charlotte F, Fedchuk L, Bedossa P, Lebray P*, et al.*, (2013) A systematic review of follow-up biopsies reveals disease progression in patients with non-alcoholic fatty liver. *J Hepatol* 59: 550-556.
10. Fattahi MR, Niknam R, Safarpour A, Sepehrimanesh M, Lotfi M, (2016) The Prevalence of Metabolic Syndrome In Non-alcoholic Fatty Liver Disease; A Population-Based Study. *Middle East J Dig Dis* 8: 131-137.
11. Paschos P, Paletas K, (2009) Non alcoholic fatty liver disease and metabolic syndrome. *Hippokratia* 13: 9-19.
12. Grundy SM, Cleeman JI, Daniels SR, Donato KA, Eckel RH*, et al.*, (2005) Diagnosis and management of the metabolic syndrome: an American Heart Association/National Heart, Lung, and Blood Institute Scientific Statement. *Circulation* 112: 2735-2752.
13. Rochlani Y, Pothineni NV, Kovelamudi S, Mehta JL, (2017) Metabolic syndrome: pathophysiology, management, and modulation by natural compounds. *Ther Adv Cardiovasc Dis* 11: 215-225.
14. Roberts CK, Hevener AL, Barnard RJ, (2013) Metabolic syndrome and insulin resistance: underlying causes and modification by exercise training. *Compr Physiol* 3: 1-58.
15. Zhou MS, Schulman IH, Zeng Q, (2012) Link between the renin-angiotensin system and insulin resistance: implications for cardiovascular disease. *Vasc Med* 17: 330-341.
16. de Kloet AD, Krause EG, Woods SC, (2010) The renin angiotensin system and the metabolic syndrome. *Physiol Behav* 100: 525-534.
17. Olivares-Reyes JA, Arellano-Plancarte A, Castillo-Hernandez JR, (2009) Angiotensin II and the development of insulin resistance: implications for diabetes. *Mol Cell Endocrinol* 302: 128-139.
18. Chappell MC, (2012) Nonclassical renin-angiotensin system and renal function. *Compr Physiol* 2: 2733-2752.
19. Sparks MA, Crowley SD, Gurley SB, Mirotsou M, Coffman TM, (2014) Classical Renin-Angiotensin system in kidney physiology. *Compr Physiol* 4: 1201-1228.

20. Wei Y, Clark SE, Morris EM, Thyfault JP, Uptergrove GM*, et al.*, (2008) Angiotensin II-induced non-alcoholic fatty liver disease is mediated by oxidative stress in transgenic TG(mRen2)27(Ren2) rats. *J Hepatol* 49: 417-428.
21. Matthew Morris E, Fletcher JA, Thyfault JP, Rector RS, (2013) The role of angiotensin II in nonalcoholic steatohepatitis. *Mol Cell Endocrinol* 378: 29-40.
22. Coimbra CC, Garofalo MA, Foscolo DR, Xavier AR, Migliorini RH, (1999) Gluconeogenesis activation after intravenous angiotensin II in freely moving rats. *Peptides* 20: 823-827.
23. Ran J, Hirano T, Adachi M, (2004) Chronic ANG II infusion increases plasma triglyceride level by stimulating hepatic triglyceride production in rats. *Am J Physiol Endocrinol Metab* 287: E955-961.
24. Ran J, Hirano T, Adachi M, (2005) Angiotensin II infusion increases hepatic triglyceride production via its type 2 receptor in rats. *J Hypertens* 23: 1525-1530.
25. Ekstedt M, Nasr P, Kechagias S, (2017) Natural History of NAFLD/NASH. *Curr Hepatol Rep* 16: 391-397.
26. Barreras A, Gurk-Turner C, (2003) Angiotensin II receptor blockers. *Proc (Bayl Univ Med Cent)* 16: 123-126.
27. Mavromoustakos T, Agelis G, Durdagi S, (2013) AT1 antagonists: a patent review (2008 - 2012). *Expert Opin Ther Pat* 23: 1483-1494.
28. Henriksen EJ, Jacob S, Kinnick TR, Teachey MK, Krekler M, (2001) Selective angiotensin II receptor antagonism reduces insulin resistance in obese Zucker rats. *Hypertension* 38: 884-890.
29. Ran J, Hirano T, Adachi M, (2004) Angiotensin II type 1 receptor blocker ameliorates overproduction and accumulation of triglyceride in the liver of Zucker fatty rats. *Am J Physiol Endocrinol Metab* 287: E227-232.
30. Borem LMA, Neto JFR, Brandi IV, Lelis DF, Santos SHS, (2018) The role of the angiotensin II type I receptor blocker telmisartan in the treatment of non-alcoholic fatty liver disease: a brief review. *Hypertens Res* 41: 394-405.
31. Reudelhuber TL, (2006) A place in our hearts for the lowly angiotensin 1-7 peptide? *Hypertension* 47: 811-815.
32. Santos SH, Braga JF, Mario EG, Porto LC, Rodrigues-Machado Mda G*, et al.*, (2010) Improved lipid and glucose metabolism in transgenic rats with increased circulating angiotensin-(1-7). *Arterioscler Thromb Vasc Biol* 30: 953-961.
33. Bilman V, Mares-Guia L, Nadu AP, Bader M, Campagnole-Santos MJ*, et al.*, (2012) Decreased hepatic gluconeogenesis in transgenic rats with increased circulating angiotensin-(1-7). *Peptides* 37: 247-251.
34. Cao X, Yang FY, Xin Z, Xie RR, Yang JK, (2014) The ACE2/Ang-(1-7)/Mas axis can inhibit hepatic insulin resistance. *Mol Cell Endocrinol* 393: 30-38.
35. Moreira CCL, Lourenco FC, Mario EG, Santos RAS, Botion LM*, et al.*, (2017) Long-term effects of angiotensin-(1-7) on lipid metabolism in the adipose tissue and liver. *Peptides* 92: 16-22.
36. Ullah R, Rauf N, Nabi G, Ullah H, Shen Y*, et al.*, (2019) Role of Nutrition in the Pathogenesis and Prevention of Non-alcoholic Fatty Liver Disease: Recent Updates. *Int J Biol Sci* 15: 265-276.
37. Neuschwander-Tetri BA, (2013) Carbohydrate intake and nonalcoholic fatty liver disease. *Curr Opin Clin Nutr Metab Care* 16: 446-452.
38. Schugar RC, Crawford PA, (2012) Low-carbohydrate ketogenic diets, glucose homeostasis, and nonalcoholic fatty liver disease. *Curr Opin Clin Nutr Metab Care* 15: 374-380.

39. Browning JD, Baker JA, Rogers T, Davis J, Satapati S*, et al.*, (2011) Short-term weight loss and hepatic triglyceride reduction: evidence of a metabolic advantage with dietary carbohydrate restriction. *Am J Clin Nutr* 93: 1048-1052.
40. Foster GD, Wyatt HR, Hill JO, Makris AP, Rosenbaum DL*, et al.*, (2010) Weight and metabolic outcomes after 2 years on a low-carbohydrate versus low-fat diet: a randomized trial. *Ann Intern Med* 153: 147-157.
41. Semiane N, Foufelle F, Ferre P, Hainault I, Ameddah S*, et al.*, (2017) High carbohydrate diet induces nonalcoholic steato-hepatitis (NASH) in a desert gerbil. *C R Biol* 340: 25-36.
42. Mihas C, Kolovou GD, Mikhailidis DP, Kovar J, Lairon D*, et al.*, (2011) Diagnostic value of postprandial triglyceride testing in healthy subjects: a meta-analysis. *Curr Vasc Pharmacol* 9: 271-280.
43. Gonzalez-Rodriguez M, Pazos-Couselo M, Garcia-Lopez JM, Rodriguez-Segade S, Rodriguez-Garcia J*, et al.*, (2019) Postprandial glycemic response in a non-diabetic adult population: the effect of nutrients is different between men and women. *Nutr Metab (Lond)* 16: 46.
44. Thorwald MA, Godoy-Lugo JA, Rodriguez GJ, Rodriguez MA, Jamal M*, et al.*, (2019) Nrf2-related gene expression is impaired during a glucose challenge in type II diabetic rat hearts. *Free Radic Biol Med* 130: 306-317.
45. Kotas ME, Jurczak MJ, Annicelli C, Gillum MP, Cline GW*, et al.*, (2013) Role of caspase-1 in regulation of triglyceride metabolism. *Proc Natl Acad Sci U S A* 110: 4810-4815.
46. Mota M, Banini BA, Cazanave SC, Sanyal AJ, (2016) Molecular mechanisms of lipotoxicity and glucotoxicity in nonalcoholic fatty liver disease. *Metabolism* 65: 1049-1061.
47. Kyvelou SM, Vyssoulis GP, Karpanou EA, Adamopoulos DN, Zervoudaki AI*, et al.*, (2006) Effects of antihypertensive treatment with angiotensin II receptor blockers on lipid profile: an open multi-drug comparison trial. *Hellenic J Cardiol* 47: 21-28.
48. Takagi H, Umemoto T, (2012) Telmisartan reduces triglyceride levels over other angiotensin II receptor blockers: a meta-analysis of randomized head-to-head trials. *Int J Cardiol* 157: 403-407.
49. Cotter TG, Rinella M, (2020) Nonalcoholic Fatty Liver Disease 2020: The State of the Disease. *Gastroenterology* 158: 1851-1864.
50. Chiang DJ, Pritchard MT, Nagy LE, (2011) Obesity, diabetes mellitus, and liver fibrosis. *Am J Physiol Gastrointest Liver Physiol* 300: G697-702.
51. Bentley-Lewis R, Adler GK, Perlstein T, Seely EW, Hopkins PN*, et al.*, (2007) Body mass index predicts aldosterone production in normotensive adults on a high-salt diet. *J Clin Endocrinol Metab* 92: 4472-4475.
52. Vaidya A, Forman JP, Underwood PC, Hopkins PN, Williams GH*, et al.*, (2011) The influence of body mass index and renin-angiotensin-aldosterone system activity on the relationship between 25-hydroxyvitamin D and adiponectin in Caucasian men. *Eur J Endocrinol* 164: 995-1002.
53. Li Y, Xiong F, Xu W, Liu S, (2019) Increased Serum Angiotensin II Is a Risk Factor of Nonalcoholic Fatty Liver Disease: A Prospective Pilot Study. *Gastroenterol Res Pract* 2019: 5647161.
54. Sloniger JA, Saengsirisuwan V, Diehl CJ, Kim JS, Henriksen EJ, (2005) Selective angiotensin II receptor antagonism enhances whole-body insulin sensitivity and muscle glucose transport in hypertensive TG(mREN2)27 rats. *Metabolism* 54: 1659-1668.
55. Hirsch D, Stahl A, Lodish HF, (1998) A family of fatty acid transporters conserved from mycobacterium to man. *Proc Natl Acad Sci U S A* 95: 8625-8629.

56. Liu J, Yang P, Zuo G, He S, Tan W*, et al.*, (2018) Long-chain fatty acid activates hepatocytes through CD36 mediated oxidative stress. *Lipids Health Dis* 17: 153.
57. Koo SH, (2013) Nonalcoholic fatty liver disease: molecular mechanisms for the hepatic steatosis. *Clin Mol Hepatol* 19: 210-215.
58. Ipsen DH, Lykkesfeldt J, Tveden-Nyborg P, (2018) Molecular mechanisms of hepatic lipid accumulation in non-alcoholic fatty liver disease. *Cell Mol Life Sci* 75: 3313-3327.
59. Inoue M, Ohtake T, Motomura W, Takahashi N, Hosoki Y*, et al.*, (2005) Increased expression of PPARgamma in high fat diet-induced liver steatosis in mice. *Biochem Biophys Res Commun* 336: 215-222.
60. Falcon A, Doege H, Fluitt A, Tsang B, Watson N*, et al.*, (2010) FATP2 is a hepatic fatty acid transporter and peroxisomal very long-chain acyl-CoA synthetase. *Am J Physiol Endocrinol Metab* 299: E384-393.
61. Doege H, Baillie RA, Ortegon AM, Tsang B, Wu Q*, et al.*, (2006) Targeted deletion of FATP5 reveals multiple functions in liver metabolism: alterations in hepatic lipid homeostasis. *Gastroenterology* 130: 1245-1258.
62. Coburn CT, Knapp FF, Jr., Febbraio M, Beets AL, Silverstein RL*, et al.*, (2000) Defective uptake and utilization of long chain fatty acids in muscle and adipose tissues of CD36 knockout mice. *J Biol Chem* 275: 32523-32529.
63. Keidar S, Heinrich R, Kaplan M, Hayek T, Aviram M, (2001) Angiotensin II administration to atherosclerotic mice increases macrophage uptake of oxidized ldl: a possible role for interleukin-6. *Arterioscler Thromb Vasc Biol* 21: 1464-1469.
64. Liu Q, Bengmark S, Qu S, (2010) The role of hepatic fat accumulation in pathogenesis of non-alcoholic fatty liver disease (NAFLD). *Lipids Health Dis* 9: 42.
65. Paschos P, Tziomalos K, (2012) Nonalcoholic fatty liver disease and the renin-angiotensin system: Implications for treatment. *World J Hepatol* 4: 327-331.
66. Nagle CA, Klett EL, Coleman RA, (2009) Hepatic triacylglycerol accumulation and insulin resistance. *J Lipid Res* 50 Suppl: S74-79.
67. Fernando DH, Forbes JM, Angus PW, Herath CB, (2019) Development and Progression of Non-Alcoholic Fatty Liver Disease: The Role of Advanced Glycation End Products. *Int J Mol Sci* 20.
68. Yu J, Loh K, Song ZY, Yang HQ, Zhang Y*, et al.*, (2018) Update on glycerol-3-phosphate acyltransferases: the roles in the development of insulin resistance. *Nutr Diabetes* 8: 34.
69. Yen CL, Stone SJ, Koliwad S, Harris C, Farese RV, Jr., (2008) Thematic review series: glycerolipids. DGAT enzymes and triacylglycerol biosynthesis. *J Lipid Res* 49: 2283-2301.
70. Arendt BM, Comelli EM, Ma DW, Lou W, Teterina A*, et al.*, (2015) Altered hepatic gene expression in nonalcoholic fatty liver disease is associated with lower hepatic n-3 and n-6 polyunsaturated fatty acids. *Hepatology* 61: 1565-1578.
71. Villanueva CJ, Monetti M, Shih M, Zhou P, Watkins SM*, et al.*, (2009) Specific role for acyl CoA:Diacylglycerol acyltransferase 1 (Dgat1) in hepatic steatosis due to exogenous fatty acids. *Hepatology* 50: 434-442.
72. Perla FM, Prelati M, Lavorato M, Visicchio D, Anania C, (2017) The Role of Lipid and Lipoprotein Metabolism in Non-Alcoholic Fatty Liver Disease. *Children (Basel)* 4.
73. Choi SH, Ginsberg HN, (2011) Increased very low density lipoprotein (VLDL) secretion, hepatic steatosis, and insulin resistance. *Trends Endocrinol Metab* 22: 353-363.
74. Feingold KR (2000) Introduction to Lipids and Lipoproteins. In: Feingold KR, Anawalt B, Boyce A, Chrousos G, de Herder WW, et al. (eds) Endotext. South Dartmouth (MA):
75. Kopp W, (2019) How Western Diet And Lifestyle Drive The Pandemic Of Obesity And Civilization Diseases. *Diabetes Metab Syndr Obes* 12: 2221-2236.

76. Moreno-Fernandez S, Garces-Rimon M, Vera G, Astier J, Landrier JF*, et al.*, (2018) High Fat/High Glucose Diet Induces Metabolic Syndrome in an Experimental Rat Model. *Nutrients* 10.
77. Godoy-Lugo JA, Thorwald MA, Hui DY, Nishiyama A, Nakano D*, et al.*, (2021) Chronic angiotensin receptor activation promotes hepatic triacylglycerol accumulation during an acute glucose challenge in obese-insulin-resistant OLETF rats. *Endocrine*.
78. Sasamura H, Itoh H, (2012) 'Memory' and 'legacy' in hypertension and lifestyle-related diseases. *Hypertens Res* 35: 272-273.
79. Lopes N, Zanini AC, Casella-Filho A, Chagas AC, (2008) Metabolic syndrome patient compliance with drug treatment. *Clinics (Sao Paulo)* 63: 573-580.
80. Alefishat EA, Abu Farha RK, Al-Debei MM, (2017) Self-Reported Adherence among Individuals at High Risk of Metabolic Syndrome: Effect of Knowledge and Attitude. *Med Princ Pract* 26: 157-163.
81. Togashi N, Maeda T, Yoshida H, Koyama M, Tanaka M*, et al.*, (2012) Angiotensin II receptor activation in youth triggers persistent insulin resistance and hypertension--a legacy effect? *Hypertens Res* 35: 334-340.
82. Volpe M, Cosentino F, Tocci G, Palano F, Paneni F, (2011) Antihypertensive therapy in diabetes: the legacy effect and RAAS blockade. *Curr Hypertens Rep* 13: 318-324.
83. Kawano K, Hirashima T, Mori S, Natori T, (1994) OLETF (Otsuka Long-Evans Tokushima Fatty) rat: a new NIDDM rat strain. *Diabetes Res Clin Pract* 24 Suppl: S317-320.
84. Kawano K, Hirashima T, Mori S, Saitoh Y, Kurosumi M*, et al.*, (1992) Spontaneous long-term hyperglycemic rat with diabetic complications. Otsuka Long-Evans Tokushima Fatty (OLETF) strain. *Diabetes* 41: 1422-1428.
85. Brunner HR, (2006) Olmesartan medoxomil: current status of its use in monotherapy. *Vasc Health Risk Manag* 2: 327-340.
86. Ghasemi A, Zahediasl S, (2012) Normality tests for statistical analysis: a guide for non-statisticians. *Int J Endocrinol Metab* 10: 486-489.
87. Mukaka MM, (2012) Statistics corner: A guide to appropriate use of correlation coefficient in medical research. *Malawi Med J* 24: 69-71.
88. Zabielski P, Blachnio-Zabielska A, Lanza IR, Gopala S, Manjunatha S*, et al.*, (2014) Impact of insulin deprivation and treatment on sphingolipid distribution in different muscle subcellular compartments of streptozotocin-diabetic C57Bl/6 mice. *Am J Physiol Endocrinol Metab* 306: E529-542.
89. Jaki T, Wolfsegger MJ, (2009) A theoretical framework for estimation of AUCs in complete and incomplete sampling designs. *Statistics in Biopharmaceutical Research* 1: 176-184.
90. Heikela H, Ruohonen ST, Adam M, Viitanen R, Liljenback H*, et al.*, (2020) Hydroxysteroid (17beta) dehydrogenase 12 is essential for metabolic homeostasis in adult mice. *Am J Physiol Endocrinol Metab* 319: E494-E508.
91. Kwak SK, Kim JH, (2017) Statistical data preparation: management of missing values and outliers. *Korean J Anesthesiol* 70: 407-411.
92. Muller-Fielitz H, Hubel N, Mildner M, Vogt FM, Barkhausen J*, et al.*, (2014) Chronic blockade of angiotensin AT(1) receptors improves cardinal symptoms of metabolic syndrome in diet-induced obesity in rats. *Br J Pharmacol* 171: 746-760.
93. Kitamura N, Takahashi Y, Yamadate S, Asai S, (2007) Angiotensin II receptor blockers decreased blood glucose levels: a longitudinal survey using data from electronic medical records. *Cardiovasc Diabetol* 6: 26.

94. Yao J, Gong X, Shi X, Fan S, Chen J*, et al.*, (2020) The efficacy of angiotensin converting enzyme inhibitors versus angiotensin II receptor blockers on insulin resistance in hypertensive patients: A protocol for a systematic review and meta-analysis. *Medicine (Baltimore)* 99: e20674.
95. Sasaki T, Noda Y, Yasuoka Y, Irino H, Abe H*, et al.*, (2008) Comparison of the effects of telmisartan and olmesartan on home blood pressure, glucose, and lipid profiles in patients with hypertension, chronic heart failure, and metabolic syndrome. *Hypertens Res* 31: 921-929.
96. Ciccarelli L, (2010) Angiotensin II receptor blockers and insulin resistance. *Hypertens Res* 33: 779.
97. Stefano JT, Guedes LV, de Souza AAA, Vanni DS, Alves VAF*, et al.*, (2021) Usefulness of collagen type IV in the detection of significant liver fibrosis in nonalcoholic fatty liver disease. *Ann Hepatol* 20: 100253.
98. Mizuno M, Shima T, Oya H, Mitsumoto Y, Mizuno C*, et al.*, (2017) Classification of patients with non-alcoholic fatty liver disease using rapid immunoassay of serum type IV collagen compared with liver histology and other fibrosis markers. *Hepatol Res* 47: 216-225.
99. Song YS, Fang CH, So BI, Park JY, Lee Y*, et al.*, (2013) Time course of the development of nonalcoholic Fatty liver disease in the Otsuka long-evans Tokushima Fatty rat. *Gastroenterol Res Pract* 2013: 342648.
100. Teixeira MZ, (2013) Rebound effect of modern drugs: serious adverse event unknown by health professionals. *Rev Assoc Med Bras (1992)* 59: 629-638.
101. Nabeshima Y, Tazuma S, Kanno K, Hyogo H, Chayama K, (2009) Deletion of angiotensin II type I receptor reduces hepatic steatosis. *J Hepatol* 50: 1226-1235.
102. Pepino MY, Kuda O, Samovski D, Abumrad NA, (2014) Structure-function of CD36 and importance of fatty acid signal transduction in fat metabolism. *Annu Rev Nutr* 34: 281-303.
103. Anderson CM, Stahl A, (2013) SLC27 fatty acid transport proteins. *Mol Aspects Med* 34: 516-528.
104. Miquilena-Colina ME, Lima-Cabello E, Sanchez-Campos S, Garcia-Mediavilla MV, Fernandez-Bermejo M*, et al.*, (2011) Hepatic fatty acid translocase CD36 upregulation is associated with insulin resistance, hyperinsulinaemia and increased steatosis in non-alcoholic steatohepatitis and chronic hepatitis C. *Gut* 60: 1394-1402.
105. Enooku K, Tsutsumi T, Kondo M, Fujiwara N, Sasako T*, et al.*, (2020) Hepatic FATP5 expression is associated with histological progression and loss of hepatic fat in NAFLD patients. *J Gastroenterol* 55: 227-243.
106. Moreno-Fernandez ME, Giles DA, Stankiewicz TE, Sheridan R, Karns R*, et al.*, (2018) Peroxisomal beta-oxidation regulates whole body metabolism, inflammatory vigor, and pathogenesis of nonalcoholic fatty liver disease. *JCI Insight* 3.
107. Chen G, Liang G, Ou J, Goldstein JL, Brown MS, (2004) Central role for liver X receptor in insulin-mediated activation of Srebp-1c transcription and stimulation of fatty acid synthesis in liver. *Proc Natl Acad Sci U S A* 101: 11245-11250.
108. Thorwald M, Rodriguez R, Lee A, Martinez B, Peti-Peterdi J*, et al.*, (2018) Angiotensin receptor blockade improves cardiac mitochondrial activity in response to an acute glucose load in obese insulin resistant rats. *Redox Biol* 14: 371-378.
109. Green CJ, Pramfalk C, Morten KJ, Hodson L, (2015) From whole body to cellular models of hepatic triglyceride metabolism: man has got to know his limitations. *Am J Physiol Endocrinol Metab* 308: E1-20.

110. Godoy-Matos AF, Silva Junior WS, Valerio CM, (2020) NAFLD as a continuum: from obesity to metabolic syndrome and diabetes. *Diabetol Metab Syndr* 12: 60.
111. Alkhouri N, Dixon LJ, Feldstein AE, (2009) Lipotoxicity in nonalcoholic fatty liver disease: not all lipids are created equal. *Expert Rev Gastroenterol Hepatol* 3: 445-451.
112. Hatziagelaki E, Karageorgopoulos DE, Chounta A, Tsiavou A, Falagas ME*, et al.*, (2012) Predictors of impaired glucose regulation in patients with non-alcoholic fatty liver disease. *Exp Diabetes Res* 2012: 351974.
113. Chatrath H, Vuppalanchi R, Chalasani N, (2012) Dyslipidemia in patients with nonalcoholic fatty liver disease. *Semin Liver Dis* 32: 22-29.
114. Legro RS, Finegood D, Dunaif A, (1998) A fasting glucose to insulin ratio is a useful measure of insulin sensitivity in women with polycystic ovary syndrome. *J Clin Endocrinol Metab* 83: 2694-2698.
115. Mori Y, Itoh Y, Tajima N, (2007) Telmisartan improves lipid metabolism and adiponectin production but does not affect glycemic control in hypertensive patients with type 2 diabetes. *Adv Ther* 24: 146-153.
116. Hanefeld M, Abletshauser C, (2001) Effect of the angiotensin II receptor antagonist valsartan on lipid profile and glucose metabolism in patients with hypertension. *J Int Med Res* 29: 270-279.
117. Nassir F, Rector RS, Hammoud GM, Ibdah JA, (2015) Pathogenesis and Prevention of Hepatic Steatosis. *Gastroenterol Hepatol (N Y)* 11: 167-175.
118. Zhou J, Febbraio M, Wada T, Zhai Y, Kuruba R*, et al.*, (2008) Hepatic fatty acid transporter Cd36 is a common target of LXR, PXR, and PPARgamma in promoting steatosis. *Gastroenterology* 134: 556-567.
119. Wilson CG, Tran JL, Erion DM, Vera NB, Febbraio M*, et al.*, (2016) Hepatocyte-Specific Disruption of CD36 Attenuates Fatty Liver and Improves Insulin Sensitivity in HFD-Fed Mice. *Endocrinology* 157: 570-585.
120. Casaschi A, Maiyoh GK, Adeli K, Theriault AG, (2005) Increased diacylglycerol acyltransferase activity is associated with triglyceride accumulation in tissues of diet-induced insulin-resistant hyperlipidemic hamsters. *Metabolism* 54: 403-409.
121. Kazantzis M, Stahl A, (2012) Fatty acid transport proteins, implications in physiology and disease. *Biochim Biophys Acta* 1821: 852-857.
122. Reidenberg MM, (2011) Drug discontinuation effects are part of the pharmacology of a drug. *J Pharmacol Exp Ther* 339: 324-328.
123. Gonzalez-Suarez I, Rodriguez de Antonio L, Orviz A, Moreno-Garcia S, Valle-Arcos MD*, et al.*, (2017) Catastrophic outcome of patients with a rebound after Natalizumab treatment discontinuation. *Brain Behav* 7: e00671.
124. Yamada S, (2011) Pleiotropic effects of ARB in metabolic syndrome. *Curr Vasc Pharmacol* 9: 158-161.
125. Kaji K, Yoshiji H, Kitade M, Ikenaka Y, Noguchi R*, et al.*, (2011) Combination treatment of angiotensin II type I receptor blocker and new oral iron chelator attenuates progression of nonalcoholic steatohepatitis in rats. *Am J Physiol Gastrointest Liver Physiol* 300: G1094-1104.
126. Benson SC, Pershadsingh HA, Ho CI, Chittiboyina A, Desai P*, et al.*, (2004) Identification of telmisartan as a unique angiotensin II receptor antagonist with selective PPARgamma-modulating activity. *Hypertension* 43: 993-1002.
127. Jiang F, Yang J, Zhang Y, Dong M, Wang S*, et al.*, (2014) Angiotensin-converting enzyme 2 and angiotensin 1-7: novel therapeutic targets. *Nat Rev Cardiol* 11: 413-426.

128. Cho KW, Cho DH, (2019) Telmisartan increases hepatic glucose production via protein kinase C zeta-dependent insulin receptor substrate-1 phosphorylation in HepG2 cells and mouse liver. *Yeungnam Univ J Med* 36: 26-35.
129. Kawano Y, Cohen DE, (2013) Mechanisms of hepatic triglyceride accumulation in non-alcoholic fatty liver disease. *J Gastroenterol* 48: 434-441.
130. Tao XR, Rong JB, Lu HS, Daugherty A, Shi P*, et al.*, (2019) Angiotensinogen in hepatocytes contributes to Western diet-induced liver steatosis. *J Lipid Res* 60: 1983-1995.
131. Lambert JE, Ramos-Roman MA, Browning JD, Parks EJ, (2014) Increased de novo lipogenesis is a distinct characteristic of individuals with nonalcoholic fatty liver disease. *Gastroenterology* 146: 726-735.
132. Song Z, Xiaoli AM, Yang F, (2018) Regulation and Metabolic Significance of De Novo Lipogenesis in Adipose Tissues. *Nutrients* 10.
133. Yvan-Charvet L, Even P, Bloch-Faure M, Guerre-Millo M, Moustaid-Moussa N*, et al.*, (2005) Deletion of the angiotensin type 2 receptor (AT2R) reduces adipose cell size and protects from diet-induced obesity and insulin resistance. *Diabetes* 54: 991-999.
134. Kurita S, Takamura T, Ota T, Matsuzawa-Nagata N, Kita Y*, et al.*, (2008) Olmesartan ameliorates a dietary rat model of non-alcoholic steatohepatitis through its pleiotropic effects. *Eur J Pharmacol* 588: 316-324.
135. Ishizaka N, Hongo M, Sakamoto A, Saito K, Furuta K*, et al.*, (2011) Liver lipid content is reduced in rat given 7-day administration of angiotensin II. *J Renin Angiotensin Aldosterone Syst* 12: 462-468.
136. Barbier-Torres L, Fortner KA, Iruzubieta P, Delgado TC, Giddings E*, et al.*, (2020) Silencing hepatic MCJ attenuates non-alcoholic fatty liver disease (NAFLD) by increasing mitochondrial fatty acid oxidation. *Nat Commun* 11: 3360.
137. Bjorndal B, Alteras EK, Lindquist C, Svardal A, Skorve J*, et al.*, (2018) Associations between fatty acid oxidation, hepatic mitochondrial function, and plasma acylcarnitine levels in mice. *Nutr Metab (Lond)* 15: 10.
138. Pellieux C, Montessuit C, Papageorgiou I, Lerch R, (2009) Angiotensin II downregulates the fatty acid oxidation pathway in adult rat cardiomyocytes via release of tumour necrosis factor-alpha. *Cardiovasc Res* 82: 341-350.
139. Boutagy NE, Marinik EL, McMillan RP, Anderson AS, Frisard MI*, et al.*, (2015) Angiotensin II receptor blockade and skeletal muscle metabolism in overweight and obese adults with elevated blood pressure. *Ther Adv Cardiovasc Dis* 9: 45-50.
140. Samuel VT, Shulman GI, (2018) Nonalcoholic Fatty Liver Disease as a Nexus of Metabolic and Hepatic Diseases. *Cell Metab* 27: 22-41.
141. Rong X, Li Y, Ebihara K, Zhao M, Kusakabe T*, et al.*, (2010) Irbesartan treatment up-regulates hepatic expression of PPARalpha and its target genes in obese Koletsky (fa(k)/fa(k)) rats: a link to amelioration of hypertriglyceridaemia. *Br J Pharmacol* 160: 1796-1807.
142. Chao HW, Chao SW, Lin H, Ku HC, Cheng CF, (2019) Homeostasis of Glucose and Lipid in Non-Alcoholic Fatty Liver Disease. *Int J Mol Sci* 20.
143. Gastaldelli A, Baldi S, Pettiti M, Toschi E, Camastra S*, et al.*, (2000) Influence of obesity and type 2 diabetes on gluconeogenesis and glucose output in humans: a quantitative study. *Diabetes* 49: 1367-1373.
144. Zhang X, Yang S, Chen J, Su Z, (2018) Unraveling the Regulation of Hepatic Gluconeogenesis. *Front Endocrinol (Lausanne)* 9: 802.

145. Gomez-Valades AG, Mendez-Lucas A, Vidal-Alabro A, Blasco FX, Chillon M*, et al.*, (2008) Pck1 gene silencing in the liver improves glycemia control, insulin sensitivity, and dyslipidemia in db/db mice. *Diabetes* 57: 2199-2210.
146. Froissart R, Piraud M, Boudjemline AM, Vianey-Saban C, Petit F*, et al.*, (2011) Glucose-6-phosphatase deficiency. *Orphanet J Rare Dis* 6: 27.
147. Rodriguez R, Lee A, Mathis KW, Broome HJ, Thorwald M*, et al.*, (2018) Angiotensin receptor and tumor necrosis factor-alpha activation contributes to glucose intolerance independent of systolic blood pressure in obese rats. *Am J Physiol Renal Physiol* 315: F1081-F1090.
148. Sahr A, Wolke C, Maczewsky J, Krippeit-Drews P, Tetzner A*, et al.*, (2016) The Angiotensin-(1-7)/Mas Axis Improves Pancreatic beta-Cell Function in Vitro and in Vivo. *Endocrinology* 157: 4677-4690.
149. Cao X, Yang F, Shi T, Yuan M, Xin Z*, et al.*, (2016) Angiotensin-converting enzyme 2/angiotensin-(1-7)/Mas axis activates Akt signaling to ameliorate hepatic steatosis. *Sci Rep* 6: 21592.
150. Santos SH, Fernandes LR, Pereira CS, Guimaraes AL, de Paula AM*, et al.*, (2012) Increased circulating angiotensin-(1-7) protects white adipose tissue against development of a proinflammatory state stimulated by a high-fat diet. *Regul Pept* 178: 64-70.
151. Tojo A, Hatakeyama S, Kinugasa S, Nangaku M, (2015) Angiotensin receptor blocker telmisartan suppresses renal gluconeogenesis during starvation. *Diabetes Metab Syndr Obes* 8: 103-113.
152. Peter A, Stefan N, Cegan A, Walenta M, Wagner S*, et al.*, (2011) Hepatic glucokinase expression is associated with lipogenesis and fatty liver in humans. *J Clin Endocrinol Metab* 96: E1126-1130.
153. Yehualashet AS, Belachew TF, (2020) ACEIs and ARBs and Their Correlation with COVID-19: A Review. *Infect Drug Resist* 13: 3217-3224.
154. Sukumaran V, Veeraveedu PT, Gurusamy N, Yamaguchi K, Lakshmanan AP*, et al.*, (2011) Cardioprotective effects of telmisartan against heart failure in rats induced by experimental autoimmune myocarditis through the modulation of angiotensin-converting enzyme-2/angiotensin 1-7/mas receptor axis. *Int J Biol Sci* 7: 1077-1092.
155. Amato D, Núñez-Ortiz A, Carmen Benítez-Flores J, Segura-Cobos D, P. L-S*, et al.*, (2016) Role of Angiotensin-(1-7) on Renal Hypertrophy in Streptozotocin-Induced Diabetes Mellitus. *Pharmacology & Pharmacy* Vol. 7: 379-395.
156. Chandarlapaty S, (2012) Negative feedback and adaptive resistance to the targeted therapy of cancer. *Cancer Discov* 2: 311-319.
157. Abuohashish HM, Ahmed MM, Sabry D, Khattab MM, Al-Rejaie SS, (2017) Angiotensin (1-7) ameliorates the structural and biochemical alterations of ovariectomy-induced osteoporosis in rats via activation of ACE-2/Mas receptor axis. *Sci Rep* 7: 2293.
158. Dias-Peixoto MF, Ferreira AJ, Almeida PW, Braga VB, Coutinho DC*, et al.*, (2012) The cardiac expression of Mas receptor is responsive to different physiological and pathological stimuli. *Peptides* 35: 196-201.
159. Diep QN, El Mabrouk M, Cohn JS, Endemann D, Amiri F*, et al.*, (2002) Structure, endothelial function, cell growth, and inflammation in blood vessels of angiotensin II-infused rats: role of peroxisome proliferator-activated receptor-gamma. *Circulation* 105: 2296-2302.

160. Knebel B, Fahlbusch P, Dille M, Wahlers N, Hartwig S*, et al.*, (2019) Fatty Liver Due to Increased de novo Lipogenesis: Alterations in the Hepatic Peroxisomal Proteome. *Front Cell Dev Biol* 7: 248.
161. Muoio DM, Newgard CB, (2008) Fatty acid oxidation and insulin action: when less is more. *Diabetes* 57: 1455-1456.
162. Moran TH, (2008) Unraveling the obesity of OLETF rats. *Physiol Behav* 94: 71-78.
163. Abbate SL, Brunzell JD, (1990) Pathophysiology of hyperlipidemia in diabetes mellitus. *J Cardiovasc Pharmacol* 16 Suppl 9: S1-7.
164. Echeverria-Rodriguez O, Del Valle-Mondragon L, Hong E, (2014) Angiotensin 1-7 improves insulin sensitivity by increasing skeletal muscle glucose uptake in vivo. *Peptides* 51: 26-30.
165. Rodriguez R, Minas JN, Vazquez-Medina JP, Nakano D, Parkes DG*, et al.*, (2018) Chronic AT1 blockade improves glucose homeostasis in obese OLETF rats. *J Endocrinol* 237: 271-284.
166. Dixon JB, Bhathal PS, O'Brien PE, (2001) Nonalcoholic fatty liver disease: predictors of nonalcoholic steatohepatitis and liver fibrosis in the severely obese. *Gastroenterology* 121: 91-100.
167. Caro JF, Triester S, Patel VK, Tapscott EB, Frazier NL*, et al.*, (1995) Liver glucokinase: decreased activity in patients with type II diabetes. *Horm Metab Res* 27: 19-22.
168. Dobrocsyova V, Slamkova M, Krskova K, Balazova L, Suski M*, et al.*, (2020) AVE0991, a Nonpeptide Angiotensin 1-7 Receptor Agonist, Improves Glucose Metabolism in the Skeletal Muscle of Obese Zucker Rats: Possible Involvement of Prooxidant/Antioxidant Mechanisms. *Oxid Med Cell Longev* 2020: 6372935.
169. Lubel JS, Herath CB, Tchongue J, Grace J, Jia Z*, et al.*, (2009) Angiotensin-(1-7), an alternative metabolite of the renin-angiotensin system, is up-regulated in human liver disease and has antifibrotic activity in the bile-duct-ligated rat. *Clin Sci (Lond)* 117: 375-386.
170. Morales MG, Abrigo J, Acuna MJ, Santos RA, Bader M*, et al.*, (2016) Angiotensin-(1-7) attenuates disuse skeletal muscle atrophy in mice via its receptor, Mas. *Dis Model Mech* 9: 441-449.
171. Rajapaksha IG, Gunarathne LS, Angus PW, Herath CB, (2021) Update on New Aspects of the Renin-Angiotensin System in Hepatic Fibrosis and Portal Hypertension: Implications for Novel Therapeutic Options. *J Clin Med* 10.
172. Rosenthal T, Erlich Y, Rosenmann E, Cohen A, (1997) Effects of enalapril, losartan, and verapamil on blood pressure and glucose metabolism in the Cohen-Rosenthal diabetic hypertensive rat. *Hypertension* 29: 1260-1264.
173. Begriche K, Massart J, Robin MA, Bonnet F, Fromenty B, (2013) Mitochondrial adaptations and dysfunctions in nonalcoholic fatty liver disease. *Hepatology* 58: 1497-1507.
174. Friedman SL, Neuschwander-Tetri BA, Rinella M, Sanyal AJ, (2018) Mechanisms of NAFLD development and therapeutic strategies. *Nat Med* 24: 908-922.
175. Takaki A, Kawai D, Yamamoto K, (2013) Multiple hits, including oxidative stress, as pathogenesis and treatment target in non-alcoholic steatohepatitis (NASH). *Int J Mol Sci* 14: 20704-20728.
176. Sies H, (1997) Oxidative stress: oxidants and antioxidants. *Exp Physiol* 82: 291-295.
177. Anderson ME, (1998) Glutathione: an overview of biosynthesis and modulation. *Chem Biol Interact* 111-112: 1-14.

178. Lushchak VI, (2012) Glutathione homeostasis and functions: potential targets for medical interventions. *J Amino Acids* 2012: 736837.
179. Kumar A, Sharma A, Duseja A, Das A, Dhiman RK*, et al.*, (2013) Patients with Nonalcoholic Fatty Liver Disease (NAFLD) have Higher Oxidative Stress in Comparison to Chronic Viral Hepatitis. *J Clin Exp Hepatol* 3: 12-18.
180. Irie M, Sohda T, Anan A, Fukunaga A, Takata K*, et al.*, (2016) Reduced Glutathione suppresses Oxidative Stress in Nonalcoholic Fatty Liver Disease. *Euroasian J Hepatogastroenterol* 6: 13-18.
181. Goutzourelas N, Orfanou M, Charizanis I, Leon G, Spandidos DA*, et al.*, (2018) GSH levels affect weight loss in individuals with metabolic syndrome and obesity following dietary therapy. *Exp Ther Med* 16: 635-642.
182. Lu SC, (2013) Glutathione synthesis. *Biochim Biophys Acta* 1830: 3143-3153.
183. Seelig GF, Simondsen RP, Meister A, (1984) Reversible dissociation of gamma-glutamylcysteine synthetase into two subunits. *J Biol Chem* 259: 9345-9347.
184. Huang CS, Chang LS, Anderson ME, Meister A, (1993) Catalytic and regulatory properties of the heavy subunit of rat kidney gamma-glutamylcysteine synthetase. *J Biol Chem* 268: 19675-19680.
185. Forman HJ, Ursini F, Maiorino M, (2014) An overview of mechanisms of redox signaling. *J Mol Cell Cardiol* 73: 2-9.
186. Zhang H, Forman HJ, Choi J, (2005) Gamma-glutamyl transpeptidase in glutathione biosynthesis. *Methods Enzymol* 401: 468-483.
187. Lauterburg BH, Adams JD, Mitchell JR, (1984) Hepatic glutathione homeostasis in the rat: efflux accounts for glutathione turnover. *Hepatology* 4: 586-590.
188. Kaneto H, Katakami N, Matsuhisa M, Matsuoka TA, (2010) Role of reactive oxygen species in the progression of type 2 diabetes and atherosclerosis. *Mediators Inflamm* 2010: 453892.
189. Chen Z, Tian R, She Z, Cai J, Li H, (2020) Role of oxidative stress in the pathogenesis of nonalcoholic fatty liver disease. *Free Radic Biol Med* 152: 116-141.
190. Wolff SP, Dean RT, (1987) Glucose autoxidation and protein modification. The potential role of 'autoxidative glycosylation' in diabetes. *Biochem J* 245: 243-250.
191. Bloemer J, Bhattacharya S, Amin R, Suppiramaniam V, (2014) Impaired insulin signaling and mechanisms of memory loss. *Prog Mol Biol Transl Sci* 121: 413-449.
192. Esterbauer H, Schaur RJ, Zollner H, (1991) Chemistry and biochemistry of 4-hydroxynonenal, malonaldehyde and related aldehydes. *Free Radic Biol Med* 11: 81-128.
193. Li Y, Xu H, Wu W, Ye J, Fang D*, et al.*, (2018) Clinical application of angiotensin receptor blockers in patients with non-alcoholic fatty liver disease: a systematic review and meta-analysis. *Oncotarget* 9: 24155-24167.
194. Taguchi I, Toyoda S, Takano K, Arikawa T, Kikuchi M*, et al.*, (2013) Irbesartan, an angiotensin receptor blocker, exhibits metabolic, anti-inflammatory and antioxidative effects in patients with high-risk hypertension. *Hypertens Res* 36: 608-613.
195. Chiarelli F, Di Marzio D, Santilli F, Mohn A, Blasetti A*, et al.*, (2005) Effects of irbesartan on intracellular antioxidant enzyme expression and activity in adolescents and young adults with early diabetic angiopathy. *Diabetes Care* 28: 1690-1697.
196. Onozato ML, Tojo A, Goto A, Fujita T, Wilcox CS, (2002) Oxidative stress and nitric oxide synthase in rat diabetic nephropathy: effects of ACEI and ARB. *Kidney Int* 61: 186-194.
197. Triguero A, Barber T, Garcia C, Puertes IR, Sastre J*, et al.*, (1997) Liver intracellular L-cysteine concentration is maintained after inhibition of the trans-sulfuration pathway by propargylglycine in rats. *Br J Nutr* 78: 823-831.

198. Salvi M, Battaglia V, Brunati AM, La Rocca N, Tibaldi E*, et al.*, (2007) Catalase takes part in rat liver mitochondria oxidative stress defense. *J Biol Chem* 282: 24407-24415.
199. Nisimoto Y, Diebold BA, Cosentino-Gomes D, Lambeth JD, (2014) Nox4: a hydrogen peroxide-generating oxygen sensor. *Biochemistry* 53: 5111-5120.
200. Bettaieb A, Jiang JX, Sasaki Y, Chao TI, Kiss Z*, et al.*, (2015) Hepatocyte Nicotinamide Adenine Dinucleotide Phosphate Reduced Oxidase 4 Regulates Stress Signaling, Fibrosis, and Insulin Sensitivity During Development of Steatohepatitis in Mice. *Gastroenterology* 149: 468-480 e410.
201. Li Y, Mouche S, Sajic T, Veyrat-Durebex C, Supale R*, et al.*, (2012) Deficiency in the NADPH oxidase 4 predisposes towards diet-induced obesity. *Int J Obes (Lond)* 36: 1503-1513.
202. Purucker E, Wernze H, (1990) Hepatic efflux and renal extraction of plasma glutathione: marked differences between healthy subjects and the rat. *Klin Wochenschr* 68: 1008-1012.
203. Sikalidis AK, Mazor KM, Lee JI, Roman HB, Hirschberger LL*, et al.*, (2014) Upregulation of capacity for glutathione synthesis in response to amino acid deprivation: regulation of glutamate-cysteine ligase subunits. *Amino Acids* 46: 1285-1296.
204. Tan Y, Ichikawa T, Li J, Si Q, Yang H*, et al.*, (2011) Diabetic downregulation of Nrf2 activity via ERK contributes to oxidative stress-induced insulin resistance in cardiac cells in vitro and in vivo. *Diabetes* 60: 625-633.
205. Swiderska M, Maciejczyk M, Zalewska A, Pogorzelska J, Flisiak R*, et al.*, (2019) Oxidative stress biomarkers in the serum and plasma of patients with non-alcoholic fatty liver disease (NAFLD). Can plasma AGE be a marker of NAFLD? Oxidative stress biomarkers in NAFLD patients. *Free Radic Res* 53: 841-850.
206. Franklin CC, Backos DS, Mohar I, White CC, Forman HJ*, et al.*, (2009) Structure, function, and post-translational regulation of the catalytic and modifier subunits of glutamate cysteine ligase. *Mol Aspects Med* 30: 86-98.
207. Lee JI, Kang J, Stipanuk MH, (2006) Differential regulation of glutamate-cysteine ligase subunit expression and increased holoenzyme formation in response to cysteine deprivation. *Biochem J* 393: 181-190.
208. Montez P, Vazquez-Medina JP, Rodriguez R, Thorwald MA, Viscarra JA*, et al.*, (2012) Angiotensin receptor blockade recovers hepatic UCP2 expression and aconitase and SDH activities and ameliorates hepatic oxidative damage in insulin resistant rats. *Endocrinology* 153: 5746-5759.
209. Sanchez-Valle V, Chavez-Tapia NC, Uribe M, Mendez-Sanchez N, (2012) Role of oxidative stress and molecular changes in liver fibrosis: a review. *Curr Med Chem* 19: 4850-4860.
210. Veal E, Day A, (2011) Hydrogen peroxide as a signaling molecule. *Antioxid Redox Signal* 15: 147-151.
211. Sies H, (2017) Hydrogen peroxide as a central redox signaling molecule in physiological oxidative stress: Oxidative eustress. *Redox Biol* 11: 613-619.
212. Cianchetti S, Del Fiorentino A, Colognato R, Di Stefano R, Franzoni F*, et al.*, (2008) Anti-inflammatory and anti-oxidant properties of telmisartan in cultured human umbilical vein endothelial cells. *Atherosclerosis* 198: 22-28.
213. Lubos E, Loscalzo J, Handy DE, (2011) Glutathione peroxidase-1 in health and disease: from molecular mechanisms to therapeutic opportunities. *Antioxid Redox Signal* 15: 1957-1997.
214. Wu X, Williams KJ, (2012) NOX4 pathway as a source of selective insulin resistance and responsiveness. *Arterioscler Thromb Vasc Biol* 32: 1236-1245.

215. Gough DR, Cotter TG, (2011) Hydrogen peroxide: a Jekyll and Hyde signalling molecule. *Cell Death Dis* 2: e213.
216. Vazquez-Medina JP, Popovich I, Thorwald MA, Viscarra JA, Rodriguez R*, et al.*, (2013) Angiotensin receptor-mediated oxidative stress is associated with impaired cardiac redox signaling and mitochondrial function in insulin-resistant rats. *Am J Physiol Heart Circ Physiol* 305: H599-607.
217. Ray R, Murdoch CE, Wang M, Santos CX, Zhang M*, et al.*, (2011) Endothelial Nox4 NADPH oxidase enhances vasodilatation and reduces blood pressure in vivo. *Arterioscler Thromb Vasc Biol* 31: 1368-1376.
218. Schroder K, Zhang M, Benkhoff S, Mieth A, Pliquett R*, et al.*, (2012) Nox4 is a protective reactive oxygen species generating vascular NADPH oxidase. *Circ Res* 110: 1217-1225.
219. Ahmed IA, Mikail MA, Mustafa MR, Ibrahim M, Othman R, (2019) Lifestyle interventions for non-alcoholic fatty liver disease. *Saudi J Biol Sci* 26: 1519-1524.
220. Panchal SK, Brown L, (2011) Rodent models for metabolic syndrome research. *J Biomed Biotechnol* 2011: 351982.
221. Figueiredo VP, Barbosa MA, de Castro UGM, Zacarias AC, Bezerra FS*, et al.*, (2019) Antioxidant Effects of Oral Ang-(1-7) Restore Insulin Pathway and RAS Components Ameliorating Cardiometabolic Disturbances in Rats. *Oxid Med Cell Longev* 2019: 5868935.
222. Verma A, Zhu P, Xu K, Du T, Liao S*, et al.*, (2020) Angiotensin-(1-7) Expressed From Lactobacillus Bacteria Protect Diabetic Retina in Mice. *Transl Vis Sci Technol* 9: 20.
223. Dioh W, Chabane M, Tourette C, Azbekyan A, Morelot-Panzini C*, et al.*, (2021) Testing the efficacy and safety of BIO101, for the prevention of respiratory deterioration, in patients with COVID-19 pneumonia (COVA study): a structured summary of a study protocol for a randomised controlled trial. *Trials* 22: 42.